



UNIVERSITÀ
DEGLI STUDI
DI PADOVA

Sede Amministrativa: Università degli Studi di Padova

Sede Consorziata: Università degli Studi di Bergamo

Dipartimento di Ingegneria Industriale

SCUOLA DI DOTTORATO DI RICERCA IN INGEGNERIA INDUSTRIALE
INDIRIZZO: INGEGNERIA CHIMICA, DEI MATERIALI E DELLA PRODUZIONE
CICLO XXVI

DEVELOPMENT OF A VIRTUAL TESTING LABORATORY FOR LOWER LIMB PROSTHESIS

Direttore della Scuola : Ch.mo Prof. Paolo Colombo

Coordinatore d'indirizzo: Ch.mo Prof. Enrico Savio

Supervisore :Ch.mo Prof.ssa Caterina Rizzi

Dottorando : Roberto Morotti

Abstract

The introduction of computer-aided tools into the product development process allows improving the quality of the product, evaluating different variants of the same product in a faster way and reducing time and costs. They can play a meaningful role also in designing custom-fit products (especially, those characterized by a tight interaction with the human body), increasing the comfort and improving people's quality of life.

This thesis concerns a specific custom-fit product, the lower limb prosthesis. It is part of a research project that aims at developing a new design platform centred on the digital model of the patient and his/her characteristics. The platform, named Prosthesis Virtual Laboratory (PVL), is being developed by the V&K Research Group (University of Bergamo) and integrates ICT tools and product-process knowledge. It provides two environments: one for prosthesis design (named Prosthesis Modelling Lab), both transfemoral and transtibial, and one for the prosthesis testing (named Virtual Testing Lab).

The main objective has been to **embed** within the Virtual Testing Environment **numerical simulation tools to analyse the interaction between the socket and the residual limb** under different loading conditions, allowing the prosthetist to **automatically run the simulation** and optimize socket shape. Simulation tools, such as Finite Element Analysis (FEA), permit to predict the pressures at the interface socket-residual limb, evaluate the comfort of socket and validate the socket design before manufacturing phase. However, the diffusion of simulation tools in orthopaedic laboratories is strongly limited by the high level of competence required to use them. Furthermore, the implementation of the simulation model is time consuming and requires expensive resources, both humans and technological, especially onerous for small orthopaedic labs. To effectively employ the numerical analysis in prosthesis design, the simulation process has been automated and embedded within the virtual design platform. Therefore, in such a context, the specific scientific objectives have been to:

- **Critically analyse the state of the art** with regard to methods and tools to evaluate socket-residual limb interaction.
- Identify the key issues to **automate the simulation** activities.
- **Define** a set of **simulation rules** and the **Finite Element Analysis model**.
- Implement and integrate within the new design platform the **automatic simulation procedure**.
- **Test** the integrated **design platform** with a case study.
- Identify **future development trends**.

Research activities have been organized into **four main activities** as follows.

The **first activity** consisted in an extensive analysis of the last two decades **State of the Art** on numerical models adopted to study residual lower-limb and prosthetic socket interaction. Starting from literature, the key issues of the simulation process (e.g., geometric models reconstruction, materials characterization, simulation steps, and boundary conditions), the methodologies and procedures have been identified. Particular attention has been also paid to the parameters commonly adopted to

evaluate socket comfort. This phase played a fundamental role since it constituted the basis for the implementation of the embedded simulation procedure. It also permitted to highlight that current finite element models are stand-alone and not integrated with prosthetic CAD or Digital Human Modelling (DHM) systems.

In the **second activity** the **tools and methods** necessary to develop the embedded simulation module have been selected. By using these tools, it was possible to identify the **simulation rules** and the **best practice procedures**, which are fundamental to implement an automatic simulation module. Initially, the modelling tools have been considered since they provide the geometric models for the numerical analysis of the socket-residuum interaction and for the virtual gait analysis of the patient's avatar. Then, particular attention has been paid on the choice of the FE solver, that has been made according to the results of preliminary FE models. They were implemented using two different solvers: Abaqus (commercial) and CalculiX (open-source). The latter has been experimented to verify the possibility to develop a design platform totally independent from commercial tools. However, according to the results, Abaqus has been chosen because it allows managing adequately simulation problems characterized by large deformations and difficult contact conditions, its results are comparable with those found in literature, and its scripting code does not require specific customization. The last considered tool was the Digital Human Modelling system (LifeMOD) since it permits to enhance the accuracy of the numerical analysis. By performing the gait simulation of the patient's avatar, it provides the directions and the magnitude of forces and moments that act on the socket.

The **third activity** consisted in **defining the architecture of the simulation module, implementing the module and the interfaces** with the socket CAD tool (namely Socket Modelling Assistant-SMA) to get the geometric models of the involved parts (socket and residual limb) and with the DHM system to acquire forces acting on the socket during patient's walking. The simulation module has been implemented using the Python language and the integrated environment works as follows. Once the prosthetist has created the 3D socket model, SMA acquires the input for the analysis (e.g., residual limb length, patient's weight, friction coefficient, material properties), and produces the files required to generate the FE model. Abaqus automatically generates the FE model without any human intervention, solves the analysis and generates the output file containing the pressure values. Results are imported in SMA and visualized with a colour map. SMA evaluates pressure distribution and highlights the areas that should be modified. Geometry modifications are needed in the areas where pressure exceeds the maximum value and are carried out automatically by the system or by the prosthetist using the virtual tools available in SMA. Then, the system re-executes the simulation. Through this iterative process of adjustments, the socket shape is modified and optimized in order to eliminate undercuts, minimize weight and, especially, distribute loads in the appropriate way so that they can be tolerated for the longest period of time.

The **fourth and last activity** concerned the **test and validation of the simulation module** integrated within the new design platform, by considering a transfemoral patient. The new virtual process and the key issues of the simulation procedure have been tested starting from the patient's data acquisition to the release of the socket using also data coming from the gait simulation with the DHM system. The geometric model of the residual limb has been reconstructed from MRI images and the socket has been modelled using SMA. Through an iterative process, the socket shape has been optimized until the pressure distribution on the residuum was consistent. Preliminary activity concerning the FE model validation has been performed comparing the pressure distribution experimentally acquired with pressure transducers over the residuum with the simulation results. To accomplish this task, the geometric model of the real socket has been acquired using reverse engineering techniques. Two numerical simulations have been implemented, they differ for the residuum geometric models adopted: from MRI and from 3D scanning. Preliminary results have been considered positive but improvements are necessary. As an example, some geometric inconsistencies, occurred during the

acquisition of the geometric model of the residual limb, have reduced the accuracy of the final results. To complete the evaluation of the simulation model, a new residuum geometric model is needed and a refinement of the material model characterization is desirable.

To conclude, the simulation module embedded within Virtual Testing Laboratory has improved the prosthesis development process with the goal of assessing and validating the socket shape under different load conditions (static or dynamic) before the manufacturing phase. The testing phase of the new procedure has demonstrated the feasibility of the virtual approach for lower limb prosthesis design. The tests carried out permitted to highlight necessary improvements and future developments, such as the definition of a protocol to acquire the residual limb through MRI and 3D scan, refinement of the FE model (e.g., non-linear viscoelastic behaviour for soft tissues, friction coefficients), parallel computing to improve simulation performances, open-source solvers to implement a design platform totally independent from commercial systems, and a massive test campaign involving transtibial and transfemoral patients to fully validate the FE model and the design platform.

Keywords: prosthesis design, socket-residuum contact interaction, finite element analysis, human modelling, gait analysis simulation, embedded simulation, pressure acquisition.

Riassunto

L'introduzione di strumenti informatizzati nel processo di sviluppo del prodotto permette di migliorarne la qualità, nonché di valutare diverse varianti del prodotto stesso in modo più veloce, riducendo in tal modo il tempo ed i costi relativi alla progettazione. Per queste motivazioni, tali strumenti possono giocare un ruolo rilevante anche nella realizzazione di prodotti personalizzati (specialmente quelli caratterizzati da una stretta interazione con il corpo umano), aumentandone il comfort e migliorando la qualità di vita delle persone.

Il presente lavoro di tesi si concentra nello specifico sull'applicazione di tali strumenti informatizzati nella creazione di protesi per arti inferiori, inserendosi in un progetto di ricerca che ha come obiettivo quello di sviluppare una nuova piattaforma di progettazione centrata sul modello digitale del paziente e sulle sue caratteristiche. La piattaforma, chiamata Prosthesis Virtual Laboratory (PVL), è stata sviluppata dal gruppo di ricerca V&K dell'Università degli Studi di Bergamo nell'ottica di integrare gli strumenti informatici con la conoscenza del prodotto e del processo. La piattaforma è strutturata in modo da offrire due ambienti di lavoro: uno dedicato alla progettazione della protesi (chiamato Prosthesis Modelling Lab), sia transfemorale che transtibiale, e l'altro destinato alla fase di verifica della stessa (chiamato Virtual Testing Lab).

L'obiettivo principale del lavoro di tesi è stato quello di **integrare**, all'interno dell'ambiente virtuale di verifica, gli **strumenti di simulazione numerica che consentono di analizzare l'interazione tra l'invaso e l'arto residuo** sotto diverse condizioni di carico, permettendo al tecnico protesico di effettuare la **simulazione in automatico** e di ottimizzare la forma dell'invaso. Gli strumenti di simulazione, come l'analisi agli elementi finiti (FEA), permettono di predire la pressione all'interfaccia tra invasore e moncone, di valutare il comfort dell'invaso e di validare la progettazione dello stesso prima della fase di manifattura. Tuttavia, la diffusione degli strumenti di simulazione nei laboratori ortopedici è fortemente limitata dall'elevato livello di competenze richieste per ottenere risultati significativi. Inoltre, l'implementazione di un modello di simulazione numerica richiede tempo e costose risorse, sia umane che tecnologiche, particolarmente onerose per i piccoli laboratori ortopedici. Affinché l'analisi numerica sia utilizzata nella progettazione delle protesi, è necessario che il processo di simulazione sia automatico ed integrato all'interno di una piattaforma virtuale di progettazione.

In questo contesto, gli obiettivi scientifici specifici sono stati:

- **Analizzare criticamente lo stato dell'arte** riguardante i metodi e gli strumenti per valutare l'interazione tra invasore ed arto residuo.
- Identificare le questioni chiave per **automatizzare le attività di simulazione**.
- **Definire** un insieme di **regole di simulazione** ed il **modello per l'analisi ad elementi finiti**.
- Implementare ed integrare nella nuova piattaforma di progettazione la **procedura di simulazione automatica**.
- **Verificare** la **piattaforma di progettazione** integrata con un caso studio.
- Identificare le **tendenze di sviluppo futuro**.

Le attività di ricerca sono state organizzate in quattro attività principali, come di seguito presentato nello specifico.

La **prima attività** è consistita in un'analisi approfondita dello **stato dell'arte** negli ultimi due decenni relativamente ai modelli numerici adottati per studiare l'interazione tra involucro ed arto residuo. Partendo dalla letteratura, sono stati individuati i temi chiave del processo di simulazione (ad esempio la ricostruzione dei modelli geometrici, la caratterizzazione dei materiali, le fasi di simulazione e le condizioni al contorno), nonché le metodologie e le procedure di simulazione. Particolare attenzione è stata posta anche ai parametri comunemente adottati per valutare il comfort dell'involucro. Questa fase ha giocato un ruolo fondamentale in quanto costituisce la base per l'implementazione della procedura di simulazione integrata. Ha permesso altresì di evidenziare come gli attuali modelli agli elementi finiti siano indipendenti e non integrati con i sistemi CAD per protesi o di Digital Human Modelling (DHM).

La **seconda attività** ha avuto come focus la selezione degli **strumenti** e dei **metodi** necessari allo sviluppo del modulo di simulazione, per mezzo dei quali è stato possibile identificare le **regole di simulazione** e le **procedure di buona prassi**, fondamentali per l'implementazione di un modulo di simulazione automatica. Inizialmente, gli strumenti di modellazione sono stati presi in considerazione in quanto forniscono i modelli geometrici sia per l'analisi numerica dell'interazione tra involucro ed arto residuo che per l'analisi della camminata virtuale dell'avatar del paziente. In seguito, particolare attenzione è stata posta sulla scelta del solutore a elementi finiti, che è stata fatta in accordo con i risultati ottenuti dai modelli preliminari implementati utilizzando due diversi solutori: Abaqus (commerciale) e CalculiX (open-source). Quest'ultimo è stato impiegato per verificare la possibilità di sviluppare una piattaforma di progettazione totalmente indipendente dagli strumenti commerciali. Tuttavia, in base ai risultati ottenuti, la scelta si è indirizzata verso Abaqus, in quanto permette di gestire in modo adeguato i problemi di simulazione caratterizzati da grandi deformazioni e da difficili condizioni di contatto. L'utilizzo di questo solutore consente di ottenere risultati paragonabili a quelli presenti in letteratura ed inoltre il suo codice di script non richiede specifiche personalizzazioni. L'ultimo strumento utilizzato è stato il sistema DHM (Digital Human Modelling) che permette di aumentare la precisione dell'analisi numerica. Attraverso l'analisi della camminata virtuale dell'avatar del paziente, questo strumento è in grado di fornire le direzioni e le intensità delle forze e delle coppie che agiscono sull'involucro.

La **terza attività** ha riguardato la **definizione dell'architettura del modulo di simulazione, l'implementazione del modulo** stesso e del suo **interfacciamento** prima con lo strumento CAD per l'involucro (chiamato Socket Modelling Assistant - SMA), allo scopo di ottenere i modelli geometrici delle parti coinvolte (involucro ed arto residuo), ed in seguito con il sistema DHM, per acquisire le forze che agiscono sull'involucro durante la deambulazione del paziente. Il modulo di simulazione è stato implementato utilizzando il linguaggio Python e l'ambiente integrato prevede diverse fasi di sviluppo, come di seguito approfondito. Una volta che il tecnico protesico ha creato il modello 3D dell'involucro, lo SMA acquisisce gli input per l'analisi (come la lunghezza dell'arto residuo, il peso del paziente, il coefficiente di attrito, le proprietà dei materiali) e rilascia i file richiesti per generare il modello agli elementi finiti. Abaqus genera automaticamente il modello di simulazione senza che vi sia alcun intervento umano, risolve l'analisi e genera il file di output contenente i valori di pressione. I risultati sono importati nello SMA e visualizzati con una mappa di colore. La modifica della geometria dell'involucro, necessaria nelle aree in cui la pressione eccede i valori massimi, è eseguita in automatico dal sistema o dal tecnico protesico tramite gli strumenti virtuali presenti nello SMA. Il sistema, quindi, riesegue la simulazione. Attraverso questo processo iterativo di rettifica, la forma dell'involucro è modificata ed ottimizzata al fine di eliminare i sottosquadri, minimizzare il peso e soprattutto distribuire i carichi in modo appropriato, così che siano tollerabili per lunghi periodi di tempo.

La **quarta ed ultima attività** ha riguardato la **sperimentazione** e la **validazione del modulo di simulazione integrato** all'interno della nuova piattaforma di progettazione considerando un paziente transfemorale. Il nuovo processo virtuale e le questioni chiave della procedura di simulazione sono state testate partendo dall'acquisizione dei dati del paziente fino al rilascio dell'invaso definitivo, utilizzando anche i dati provenienti dalla simulazione della camminata con il sistema DHM. Il modello geometrico dell'arto residuo è stato ricostruito partendo dalle immagini MRI e l'invaso è stato modellato utilizzando lo SMA. Attraverso un processo iterativo, la forma dell'invaso è stata ottimizzata fino ad avere una distribuzione appropriata della pressione sul moncone. L'attività preliminare riguardante la validazione del modello agli elementi finiti è stata eseguita comparando la distribuzione delle pressioni acquisite sperimentalmente sul moncone con i risultati della simulazione. Per realizzare questo compito, il modello geometrico dell'invaso reale è stato acquisito utilizzando tecniche di reverse engineering. Sono state implementate due diverse simulazioni numeriche che differiscono per il modello geometrico del moncone adottato: attraverso MRI nel primo caso, da scansione 3D nel secondo. I risultati preliminari possono considerarsi positivi ma ulteriori sviluppi sono necessari. Ad esempio, alcune incongruenze geometriche che si sono verificate durante l'acquisizione del modello geometrico hanno ridotto la precisione dei risultati finali. Per completare la valutazione del modello di simulazione è quindi necessario utilizzare un nuovo modello geometrico del moncone e sarebbe anche auspicabile raffinare il modello di caratterizzazione del materiale.

Concludendo, il modulo di simulazione integrato all'interno del Virtual Testing Laboratory – VTL ha permesso di migliorare il processo di sviluppo della protesi con l'obiettivo di valutare e validare la forma dell'invaso sotto diverse condizioni di carico (statiche o dinamiche), prima della fase di manifattura. La fase di test del nuovo processo ha inoltre dimostrato la fattibilità del nuovo approccio virtuale per la progettazione delle protesi per arti inferiori. I test effettuati hanno indicato quali miglioramenti siano necessari ed i possibili sviluppi futuri, tra cui: la definizione di un protocollo di acquisizione dell'arto residuo attraverso MRI o scansione 3D, il calcolo parallelo per migliorare le prestazioni della simulazione, l'utilizzo di solutori open-source per implementare una piattaforma di progettazione totalmente indipendente dai sistemi commerciali, la realizzazione di una massiccia campagna sperimentale che coinvolga pazienti transtibiali e transfemorali al fine di convalidare pienamente il modello FE e la piattaforma di progettazione.

Parole chiave: progettazione di protesi, interazione di contatto tra invasore e moncone, analisi agli elementi finiti, modelli umani digitali, simulazione dell'analisi della camminata, simulazione integrata, acquisizione della pressione.

Table of Contents

Abstract	iii
Riassunto	vii
Table of Contents	xi
List of Figures	xv
List of Tables	xix
List of Abbreviations	xxi
1 Introduction	1
1.1 Context.....	1
1.2 Background and motivation.....	3
1.3 Thesis organisation	4
2 Lower Limb Prosthesis Design Framework	5
2.1 Traditional design process	5
2.2 A virtual approach for prosthesis design	7
2.2.1 Prosthesis Modelling Lab.....	9
2.2.2 Virtual Testing Lab	10
3 State of the Art	11
3.1 Patient’s digital model	11
3.1.1 Residual limb model.....	12
3.1.2 Prosthetic socket model and liner.....	15
3.2 Numerical models	17
3.2.1 Geometries and mesh	18
3.2.2 Material properties	20
3.2.3 Interaction.....	23
3.2.4 Boundary conditions and analysis steps.....	25
3.3 Evaluation parameters	28
3.3.1 Numerical model validation	32
3.4 Discussion.....	32
4 Tools and Methods	35
4.1 Modelling tools.....	35
4.1.1 Socket Modelling Assistant.....	35
4.1.2 Prosthesis configuration and assembly	37
4.2 FE solvers	38
4.2.1 Abaqus FE model	39

4.2.2	CalculiX FE model.....	42
4.2.3	Discussion	45
4.3	Digital Human Modelling.....	45
4.3.1	Patient’s avatar implementation	45
4.3.2	Avatar simulation	46
5	Embedded Simulation Module	49
5.1	FEA module architecture	49
5.2	Simulation rules	52
5.2.1	Geometric model	52
5.2.2	Mesh properties	52
5.2.3	Material properties	56
5.2.4	Boundary conditions and analysis steps.....	58
5.2.5	Evaluation parameters	59
5.3	Module Implementation.....	60
6	Case Study	67
6.1	Patient’s case history	67
6.2	3D reconstruction of the residual limb	68
6.3	Prosthesis design.....	69
6.4	Gait analysis.....	69
6.5	Finite element analysis	70
6.6	Results.....	72
7	FEA Model Assessment	77
7.1	Pressure sensors systems	77
7.1.1	Novel Prosthesis System	79
7.1.2	SensorTech Zebra™ 3D System	79
7.1.3	Tekscan F-Socket™ System	80
7.1.4	Selection of the system.....	81
7.2	Pressures distribution acquisition	81
7.2.1	Sensors specifications	81
7.2.2	Acquisition protocol.....	82
7.2.3	Calibration method.....	83
7.3	Finite element analysis	84
7.3.1	Geometric models acquisition and reconstruction	85
7.3.2	FE analysis	86
7.4	Comparison of the results	87
	Conclusions	91
	Bibliography	93

Appendices	101
A Prosthesis components	103
A1. Socket	104
A2. Liner	106
A3. Knee	107
A4. Foot	107
A5. Other components	108
B Workstation technical specification	111

List of Figures

Figure 1.1 - Examples of lower limb amputees without and with prosthesis: transfemoral (left) and transtibial (right) [1].	2
Figure 1.2 - Examples of modular transfemoral (left) and transtibial (middle) prosthetic device, and scheme of main components of modular transfemoral prosthesis (right).	3
Figure 2.1 - Workflow of the traditional manufacturing of modular lower limb prosthesis.	7
Figure 2.2 - Prosthesis design platform and the associated modules.	8
Figure 2.3 - Workflow and modules interaction of the new design platform for modular lower limb prosthesis.	9
Figure 3.1 - (A) portable indentation device, (B-D) images of various indentation steps, (E) deformed shapes [46].	22
Figure 3.2 - 3D model to compute load magnitude at the knee joint [53].	26
Figure 3.3 - Boundary conditions applied to an FE model (fixed region and load direction) and frames sequence of the donning simulation.	27
Figure 3.4 – Critical areas of transtibial residual limb (in green the load areas and red the off-load areas) [65].	28
Figure 3.5 – Critical areas of transfemoral residual limb (in green the load areas and red the off-load areas).	29
Figure 4.1 - Example of Marker Tool functionalities with highlighting the critical zones (left) and Circumferences Scaling Tool (right).	36
Figure 4.2 - Example of the creation of the reference socket surface (left) and the socket top rounding (right).	37
Figure 4.3 - Examples of Sculpt Tool functionality (left) and the use of the Section Tool for moving the surface control point in green (right).	37
Figure 4.4 - Example of an assembly of transfemoral prosthesis (left) and prosthesis modules (right).	38
Figure 4.5 - Three-dimensional models of the socket; the residual limb and the femur; and, finally, the results of the Boolean operation of union of residuum and bone.	40

Figure 4.6 - Meshed models of the socket and residuum with initial over-closure (left) and FE model boundary condition relative to the fixed nodes of the residuum (right).....	41
Figure 4.7 - Donning simulation of a transfemoral socket.....	41
Figure 4.8 - Pressure distribution on residuum surface after loading simulation performed with Abaqus.....	42
Figure 4.9 - Residual limb without residual femur and prosthetic socket used for the FE analysis.	42
Figure 4.10 - Discretization of the socket and residuum with initial over-closure (left) and FE model boundary condition relative to the fixed nodes of the residuum (right).....	44
Figure 4.11 - Pressure distribution on residuum surface after loading simulation performed with CalculiX.	44
Figure 4.12 - Patient's avatar (left); avatar wearing the prosthesis (right).	46
Figure 4.13 - Load components acting on the socket during walking.	47
Figure 5.1 - Logic schema of the framework: socket design process integrated with the FEA module and the DHM module.	50
Figure 5.2 - Integrated FE analysis procedure within the design platform.	51
Figure 5.3 - Graphic correlation between model size and computational time (dot-dashed line refers to linear trendline).	53
Figure 5.4 - Simulation results with different mesh size (from 3 to 5): legenda (first row), yx view (second row), zy view (third row), xy view (fourth row),yz view (fifth row), zx view (sixth row).	54
Figure 5.5 - Simulation results with different mesh size (from 6 to 8): legenda (first row), yx view (second row), zy view (third row), xy view (fourth row),yz view (fifth row), zx view (sixth row)	55
Figure 5.6 - Simulation results with different model material: legenda (first row), yx view (second row), zy view (third row), xy view (fourth row),yz view (fifth row), zx view (sixth row).	57
Figure 5.7 - Example of the simulation steps: from the initial position to the end of phase static load.....	59
Figure 5.8 – Critical areas of transtibial residual limb (in green the load areas and red the off-load areas) [65].....	59
Figure 5.9 – Critical areas of transfemoral residual limb (in green the load areas and red the off-load areas).	60
Figure 5.10 - Abaqus Scripting Interface commands and Abaqus/CAE.....	61
Figure 6.1 - Example of definition of the patient's characteristics.	68
Figure 6.2 - Socket model within the SMA and complete prosthetic device.....	69

Figure 6.3 - Load components acting on the socket during stance phase: Initial Loading Response, Midstance, and Terminal Stance.....	70
Figure 6.4 - Three-dimensional models of the socket; the residual limb and the femur; and, finally, the results of the Boolean operation of union of residuum and bone.	71
Figure 6.5 - Socket and residual limb meshed.	71
Figure 6.6 - Complete assembled model with the fixed surface contoured in orange.	71
Figure 6.7 - Simulation results visualized in SMA (left) and Socket shape modification (right).....	72
Figure 6.8 - Donning and loading simulation: front, back and side views.	73
Figure 6.9 - Comparison of the pressure maps obtained with FE analysis between the preliminary socket model (first row) and the refined socket model (second row).	73
Figure 6.10 - Pressure distribution on residuum surface during loading step in three different stance phases.	74
Figure 7.1 - Novel Prosthesis System: Pliance-RLS system, RLS sensors with different standard shapes.....	79
Figure 7.2 - Zebra™ 3D System: Zebra sheet sensors and thermoformed sensors within the prosthetic socket.	80
Figure 7.3 - F-Socket Pressure System: scanning electronics (left), software (middle) and patented thin-film sensors (right).	80
Figure 7.4 - Socket made by CEMPLEX from different views.	81
Figure 7.5 - Example of trimmed sensor (left) and sensors positioning within the socket (middle and right).....	82
Figure 7.6 – Patient wearing the instrumented socket (left and middle) and patient with the prosthetic socket positioned on the trestle for the acquisition phase (right).	83
Figure 7.7 - Examples of the material behaviour at the sensor-interface according to the material stiffness: hard material (left) soft material (right).....	83
Figure 7.8 - Examples of calibration system and flat plane of Plexiglas.	84
Figure 7.9 - Examples of the reconstruction phase within the Skanect.	85
Figure 7.10 - Points cloud of the CEMPLEX socket (left) and the patient’s residual limb (right) before editing phase from different views.	86
Figure 7.11 - Three-dimensional models of the CEMPLEX socket and the residuum.....	86
Figure 7.12 - The meshed models of the socket (left), the residual limb from MRI (middle) and the residual limb acquired with Kinect (right).	87
Figure 7.13 - Complete assembled model with the fixed surface contoured in orange.	87
Figure 7.14 - Simulation steps of the numerical analysis from the initial position to the end of static load phase.	87

Figure 7.15 - Pressure map on the socket inner surface.....	88
Figure 7.16 - Pressure map after the loading phase using the residuum model acquired with Kinect.	89
Figure 7.17 - Pressure map after the loading phase using the residuum model reconstructed from MRI.....	89
Figure 7.18 - Pressure map obtained with FE analysis considering the designed socket.	90
Figure A.1 - Mind map of modular lower limb prosthesis components [3].....	104
Figure A.2 - Examples of transfemoral prosthesis socket: quadrilateral (left) and ischial-containment (right) [122]	105
Figure A.3 - Examples of Patellar Tendon Bearing (PTB) and Total Surface Bearing (TSB) [122].	105
Figure A.4 - Examples of transfemoral flexible sockets (left) and transtibial flexible sockets (right).....	106
Figure A.5 - Different typologies of liners by Össur.	107
Figure A.6 - Examples of monocentric and polycentric knee.....	107
Figure A.7 - Examples of prosthetic feet by Otto Bock: carbon foot, adjust foot, dynamic foot and SACH.	108
Figure A.8 - Examples of adapters: socket adapter, pylon clamps, double adapter, foot adapter.	109

List of Tables

Table 3.1 - Characteristics of 3D imaging techniques.	12
Table 3.2 - Some CAD/CAM prosthetic systems available on the market [3]	16
Table 3.3 - Source of geometric data.	18
Table 3.4 - FE models and solvers.	19
Table 3.5 - Material properties used in literature.	21
Table 3.6 - Constitutive parameters for residuum soft tissues.	22
Table 3.7 - Summary of studies involving interface pressure and shear force measurement. .	30
Table 3.8 - Pressure pain threshold and pain tolerance in different transtibial residuum regions [64].	31
Table 4.1 – Open-source finite element software specifications.	39
Table 4.2 - Mesh characteristics: seed value, node number and elements number.....	40
Table 4.3 – Material properties.	40
Table 4.4 - Mesh characteristics: size, node number and elements number.	43
Table 5.1 - Mesh characteristics and simulation times for transfemoral model according to seed values.....	53
Table 5.2 - Mechanical properties for linear characterization.	56
Table 5.3 - Second order coefficients of Mooney-Rivlin hyperelastic model used for the characterization of soft tissues.	56
Table 5.4 - Simulation time for the entire process according to material characterization.....	56
Table 5.5 - Pressure pain threshold and pain tolerance in different transtibial residuum regions [64].	60
Table 5.6 - Material properties.	62
Table 5.7 - Mesh characteristics: element type, seed value, deviation factor and minimum size factor.....	65
Table 6.1 - Numerical values of simulation parameters.....	70
Table 7.1 - Commercial pressure sensors and systems.	78
Table 7.2 - Numerical values of sensors calibration.	84
Table 7.3 - Numerical values of simulation parameters.....	86

Table B.1 - Workstation technical specifications..... 111

List of Abbreviations

CAE	<i>Computer Aided Engineering</i>
CAM	<i>Computer Aided Manufacturing</i>
CT	<i>Computed Tomography</i>
DHM	<i>Digital Human Modelling</i>
FE	<i>Finite Element</i>
FEA	<i>Finite Element Analysis</i>
ISNY	<i>Iceland-Swedish-New York</i>
KBE	<i>Knowledge-based engineering</i>
MAS	<i>Marlo Anatomical Socket</i>
MRI	<i>Magnetic Resonance Imaging</i>
PET	<i>Positron Emission Tomography</i>
PML	<i>Prosthesis Modelling Laboratory</i>
PTB	<i>Patellar Tendon Bearing</i>
PTB	<i>Patella Tendon Bearing</i>
PVL	<i>Prosthesis Virtual Laboratory</i>
RE	<i>Reverse Engineering</i>
SC	<i>Supracondylar Suspension</i>
SCSP	<i>Supracondylar Suprapatellar Suspension</i>
SMA	<i>Socket Modelling Assistant</i>
SPECT	<i>Single Photon Emission Computerized Tomography</i>
TF	<i>Transfemoral</i>
TSB	<i>Total Surface Bearing</i>
TT	<i>Transtibial</i>
VHM	<i>Virtual Human Modelling</i>
VTL	<i>Virtual Testing Laboratory</i>

1

Introduction

This thesis concerns the design of lower limb prosthetic devices both of above knee amputees, also called “transfemoral”, and below knee, called “transtibial”. The process and procedures of the prosthesis design, especially the socket, are crucial to improve the quality of the device, which has directly consequences on the quality of the amputee’s life.

In the following, the context of the research work is briefly introduced; then, the motivations and the background know-how are exposed; finally, an overview of thesis organization is described.

1.1 Context

The loss of a limb represents a very traumatic event in one’s life. Amputation has important economic costs and strong physiological effects due to the loss of functionality. Prosthetic devices represent the best solution to restore lost functions to individuals that have undergone an amputation after vascular diseases or accidents. They have a deeply interaction with human body and their functionality, comfort, and fit, depend on the way in which the device is interfaced with the residual limb.

The most common causes of lower-limb amputation are: peripheral vascular disease, diabetes, trauma, infection, tumours and limb deficiencies [1]. While not all causes of limb loss are preventable, the leading causes of amputation, complications from diabetes and peripheral artery disease, can often be prevented, and then reduced, through patient education, disease management and regular foot screening.

Unfortunately, amputations involve a lot of people around the world and they represent an important health care cost, both public and private. The following examples can identify the phenomenon size about lower limb amputations. In the United States in the year 2005, Ziegler-Graham et al. [2] observed 1.6 million persons living with the loss of a limb and they estimated that this number double by the year 2050 up to 3.6 million. Approximately, the 65% of the cases involve lower limb. In 2005 in Italy, Italian National Institute of Statistics assessed about 3 millions of amputated people, including 250000 of lower limb. According to Italian Federation of Orthopaedic Technicians every year there are 11000 new lower limb amputations, of which 1000 transtibial and 4000 transfemoral [3]. In China, approximately 600000 lower amputations are performed each year and below-knee amputations are dominant [4].

The stages from the amputation surgery to a residual lower limb stable condition are complex and long. The surgery is the first step of an amputation, where it is necessary to choose the best strategy to

maintain the remaining functional of the residual limb. This phase is crucial for the future of the amputees and doctors and surgeons should reconsider this phase as a new starting point for the patient's life and not as a failure of their previously therapies. During the post-surgical phase, the focus is on the prevention of infections and blood curdling. Once the residuum is stabilized, the swellings have been absorbed and the injures have healed, rehabilitative therapy takes pace and the amputees can retrieve the natural movements of their articulations. Then, the patient starts to wear a temporary prosthesis for a short period of time, increasing day by day the periods of use in order to adapt skin and soft tissues to the prosthetic socket. Just at the end of this healing process it is possible start to design the final prosthetic socket device.

Nowadays in lower limb amputation, both transfemoral and transtibial (see example in Figure 1.1), the prosthetic devices are modular, that is most of parts are standard (Figure 1.2) and they are selected from commercial catalogues in accordance with patient's characteristics. The only exception is the socket that acts as an interface between the prosthetic device and residuum and for this reason is custom-made on the basis of the residual limb morphology. The whole prosthesis functionality and comfort depend on the socket, making it the most critical component; the key issue is the shape definition in order to ensure the best comfort and fit. The socket shape has significant differences from the residuum silhouette: it is smaller and its shape allows distributing appropriately on specifics areas the contact pressure due to stresses. At present, socket design and manufacture are still performed almost in a manual way, starting from a positive chalk cast. The cast can be manufactured following a fully hand-made procedure or partially based on digital tools, such as CAD/CAM systems. Actually, the product quality deeply relies on the experience and manual skills of the orthopaedic technicians, causing a high rate of inappropriate prosthetic devices and increasing costs and times.

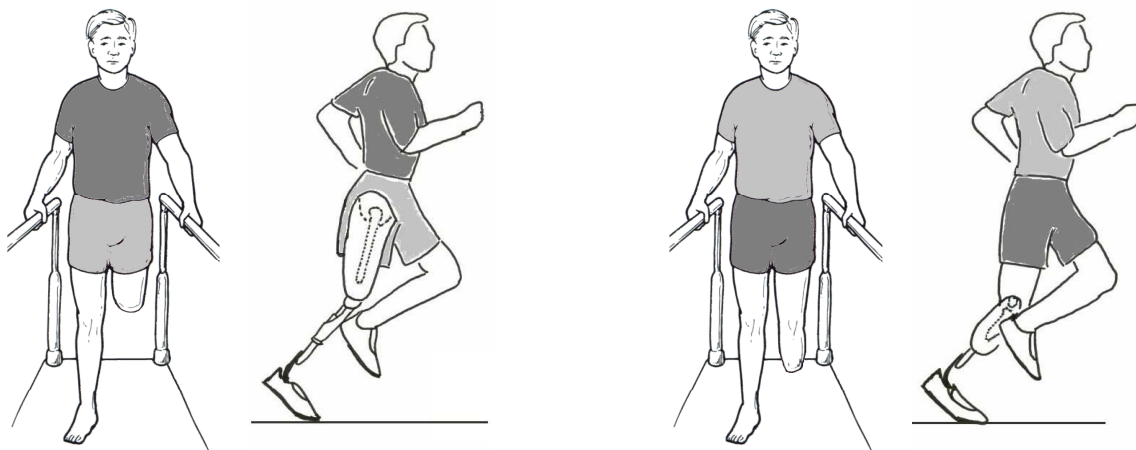


Figure 1.1 - Examples of lower limb amputees without and with prosthesis: transfemoral (left) and transtibial (right) [1].

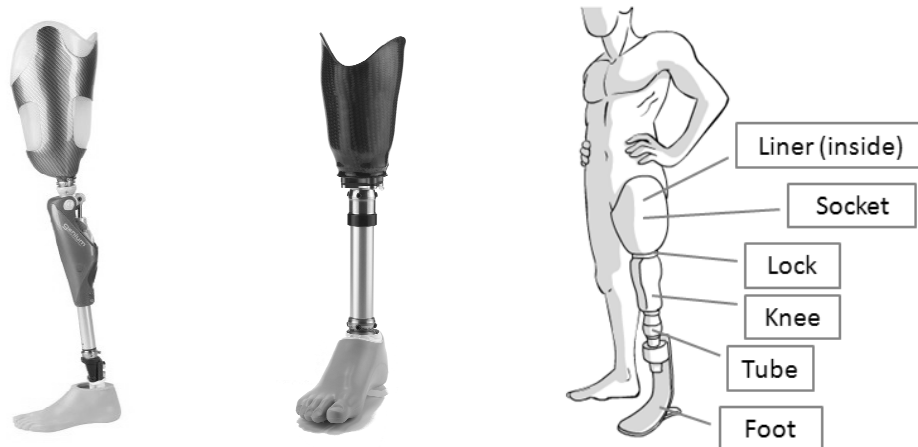


Figure 1.2 - Examples of modular transfemoral (left) and transtibial (middle) prosthetic device, and scheme of main components of modular transfemoral prosthesis (right).

1.2 Background and motivation

Systematically manufacturing of high quality prosthetic devices could permit to limit the physiological and psychological impact of amputations, and contain the considerable cost both for health care system and for amputees themselves. Actually, traditional process depends on orthopaedic technician's skills and knowledge, so it is far from being methodical. To overcome these limits, the introduction of new appropriate tools and design procedures becomes a key issue, as well as the identification of objective design parameters and best practice rules.

Computer-aided technologies can play a crucial role in improving design, analysis, and manufacture of products. Unfortunately, custom-fit products cannot be completely designed using methods and tools developed in industrial fields, but it is necessary to implement *ad hoc* design methodologies and to integrate tools coming from different research and application fields, such as reverse engineering, medical imaging, virtual prototyping, numerical simulation, and rapid prototyping.

In such a context, the V&K research group (University of Bergamo) is developing a 3D design platform for transtibial and transfemoral prosthesis automating as much as possible design steps. The platform is centred on 3D digital model of the amputee and it integrates *ad hoc* tools to acquire patient's data, CAD tools to model prosthesis components, human modelling system to perform gait analysis, and numerical analysis package to analyse the socket-residual limb interaction. The virtual design environment, called Prosthesis Virtual Laboratory, guides the prosthetic during each design task providing specific knowledge and rules (e.g., selection rules for standard parts or where and how to modify the socket shape), coherently with the traditional procedures.

The goal of this thesis has been to integrate within the new design platform an embedded and automated numerical simulation module that supports the design process during the assessment phase of the prosthetic socket. Numerical analysis allows to predict the interaction between socket and residual limb and to compute the pressures values at the socket-residuum interface. In fact, the challenge in socket design is to distribute pressure loads over desired regions of the residual limb according to its morphology, improving the socket fit.

The need to automate the simulation process increases dramatically the difficulty of the work but it is due to the fact that orthopaedic technicians have not the necessary competences to perform numerical

analysis. Furthermore, to reach significant results in virtual simulations it requires high level skills and expensive resources, both humans and technological, and in terms of time.

1.3 Thesis organisation

The contents of this thesis work are organized as follows.

Chapter 2 analyses the traditional design process commonly adopted for lower limbs amputees and identifies the limits of this procedure. Then, the new design approach to develop lower limb prosthetic devices is introduced and described.

Chapter 3 presents a critical analysis of the State of the Art of the techniques and the tools that allow implementing an integrated virtual environment to design the prosthetics socket. The main issues concern: (i) the numerical models to predict the socket-residuum interaction in lower limb prosthesis; (ii) the parameters commonly used to evaluate socket comfort and fit; (iii) the methods to get in digital model of anatomical districts. The role of this activity was fundamental to identify the basis for the implementation of the embedded simulation procedure.

Chapter 4 focuses the attention on the tools and methods adopted to develop the embedded simulation module. Modelling tools have been considered since they allow creating the geometric models for the FE analysis and the whole prosthesis model for the gait analysis. To identify the suitable FE solver able to analyse the residuum-socket interaction, some FE models has been implemented using both commercial and open source solvers. Digital Human Modelling system has been adopted in order to perform a gait simulation of the patient's avatar and get the forces applied to the socket.

Chapter 5 describes the FEA module architecture and its integration within the platform, concentrating the attention on the simulation task, the involved players and the definition of the simulation rules. By the use of a Python script, the FE model has been automated and integrated within the design platform.

Chapter 6 concerns the testing of the new design procedure and the verification of the key issues of the integration, such as the data exchange among the modules and the automatic execution of the FE analysis. According to the patient's data and the residual limb geometric model reconstructed from MRI images, the socket has been modelled and the standard parts are selected to create the whole prosthesis model. The socket evaluation has been performed by the simulation module considering both the patient's weight and data coming from the gait simulation performed by the DHM system.

Chapter 7 is dedicated to a preliminary assessment of the FE model. This task has been completed comparing the pressure values from numerical analysis with experimental data from the pressure transducer measurements. A real prosthetic socket, designed by a prosthetist, has been considered for the experimentation. This socket has been digitalized and the geometric model was used for the numerical simulations. The FE models considered two geometrical models of the residual limb, from MRI and from 3D scanning, in order to investigate how acquisition techniques influence the final results.

2

Lower Limb Prosthesis Design Framework

This chapter provides a brief overview of the traditional design process about lower limb prosthesis, and then a description of the new design platform. In particular, the research work focuses on above knee prosthesis (or transfemoral - TF) and below knee (or transtibial - TT). Hemi-pelvic amputation, toe amputation, partial foot amputation, and disarticulation were not considered.

2.1 Traditional design process

Nowadays, the prosthesis socket design and manufacturing are still carried out manually and deeply relies on the prosthetic's know-how (skill and experience). This subjective and static assessment causes a high rate of inappropriate prosthetic devices, increasing costs and times.

The socket is the interface between the residuum and the mechanical part of the prosthesis and requires a high level of customization to satisfy functional and comfort requirements. The socket therefore plays a fundamental interfacing role. In addition, the residual limb is subjected to continuous morphological changes and, when a significant variation occurs, a new socket has to be made. The design and manufacture of high quality sockets must fulfil the following requirements: accurate evaluation of the residuum, perfect close fitting, good response to forces and mechanical stress, safety, and no effect on blood circulation.

The traditional design process, schematized in Figure 2.1, can be divided in four main phases:

- **Patient evaluation.** During this phase, medical doctor and prosthetist evaluate both general physical and mental conditions of the patient (e.g., age, weight, height, disease, and psychological condition, such as self-esteem and adaptation capacity) and general condition of the residual limb (shape, skin, length, bones, etc.). In addition, the measurement of residual limb and knee are manually acquired in order to choose the proper components in the next phase.
- **Standard components evaluation.** Once the general evaluation is completed, the technician selects the better standard components according to the measures and characteristics recognized in the previous step. Standard parts are: knee (only for transfemoral amputees), pylon, foot, adapters, and cosmetic part.

- **Socket manufacture.** That is the crucial phase of the development process because the socket shape has to be modelled on the basis of the residuum morphology. The technician realizes first the plaster cast directly on the patient's residual limb, manipulating the plaster bandages in some specific areas, and then a positive plaster cast is obtained. The positive cast is modified, adding or removing material, in agreement with the residuum morphology and the characteristics of the patient acquired during first phase. In particular, during the modelling phase, the technicians identifies two different zones: (i) the "load areas", where the socket constricts the residuum creating pressure zones that sustain the body weight; (ii) the "off-load area", where the presence of bony structure or tendons could cause skin or other problems if pressed and so the socket is wider than load areas. Once the positive is completed, the technician manufactures a thermoformable socket directly on the cast.

After manufacturing the socket, the technician pre-assembles all the components; then, he/she verifies the socket accuracy and identifies all necessary modifications with the patient. During this phase, if the adjustments are of minor entity, the shape changes are applied directly on the socket, otherwise adding or removing material on the positive cast. In the latter case, another thermoformable socket is produced and a new pre-assembly operation is performed. The manufacturing process of the socket ends when the socket fits perfectly on the patient's residual limb.

- **Prosthesis assembly.** Once checked the definitive socket, last phase concerns the assembly of the prosthesis components. During this phase, the correct alignment of standard components, according to the patient's characteristics and way of walking, is fundamental because it significantly affects the effectiveness of the prosthesis device, and, consequently, on the comfort and its use. The alignment accuracy has order of magnitude less than a millimetre and it is checked during static postures or gait conditions. In practice, perform the right alignment means to find the correct lengths and the proper angles of the components. During the static optimization, the components are aligned through a vertical line in the frontal and lateral plane and considering the knee as reference point. Then, the reaction forces, due to the loads applied, are measured by a dynamometric platform and the joints are consequently regulated in order to optimize load line of the leg, referring to the patient's centre of mass. Any minor regulations are made inserting special orthotics within the prosthetic foot. Throughout the dynamic optimization, the technician analyses the patient's walking and the residuum movements in different gait conditions; applying further adjustments of the joints according to his/her observations and the patient perceptions.

Typically, the prosthesis set-up has to be made at least every 4÷6 months, because the device contains many moving mechanical components that require maintenance, cleaning, or replacement at some specific intervals and that have a directly affect the prosthetic function. Moreover, the set-up updates allow improving the fit of the prosthesis when volume or shape of the patient's residuum occur, particularly frequent during the first month of wearing a new prosthesis.

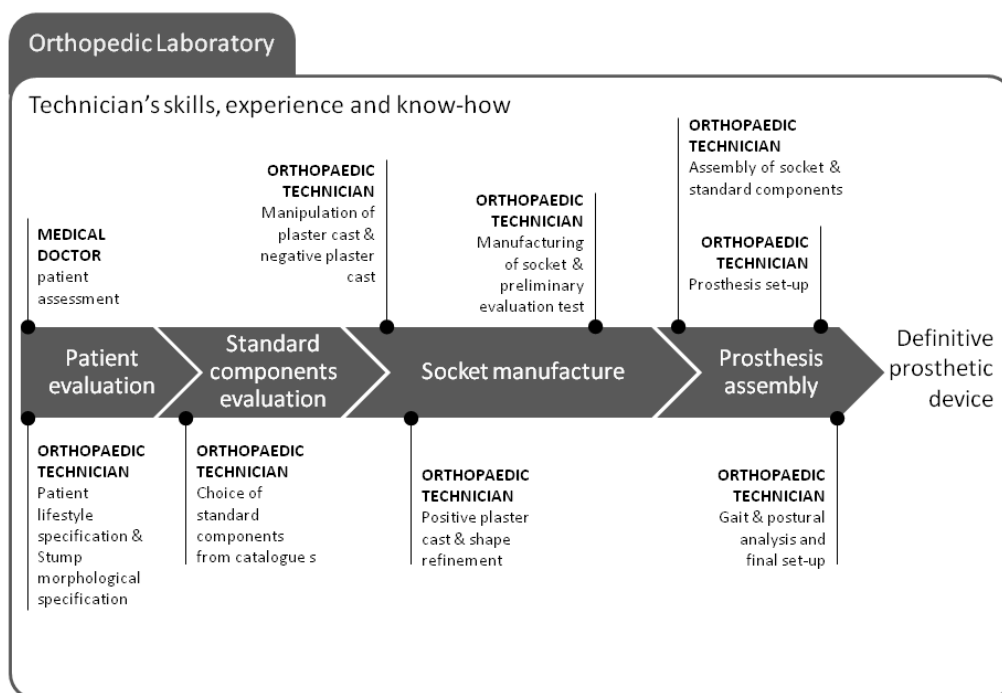


Figure 2.1 - Workflow of the traditional manufacturing of modular lower limb prosthesis.

2.2 A virtual approach for prosthesis design

The challenge in prosthetic devices is to manufacture an optimal socket shape, which distributes loads over desired regions of the residual limb, and to identify the correct standard components (such as liner, knee, pylon, foot, adapters, and cosmetic) in order to assemble a prosthetic device that satisfy the amputees' requirements. The analysis of the current prosthesis design for lower limb amputees suggests that the subjective and static assessment causes a high rate of inappropriate prosthetic devices, increasing costs and times. In addition, the commercial ICT tools, that partially digitalize the socket design process, do not provide support to the designer or numerical tools to evaluate the design quality.

Computer-aided tools and numerical simulation tools have reached a good level of maturity and could play an important role in orthopaedic field, especially if integrated with each other. These tools could support the prosthetic technicians in order to achieve in the prosthetic socket a higher quality, a more objective design and a faster manufacturing process. Actually, their diffusion is limited by investment costs for hardware and software equipment and the lack of human resources with high-level IT skills. Moreover, even if the human resources are available, time and resources necessary to define the right methodologies and to create the accurate models represent a meaningful limit.

In such a context, the V&K group of University of Bergamo is implementing a new design platform that integrates ad hoc tools to acquire patient's data, CAD tools to model prosthesis components, both standard and custom-fit, FEA package to deeply analyse the socket-residual limb interaction, and human modelling system to perform gait analysis. Specifically, the framework works both for transtibial and transfemoral prosthesis and it is centred on 3D digital model and characteristics of the amputee patient. The underlying idea of this approach is that the end-user should be guided step-by-step during the design process by system, which suggests rules and procedures to design and optimize products. Each activity within the system is supported in direct way by the management of specific domain knowledge. The knowledge has been acquired by handbook [5, 6], scientific literature,

commercial catalogues (i.e., Össur, Otto Bock) and a strong interaction with technical staff of a qualified orthopaedic laboratory. This has allowed identifying design rules and best practice standards of each process task.

The platform, called Prosthesis Virtual Laboratory (PVL) (Figure 2.2), provides the prosthetic technician a set of interactive tools to design, configure and test the prosthesis. It comprehends two main environments: (i) the Prosthesis Modelling Laboratory (PML) and (ii) the Virtual Testing Laboratory (VTL). The first permits to configure and generate the three dimensional model of the prosthesis, whereas the second allows the prosthetist to virtually set up the artificial leg and to simulate the patient's postures and movements, validating prosthesis functionality and configuration. The backbone of PVL is the digital patient's model, composed by a biomechanical model and a set of patient's data (such as physical and physiological characteristics, anthropometric measurements, and health conditions). PVL manages the entire design and testing process basing on the rules and knowledge of the experts that are implemented into the system.

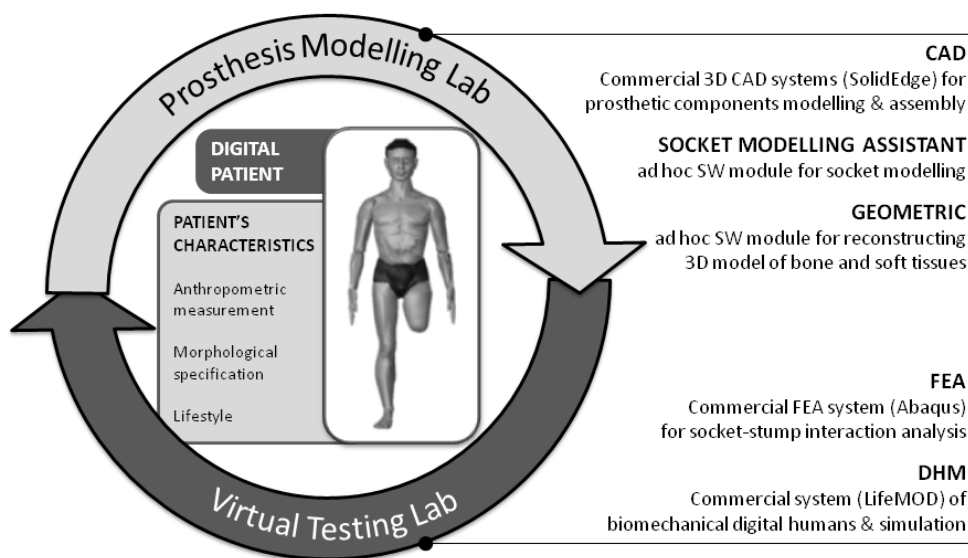


Figure 2.2 - Prosthesis design platform and the associated modules.

The Prosthesis Modelling Lab (PML) is the environment where the orthopaedic technician can design the whole prosthesis for both transtibial and transfemoral amputees. S/he directly creates the 3D socket model onto the residual limb digital model using a dedicated CAD tool. The system guides the prosthetic during each design task, coherently with the traditional procedures.

The Virtual Testing Lab (VTL) interacts with PML to assess the prosthesis design. It should permit to evaluate automatically or semi-automatically the socket shape thanks to the integration of numerical simulations tools, such as Finite Element Analysis. Moreover, by the use of Human Modelling systems, it allows to virtually set up the artificial leg and simulate patient's posture and walking, validating prosthesis functionality and configuration.

Through an iterative process between PML and VTL environments, the socket shape and the parts alignments of the assembly are optimized. The socket shape is modified and adjusted by prosthetic technician until the loads distribution on the residuum is consistent with the adopted parameters, removing undercuts and minimizing weight. The alignments between the assembled elements are modified according to the patient's way of walking in order to reach the better cadence during the walking.

The PML environment has been implemented during previous research activities [7, 8] and PhD thesis [3]; while the development of the Virtual Testing Laboratory is the specific purpose of this thesis work. In particular, I focused the attention on the development of the numerical analysis module for simulating the contact interaction between socket and residual limb, making it more automated as possible. Moreover, the numerical simulation has been integrated with the Digital Human Modelling system to reach the dynamic forces the act on the socket during the patient's walking.

Figure 2.3 describes the workflow and modules interaction of the virtual approach; while the following paragraphs describe the modules functionalities composing each environment.

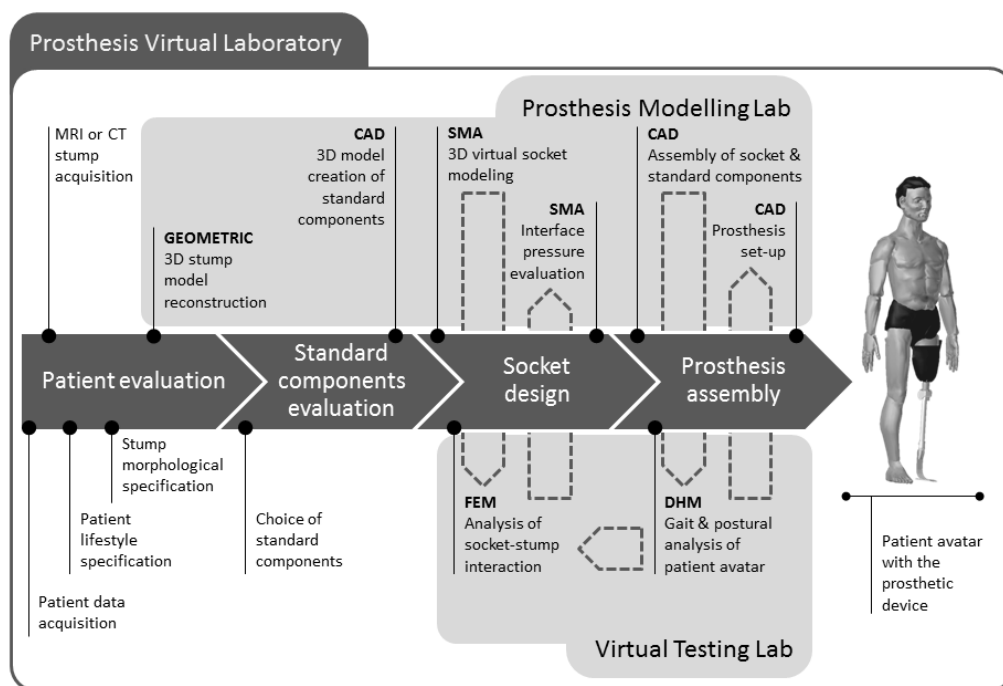


Figure 2.3 - Workflow and modules interaction of the new design platform for modular lower limb prosthesis.

2.2.1 Prosthesis Modelling Lab

The Prosthesis Modelling Laboratory integrates three main modules:

- The *Geometric* module, implemented ad hoc to reconstruct automatically 3D detailed model of residual limb, starting from the 2D images acquired with MRI. The 3D residuum models (bones and soft tissues) are generated in a neutral format (.IGES), which permits data exchange among the modules composing the design platform. The reconstruction procedure consists of three different phases: image pre-processing, voxel segmentation, 3D models generation [9].
- The *Socket Modelling Assistant (SMA)*, implemented ad hoc to model the socket directly around the digital residual limb, following rules and procedures, which replicate the activities performed in an orthopaedic laboratory. It embeds a set of design rules and procedures (e.g., where and how to modify the socket shape) that emulate the operations performed by the prosthetist during the traditional manufacturing process. The technician is guided step-by-step by the system that applies in automatic or semi-automatic way rules and modelling procedures. For example, SMA makes available a set of interactive virtual tools (e.g., Surface Tool or Sculpt Tool) that permit to manipulate the socket shape according to traditional procedures [8].

- The commercial *3D CAD system* (SolidEdge) selects standard components, configures and assembles all prosthesis components. It permits to generate the 3D parametric models of the standard parts according to patient's physical characteristics (such as weight and height) and then to compose the final assembly, considering both custom part and standard elements. The 3D model of the assembled prosthesis is crucial to virtually study the prosthesis set-up and patient's walking [3].

2.2.2 Virtual Testing Lab

The Virtual Testing Laboratory provides a second virtual environment where the orthopaedic technicians should test and validate the prosthesis device, created and configured using the PML. It incorporates two main modules:

- The *Digital Human Modelling system* (LifeMOD), that allows to realize a complete amputee's digital model (the patient's avatar) and simulate the patient's gait. The idea is get geometric and/or dynamic data to identify gait deviations and forces acting on the socket. The prosthesis set-up means finding the correct components alignments, analysing and assessing the gait cadence. Wrong configurations, in terms of interfacing angles and parts lengths, cause bigger asymmetry in walking.
- The *Finite Element Analysis solver* (Abaqus) to simulate and to analyse the interaction between the residuum soft tissues and the socket wall in order to achieve a socket shape that ensures better fit and comfort on the basis of residuum's morphology. Socket evaluation is made by analysing the interface pressure in critical region. Pressure values should not exceed the respective pain threshold in order to be tolerated for a certain time period. So, this tool allows predicting pressure distribution over residual limb surface considering different loads acting on the socket. The static load is equal to patient's weight, while the dynamic loads are acquired from virtual gait performed with LifeMOD.

3

State of the Art

Modern imaging techniques, computer-aided tools and numerical analysis can support the prosthetic technicians in order to achieve in the prosthetic socket a higher quality, a more objective design and a faster manufacturing process.

The chapter presents the analysis of the State of the Art related to the three main issues of this thesis: techniques to acquire the residual limb geometry, numerical models for finite element analysis, and evaluation parameters to assess the socket shape. The last issue has been fundamental to identify the procedure and the rules to implement the automatic numerical simulation model. This phase played a fundamental role since it constituted the basis for the implementation of the embedded module that automatically execute the simulation of the socket-residuum contact interaction without the manual intervention of the prosthetist. Moreover, this activity permitted to highlight that current finite element models are stand-alone and not integrated with prosthetic CAD or Digital Human Modelling (DHM) systems.

3.1 Patient's digital model

Detailed 3D models of the residual limb (skin, soft tissues and bones), socket and liner (when considered) are fundamental to run a numerical analysis, which allows predicting the interaction between prosthetic socket and residual the limb. The right geometries and correct alignment among parts have an influence on the quality of simulations and convergence of results [10].

Digital imaging and reverse engineering techniques allow obtaining the required digital models, taking into account the real morphologies of the residuum. These systems can be classified according to the capability to acquire internal and external parts, as Zheng et al. [11] did in 2001. They listed and analysed all the possible techniques to acquire both inner (water immersion, circumferential measurement, contacting methods, Moiré contourography, laser video scanning, silhouetting, hand-held digitizer and scanner) and outer geometries (x-ray and computed tomography, magnetic resonance imaging and ultrasound) of the residual limb, and, eventually, also the socket. However some technologies have become obsolete, others have been improved and new ones have been developed, speeding up the process and increasing the details.

In the following paragraphs, the solutions, found in literature, are reported and analysed. Digital imaging systems are mainly oriented to get the 3D virtual models of the residual limb, but they can be used also to reconstruct the inner socket shape. In some research works, the socket model has not been

shaped within a virtual environment, generally a CAD system, but it has been reconstructed starting from an existing one.

3.1.1 Residual limb model

Different techniques are available to acquire internal and external parts of anatomical districts. Table 3.1 summarizes some characteristics of the most diffused 3D imaging techniques available on market.

Table 3.1 - Characteristics of 3D imaging techniques.

Technique	Physical property adopted	Inner tissue detection	Bone structure detection	Harmful
Internal acquisition				
MRI	Magnetic field	Yes	Yes	No
CT	X-Ray	Yes	Yes	Yes
PET	γ -rays, Electron positron annihilation	Yes	Yes	Yes
SPECT	γ -rays	Yes	Yes	Yes
Ultrasound	Ultrasound	Yes	Yes	No
External acquisition				
Laser scanning	Triangulation of reflected light source	No	No	No
Structured light	Triangulation of reflected light patterns	No	No	No
Stereophotogrammetry	Photography at different angles	No	No	No

In the following a brief description of listed techniques is provided, subdivided according to the capability to acquire or not internal geometries.

Internal geometries

Biomedical imaging, or diagnostic imaging, includes all the medical systems used to create internal images of the human body, and main techniques for acquiring residual limb parts (bone, muscle, soft tissue and skin) incorporate Radiology, Magnetic Resonance Imaging, Nuclear medicine, and Ultrasound. These noninvasively methods generate cross-section images of the human body and it is possible to reconstruct and to visualize 3-dimensionally the inner organs and apparatus by the use of computers.

Computed Tomography

Computer tomography (CT) is a part of traditional radiology. It utilizes a wide beam of ionizing radiation, in the form of X-rays, in conjunction with a computer for image acquisition. The 3D model of the residuum, both soft and hard tissues, can be reconstructed starting from 2D images obtained transversely to the limb axis using CT [12]. CT obtains better results than traditional radiology with regard to diagnostic imaging of soft tissue, but using a quite high radiation dose for the patient. In literature it is documented that CT can reach a precision of 0.88 mm and an accuracy of 2.2 mm [13]. Compared to an axial CT, a helical CT offers faster scanning (less than a minute is needed to obtain a full scan for a multi-section CT [14] against the 8-10 minutes normally required [15]), a reduction of the motion artefact, continuous slice acquisition allowing image slice interpolation [16], as well as better images quality with a lower dose of X-rays [17]. In CT images, there is a correlation between the Hounsfield units and tissue density, and this allows a simpler automatic segmentation using thresholding and a sufficiently accurate 3-D geometry for numerical analysis [15].

Actually, CT is associated with other nuclear medical techniques that use gamma ray, in particular Single Photon Emission Computerized Tomography (SPECT) and Positron Emission Tomography

(PET). SPECT and PET images are reconstructed detecting the gamma rays emitted by a short-life radioisotope injected into the patient. This simultaneous acquisition ensures registration and image fusion of metabolic and spatial information [18] and allows to obtain advantages such as scan time reduction and improvement of longitudinal resolution [19]. PET images have higher signal-to-noise ratio and a better spatial resolution (~2mm) than SPECT images; however, PET systems are much more expensive [20].

Ionizing radiation (x-rays or γ -ray) have sufficient energy to ionize atoms and molecules within the body, causing serious and lasting biological damage. The adsorbed dose, measured per unit mass of body, is usually considered acceptable, but it strictly depends on the time of exposition [20]. Frequently expositions and extensive scanned areas lead to increment considerably the adsorbed dose, making this technique harmful and then unsuitable.

Magnetic Resonance Imaging

Magnetic Resonance Imaging (MRI) exploits a strong magnetic field to align hydrogen atoms in water molecules. The atoms alignment creates a measurable rotating magnetic field that changes according to the transmitter radiofrequency. The cross-section images can be reconstructed thanks to the successive changes in the radiofrequency field of the transmitter [18]. The contrast resolution of the images can be improved changing the nature and timing of the radiofrequency pulses. It depends on different factors: proton density of the tissues; the spin-lattice relaxation time or T1 (the rapidity of protons to come back to the original alignment) and the spin-spin relaxation time or T2 (the rapidity of destruction of tissue magnetization) of various tissues within the body; and, flow and diffusion effects [20].

Similar to CT, MRI requires the patient to adopt a horizontal position. This posture suffers the effect of gravitational forces on soft tissue distribution of the residuum in connection with the skeletal structure. Nowadays, alternative MRI scanner designs, such as upright systems, allow the patient to be acquired also in vertical position, avoiding the soft tissues fluttering. MRI images look similar to a CT image, but in MRI images bones are dark. MRI provides high-resolution images that show a clear difference between the tissues. However, it is expensive and requires a long scan time: for the whole residual limb, a compromise solution between details and scan time (less than 10 minutes) is obtained by using a slice thickness of 2 mm associated with 0.6 mm of in-plane resolution [21].

Because of the strong magnetic field created during an MRI, metal objects can move and provoke harms to the patient's tissues. Due to that, it should avoid wearing metal objects and particular attention has to be paid in patients that have metal fragments or chips into their body, due to previous operations/accidents. In prosthetic field, Torres-Moreno et al. [22] went into deep of the advantages and disadvantages of MRI for 3D models in finite element analysis. They obtained cross section images of residual limb inner structures, which can help the theoretical evaluation of soft tissue behaviour under load and prediction of the stress interface.

Ultrasound

Like the previous techniques, ultrasound imaging generates cross-section images of the human body, using high frequency sound waves. While scanning, the images tend to overlap each other so the quality of these has to be improved by piecing together different directions [23]. During the past years, commercial scanning systems have improved their accuracy. As reported in literature, the pixel resolution is increased from 3 to 0.5 mm, but 1 mm seems to be the right limit to reduce patient movements to a minimum [24].

The scan time is relatively high in landscape mode. For a typical system, image acquisition takes place every 10 degrees, vertical sections are given at intervals of 3-5 mm, the digitization time for each level is 12 seconds and the total scanning time is about 12-15 minutes, depending on the length of the

residuum [23, 25]. A vertical acquisition mode has been developed to improve the scanning speed [26]. For a 26 cm residuum, a vertical scan may take about 80 seconds and the skin surface acquires a resolution of about 2.5 degrees in the transverse direction and a resolution of about 28 points/cm in the longitudinal direction [26]. Each residuum movement during the scan may damage the image which has to be reconstructed later: the motion compensation methods are reported in the literature [27]. Douglas et al. [24], in their review on ultrasound imaging in lower limb prosthetics, noticed that the images generated with this technique do not allowed detection of muscle contours and has a low quality, if compared with MRI and CT.

External geometries

Besides diagnostic imaging to analyse internal human parts, there are techniques to acquire external parts. These techniques measure and acquire external surfaces of the human body, allowing precise and repeatable acquisitions with high accuracy, without direct contact with the human body and quite short acquisition times (few seconds). These systems, based on optical triangulation and time delay of the light signal, can rebuild an object by measuring the time required for a light spot to bounce back from the objects in the scene. When the information is directly derived from the illumination of the scene and from the reflection of the object, one speaks of passive methods, otherwise of active methods when a specific light source is used. Some examples of these are: stereo vision, photogrammetry, structured light and laser scanning [28]. The latter technique is the one mostly used by the CAD/CAM prosthetic systems available on the market to design the socket shape [29-31].

Laser scan

Laser scan bases on the active triangulation principle because it uses a light source the laser beam. A sensor captures the back scattered beams as single points or laser stripe, and, then, the scene is scanned and the object surfaces are reconstructed by means of simple geometric considerations. Laser scan systems are quite diffused method available thanks to their accuracy and relative insensitivity to illumination conditions and surface texture effects [28]. These systems are usually composed by more than one laser source, light sensors and a motion capture system. This because the reconstruction of the whole object requires more acquisitions from different angulations.

Structured light

Structured light is the process of projecting a planar pattern of non-coherent light (often grids or horizontal strips) onto an object and it is based on the active triangulation approach. According to the deformations of the light pattern striking the object surfaces, the system elaborates the surface information of the objects acquired by a camera and reconstructs the scene, calculating the distance of every point in the field of view. Structured light scanners scan contemporarily multiple points or the entire field of view. This makes this technology quite fast.

Stereophotogrammetry

Stereophotogrammetry system is based on the passive triangulation (no external light source are used) and it permits to capture and then reconstruct the scene just adopting at least two cameras. The key problem is the identification of common points with the image pairs and the quality of the shape extracted depend on the sharpness of the surface texture [28]. The acquired data have a low level of accuracy and the use of the method is limited to the static scene because to achieve the complete scene it is necessary to use a sequence of images from different point of views. On the other hand, the process is simple and low cost.

3.1.2 Prosthetic socket model and liner

The 3D socket model represents the second fundamental component necessary to perform a numerical analysis and it can be obtained in two ways.

The first method is to reconstruct the inner socket shape through the use of biomedical imaging techniques. For example, Sanders and Daly [55] and Faustini et al. [19] obtained the socket 3D model respectively from Magnetic Resonance Imaging and Computed Tomography.








In the second method, starting from the residuum surface of the patient previously acquired, the inner surface of the 3D socket model is obtained as an offset of the residual limb external surface and then it is modelled. The modelling phase is performed by commercial specific prosthetic software or by commercial CAD tools (e.g., Rhinoceros, 3-matic's, Solid Edge, or Solid Work). In the academic field, during the last two decades, Facchetti et al. [8] and Rogers et al. [32] implemented a specifically CAD software to design lower limb prostheses.

As mentioned before, there are commercial software packages generally aimed at manufacturing orthoses and socket prostheses [29-31, 33-36] that allow creating the 3D socket model onto the external shape of the residuum digital model (acquired by reverse engineering technique) using also standard libraries. The virtual model generated is subsequently used to produce positive models with CAM systems and CNC machines. The checked socket is thermoformed on the amended shape of the residual limb. To create the socket prototype as a 3D model, the majority of these devices consider only the external shape of the limb, using reverse engineering techniques such as laser scanning or a digital camera. This type of solution is convenient from the viewpoint of costs and times, but precludes the possibility of including bony structure in the digital model necessary to perform a finite element analysis.

Commercial CAD/CAM prosthesis systems permit to create the 3D model of the socket but do not provide any type of numerical analysis. Table 3.1 lists and compares some prosthetic CAD/CAM tools, taking into consideration the acquisition technique, the acquired data and the residuum-socket modelling for transtibial and transfemoral prostheses.

Another important element related to the prosthetic socket is the liner: a sock usually made of silicone worn on the residuum. It provides skin protection and reduces friction between the skin and socket, creating a more comfortable interface. It also allows obtaining a better distribution of the loads acting on the socket according to its material stiffness. The digital liner model can be obtained as an offset of the outer residuum surface or of the inner socket shape, or by combining different reverse engineering techniques. In fact, it is barely visible in computed tomography or magnetic resonance imaging [37].

Table 3.2 - Some CAD/CAM prosthetic systems available on the market [3]

Company	Specifications	
 BioSculptor [®] innovative solutions	Acquisition Technique	Laser scanner with 2 cameras, a miniature transmitter for the body and scan through-glass technology, or manual measurements
	Acquired Data	External shape of AK and BK residual limb
	Residuum-Socket Modelling	AK: starting from library template → external shape of the socket AK/BK: using oblique, transverse and circumferential measurements → automatic generation of the checked socket
 infinity CAD systems	Acquisition Technique	Laser scanner with 1 or 2 cameras
	Acquired Data	External shape of AK and BK residual limb
	Residuum-Socket Modelling	BK: proximal brim and shape utilities help to transform areas anywhere on the acquired shape → external shape of the socket AK: standard shape from library, tool to change volume, length, circumferences → model of the socket
 orten I' orthomesure	Acquisition Technique	Structured light projection, digital camera or manual measurements
	Acquired Data	External shape of AK and BK residual limb BK: on the geometry of the residual limb in defined areas you can apply compression or create build-up areas → external shape of the socket
	Residuum-Socket Modelling	AK: the desired shape is created using a protocol based on manual measurements → positive model of the socket
 proolutions the service company for prosthetic solutions	Acquisition Technique	Manual measurements
	Acquired Data	External shape of AK and BK residual limb
	Residuum-Socket Modelling	BK: calculates circumferences and volume of the residuum and allows modification of the acquired shape → positive model of the socket AK: measurements taken from the residual limb → model of the checked socket
 RODIN	Acquisition Technique	Laser scanner with 1 camera
	Acquired Data	External shape of AK and BK residual limb
	Residuum-Socket Modelling	AK/BK: starting from a shape library, adding check measurements, checking volume and circumferences → positive model of the socket
 Vorum Research Corporation	Acquisition Technique	Manual measurement and an appropriate proximal brim
	Acquired Data	External shape of AK and BK residual limb
	Residuum-Socket Modelling	AK/BK: fitting an appropriate brim to the patient and taking circumference measurement, supported by a variety of socket styles → model of the socket
 WillowWood	Acquisition Technique	Structured light scanner, electromagnetic tracing device or manual measurements
	Acquired Data	External shape of AK and BK residual limb
	Residuum-Socket Modelling	AK/BK: tool to change volume, length, circumferences → positive model of the socket

KEY: BK – Below Knee (transtibial) amputation; AK- Above Knee (transfemoral) amputation

3.2 Numerical models

Computer Aided Engineering (CAE) tools are becoming more and more important in different industrial contexts. They permit to reduce costs and development times; improve safety, comfort, and durability of the products; and decrease the number of physical prototypes. These tools can be employed in the development of lower limb prosthesis, in particular to investigate and to understand the interactions between the socket and the residuum.

Since the late 1980s, the numerical analysis has been used to study and simulate interaction between the soft residuum tissue and the hard socket wall. As reported in some state-of-the-art [11, 38-41], simulations were mainly performed using the Finite Element Method (FEM) because it allows getting the deformations and the stress states in parts or elements subjected to load. To analyse the socket-residuum interaction, general-purpose FE packages (e.g., Marc, Nastran, Ansys, LS-Dyna and Abaqus) have been used; *de facto*, open-source software or in-house codes have not been considered.

In recent years, some researchers have considered the use of artificial intelligence and soft computing together with standard computational and experimental techniques [42-45]. Neural networks are increasingly used to solve different engineering problems of artificial intelligence; in particular, in those contexts where the data may be partially incorrect, or where there is no analytical models able to deal with the problem. Although neural networks are able to partially overcome the problems of model characterization, they require a significant development work. Specifically, the network must be trained through the use of examples in which the inputs and output are known. The neural network behaves as black box, since it is no possible explain input-output association, and its success depends on creator's skills, since there are no theorems or models enabling optimize it. In prosthetic field, the method requires an initial phase to find the relationship between the surface strain and internal pressure by measuring the strain response on the socket due to the know pressure load. The socket strain is measured with a strain gauge transducer, one for each patch in which the socket surface is subdivided. Then, the artificial neural network is trained according to experimental results and determines an algorithm able to simulate socket-residuum interaction.

Another approach, that deserves mention because it is widely used for visualization purposes and real-time simulation, is particle-based modelling. This technique may be computationally convenient, but requires discretization of the continuum in terms of mass-spring elements, which is difficult to set according to mechanical properties of skin and soft tissue.

The choice of using FEM seems to be the right option to obtain better qualitative and quantitative results than particle-based modelling [46]. FE analyses can provide information on the stress/strain distribution at the residual limb and socket interface, allowing the prosthetists to make their decision to reach the optimal design. However, for complex models, an accurate solution is affected by [38, 47, 48]:

- Difficulties in arranging the three-dimensional geometry of the limb as well as the exact distribution of the soft tissue around the bone of the residuum;
- Non-linear behaviour of biological tissue that undergoes large deformation;
- Contact conditions between the socket and residuum;
- Evaluation of material mechanical properties;
- Values and direction of the loads within the model.

Over the past two decades, improvements to FE models have been made to overcome various model limits [11, 38-40, 49, 50]. For example, biological soft tissues are usually characterized using a linear material model; however, they have non-linear, viscoelastic, time-dependent and anisotropic behaviour. Some studies have been developed hyperelastic and viscoelastic material models [51, 52].

Other researches [10, 53, 54] introduced inertia, contact problems and friction, or tried to better identify discretization elements. Silver-Thorn et al. [49] summarized experimental measurement investigations, identifying associated limitations, and presented an overview of various computer models used to examine the residual limb interface. Zachariah and Sanders [50] investigated the mechanical behaviour at the interface between socket and residual limb in detail, considering the sensitivity of the FE models and comparing the FE estimates of interface stress against experimental data from various analysts.

From the analysis of the State of the Art some key issues have been identified to meet our goal. They are: residuum and socket geometries, mesh grid, material modelling and characterization, boundary conditions, and analysis steps. Even if, research works were mainly related to the transtibial amputees, I tried to generalize also to the transfemoral cases. In the following paragraphs these key issues are described.

3.2.1 Geometries and mesh

As previously stated, the necessary 3D models are the socket and the residual limb, in terms of soft tissues and bones, and liner when considered. Table 3.3 summarizes the acquisition techniques adopted by researchers to get the geometries. Computed Tomography and Magnetic Resonance Imaging are the most widely used technologies to acquire both bone structure and soft tissue; Laser Scan is mainly adopted to reconstruct the external shape of soft tissues; and, the socket model is achieved by the use of CAD system. Unfortunately, as Silver-Thorn et al. [49] assessed, not all reconstruction techniques for the internal geometry are completely safe, above all X-ray and tomography techniques which expose the patient to ionizing radiation.

Table 3.3 - Source of geometric data.

Authors	Bone structure	Soft tissues	Liner	Socket
Colombo et al. [55, 56]	CT/MRI	CT-MRI/LS	-	CAD
Lee and Zhang [57]	MRI	MRI	Offset Socket	CAD
Faustini et al. [47]	CT	CT	CT	CT
Frillici et al. [46]	MRI	LS	-	CAD
Goh et al. [48]	AS	LS	-	CAD
Jia et al. [10, 53]	MRI	MRI	Offset Socket (?)	CAD
Kistenberg et al. [58]	MRI	MRI	MRI	CAD
Kovacs et al. [15]	MRI	MRI	-	CAD
Lacroix and Ramirez Patino [59]	CT	LS	-	LS
Lee et al. [54]	MRI	MRI	SW	CAD
Lin et al. [37]	CT	CT	Offset Socket	CT
Portnoy et al. [60-62]	MRI	MRI	-	MRI
Ramirez and Vélez [63]	CT	LS	-	LS
Wu et al. [64]	CT	CT	Offset Residuum	?
Zhang and Roberts [65]	X-ray	Offset Socket	Offset Socket	CAD

LEGENDA: CT – Computed Tomography; LS – Laser Scan; MRI – Magnetic Resonance Imaging; X-ray – X Ray; CAD – dedicated CAD systems; ? – Not clearly specified.

Colombo et al. [55, 56] evaluated three different equipment and techniques (laser scanner, CT and MRI) to obtain the residual limb digital model and identify the most suitable for a detailed reconstruction. They described a mixed model obtained by integrating MRI and CT images for internal part and laser scanning data for the skin. The model reconstructed from laser-scanning allows

the acquisition of high quality morphological details (e.g., scars and abrasions). CT models have good quality for 3D bone reconstruction, while the external surface is not sufficiently adequate for skin representation. Finally, they used MRI data to generate detailed representations of internal soft tissues.

The use of different sources required the correct positioning of the different parts in the complete geometric model, because the alignment among parts have a significantly influence on the quality of simulations and convergence of results, as observed by Lin et al. [10]. To face this task, Colombo et al. [55, 56] used markers during the acquisition phases, but their positioning is not trivial issue because the acquisition of external and internal parts were done at different times.

The digital model of the liner can be obtained as an offset of the residuum model or by combining different RE techniques. The socket liner is involved in numerical simulation only in few cases that tray to understand its behaviour within the socket. From the study by Lin et al. [37], liner key role in the redistribution of stresses and interface pressures comes to light. It emerged how a less rigid liner increases the slippage distance between the residuum and socket, but without ensuring a reduction of peak stress. This rather complicated behaviour is due to the combined effects of non-uniformity of the socket shape and of the different sliding distances caused by the different stiffness of the liner.

Meshing step is very important since it influences the accuracy of the FE model. Subdivision topology can be carried out with different elements and methods (manually or automatically), according to the solver. Table 3.4 resumes the main characteristics of the FE models used (model size, nodes and elements and type), the mesh generation (automatic vs. manual) and the solver used to analyze socket-residuum interaction.

Table 3.4 - FE models and solvers.

Referents	Model size		Mesh generator	Solver
	Elements	Nodes		
Colombo et al. [55]	-	-	Automatic	LS-DYNA
Colombo et al. [66]	23460 – C3D4/S3R	5323	Automatic	Abaqus 6.9
Faustini et al. [47]	38855 - 10 T	66858	Automatic	I-deas
Goh et al. [48]	9477 - 10 T	14140	Automatic	ANSYS
Jia et al. [10, 53]	22301 - 4 T	6030	Automatic	Abaqus 6.3
Kistenberg et al. [67, 68]	549327 - C3D4	647565	Automatic	Abaqus
Lacroix and Ramírez Patiño [59]	300000÷480000 – T	-	Automatic	Abaqus 6.10.2
Lee and Zhang [69]	18794 T	-	Automatic	Abaqus 6.4
Lee at al. [54]	22301 - T	-	Automatic	Abaqus 6.3
Lin et al. [37]	11788 – T and B	-	Automatic	ANSYS 5.5
Portnoy et al. [70]	Up to 40855 SFM3D4, C3D10M, M3D3, M3D6	-	Manual	Abaqus 6.8
Ramirez and Vélez [63]	35000÷221000 – C3D4		Automatic	Abaqus 6.9.2
Silver-Thorn and Childress [71, 72]	1688 - 8 T	2221	Manual	MARC
Senders and Daly [73]	840 -8 B	795	Manual	ANSYS
Tonuk and Silver-Thorn [51, 52]*	328÷490 – 4 Q	383÷562	Manual	MARC
Torres-Moreno et al. [22]	26282 – T and E	1962	Automatic	Abaqus
Wu et al. [64]	12320 - 8 E	12368	Manual	ANSYS 5.6
Zachariah and Senders [74, 75]	1826 – 4 Q	2386	Manual	MARC
Zhang and Roberts [65]	8 B	-	Manual	Abaqus
Zhang et al. [76, 77]	2304 - C3D8/6	2421	Manual	Abaqus

*FE model only used to characterized soft tissues

KEY: Element type: T–Tetrahedron; Q–Quadrangle; E–Hexahedron; B–Brick

To simplify and reduce the computational time, Sander and Daly [73] used different types of mesh: 8-node isoparametric brick elements for soft tissues and quadrilateral liner shell elements for the socket and beam elements for the shank. No elements were generated for the bone and knee joint because they assumed these surfaces to have zero displacement. For the same purpose, Colombo et al. [66] used 4-node tetrahedral elements for soft tissues and bones and triangular shell elements for the socket. Ramos and Simoes [78] compared tetrahedral linear elements with hexahedral quadratic elements in their numerical analysis of femurs. They concluded that the former allows results closer to the theoretical ones to be obtained, while the latter seem to be more stable and less influenced by the degree of freedom of the mesh. Faustini et al. [47] subdivided the parts using an automated mesh generator through a 10-node parabolic tetrahedral with the Delaunay option.

Automated mesh seems to be obligatory to discretize complex shapes, such as bones, residuum and socket, in the correct way. The shape of the element is set according to the algorithm used. The geometric order and the mesh size determine the computational cost of the FE model: the more sophisticated the model is in terms of degrees of freedom, the longer the time needed to solve it is.

3.2.2 Material properties

To define a true distribution of stiffness in the FE model, each composing part (bones, soft tissues, the socket and sometimes the liner) must be characterized by different mechanical properties. In most cases, model properties were assumed to be linearly elastic, isotropic and homogeneous and they are described by specifying Young's module and Poisson's ratio. Table 3.5 reports material properties found in literature.

Colombo et al. [66], Lee and Zhang [69], Senders and Daly [73], Silver-Thorn and Childress [72] and Zachariah and Senders [74] considered bony structure as rigid or fixed, whereas Goh et al. [48], Jia et al. [10, 53], Lee et al. [54] and Wu et al. [64] assumed a fixed socket. For the bone structure, common value of Young's modulus E is 10000 or 15000 MPa with a Poisson's ratio ν equal to 0.3 [10, 37, 46, 48, 53-55, 63, 79]; for the socket, E is usually considered lower than 15000 MPa and ν from 0.3 to 0.39.

Young's modulus for soft tissue is around 0.2 MPa, while Poisson's ratio is 0.45 or 0.49. Only Zachariah and Senders [74] assumed E equal to 0.965 MPa. Lin et al. [37], Zhang et al. [76] and Zhang and Roberts [65] considered a more refined model for soft tissues, subdividing them into specific regions, such as patellar tendon and popliteal depression. To consider the stiffening of soft tissue during the load bearing condition [80], Faustini et al. [47], who used a linear model material, increased Young's soft tissues modulus by 25% where the pre-stresses were the highest (e.g. in the patella-tendon region [65]).

Table 3.5 - Material properties used in literature.

Referents	Bone structure		Soft tissue		Liner		Socket	
	E [MPa]	ν	E [MPa]	ν	E [MPa]	ν	E [MPa]	ν
Colombo et al. [55]	10000	0.3	0.2	0.49	-	-	15000	0.3
Colombo et al. [66]	Rigid		0.2	0.49	-	-	Rigid	
Faustini et al. [47]	15000	0.3	0.2-0.25	0.49	0.38	0.39	1600	0.39
Frillici et al. [46]	10000	0.3	0.2	0.49	-	-	15000	0.3
Goh et al. [48]	15500	0.33	0.105	0.499	-	-	Rigid	
Jia et al. [10, 53]	10000	0.3	0.2	0.49	0.38	0.39	Rigid	
Kovacs et al. [15]	73000	0.3	Non Linear		-	-	30000	0.3
Lee et al. [54]	10000	0.3	0.2	0.49	-	-	15000	0.3
Lee & Zhang [69]	Rigid		0.2	0.45	-	-	Fixed	
Portnoy et al. [61]	Rigid		Non Linear		-	-	1000	0.3
Ramirez and Vélez [63]	15000	0.3	0.2	0.475	-	-	1500	0.3
Senders & Daly [73]	Rigid		0.131	0.49			1800	0.39
Silver-Thorn & Childress [72]	Fixed		0.06	0.45	0.38	0.49	10000	0.3
Wu et al. [64]	15500	0.3	0.1÷0.4	0.49	1	0.49	Fixed	
Zachariah & Senders [74]	Rigid		0.965	0.45	-	-	1000	0.35

	Lin et al. [37]		Zhang et al. [76]		Zhang and Roberts [65]	
	E [MPa]	ν	E [MPa]	ν	E [MPa]	ν
Bone structure	15500	0.28	10000	0.49	15000	0.3
Soft tissue						
Patellar tendon	2.49	0.45	0.26	0.49	0.26	0.49
Popliteal depression	0.7	0.45	0.16	0.49	0.16	0.49
Anterolateral tibia	0.35	0.45	0.2	0.49	0.22	0.49
Anteromedial tibia	0.3	0.45	0.16	0.49	0.160	0.49
Others	0.06	0.45	0.2	0.49	-	-
Liner	0.4÷0.8	0.45	0.38	0.49	0.38	0.3
Socket	Rigid		Rigid		Rigid	

The mechanical properties of bones, liner and socket seem not to be a problem, whereas the problem of obtaining the soft tissue characteristics remains because these show non-homogeneity, anisotropy, viscoelasticity and time-dependent behaviour. Only in the last few years, non-linear elastic and also non-linear viscoelastic models have been used to obtain better approximation of soft tissue behaviour. Tonuk and Silver-Thorn [51, 52] tried to characterize the soft tissue of transtibial amputees with an appropriate set of non-linear viscoelastic material coefficients of James-Green-Simpson formulation, normally used to model elastomer material, such as rubber. They were able to simulate the compressive behaviour of 90% of the soft tissues using only the first two viscoelastic terms in the Prony series. They noted that these coefficients couldn't be readily extrapolated from those of other anatomical zones. Moreover, non-linear characterization adds complexity to the FE model and increases computational time.

The soft tissue characterization is the crucial point of material properties because it significantly influences FE results. The non-linear behaviour is accepted and desirable, but the lack of clear and specific information, combined with higher computational costs, limits their diffusion. Table 3.6 specified the constitutive parameters adopted in literature. Soft tissues were assumed to be homogeneous and isotropic with hyperelastic behaviour. The generalized Mooney–Rivlin solid strain energy function, both linear and quadratic polynomial functions, was adopted.

Table 3.6 - Constitutive parameters for residuum soft tissues.

Referents	Part	C ₁₀ [kPa]	C ₀₁ [kPa]	C ₂₀ [kPa]	C ₁₁ [kPa]	C ₀₂ [kPa]	D ₁ [MPa ⁻¹]	D ₂ [MPa ¹]
Kovacs et al. [15]	Muscle	30	10	-	-	-	1.667E ⁻⁵	-
	Fat	85.56	-58.41	39	-23.19	85.1	3.653	0
Lacroix and Ramírez Patiño [59]	Residuum	4.25	-	-	0	-	2.36	-
Portnoy et al. [70]	Fat	0.143	-	-	0	-	70.2	-
	Flaccid muscle	4.25	-	-	0	-	2.36	-
	Contracted muscle	8.075	-	-	0	-	1.243	-
	Skin	9.4	-	-	82	-	0	-
	Scar	148.9	-	-	0	-	0	-
Portnoy et al. [61]	Skin	9.4	-	-	82	-	0	-

The parameter values refer to the literature and/or are estimated by *in vivo* indentation tests. *In vivo* indentation tests estimate the mechanical properties of the patient’s soft tissues in different zones, allowing a more realistic stiffness distribution of the soft tissues. More specifically, the indentation test measures the surface lowering of the residual limb due to the indentation pressure. The load-displacement curve is recorded and used to set the unknown parameters defining the characteristics of the material. Figure 3.1 shows the indentation tool and some analysis steps developed by Frillicci et al. [46].

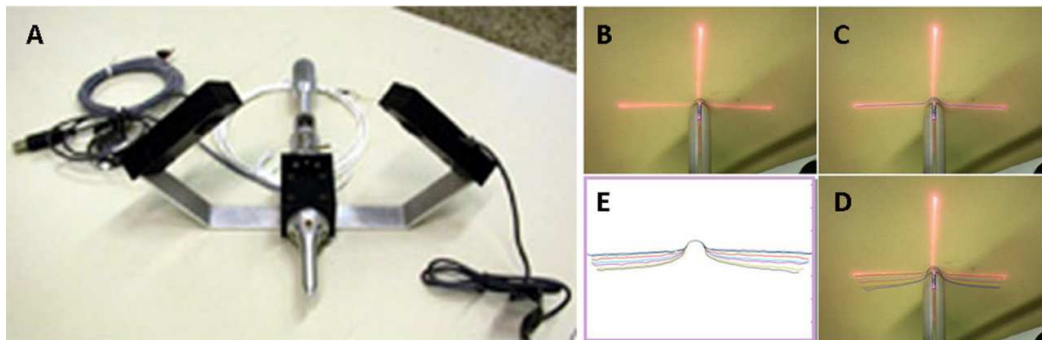


Figure 3.1 - (A) portable indentation device, (B-D) images of various indentation steps, (E) deformed shapes [46].

Starting from the Hayes et al. study (1972), Zhang et al. [57] investigated the influence of friction on calculation of the effective Young’s modulus of soft tissues using indentation test data. They found that friction becomes considerable when the Poisson’s ratio and the ratio of indenter radius and tissue thickness assume large values. The stress-strain curves obtained from tests on organic samples are non-linear. The stiffness increases as the penetration depth increases. In order to determine the effective elastic modulus, it is necessary to remove non-linearity due to the geometry. Young’s modulus E can be calculated as follows:

$$E = \frac{p(1 - \nu^2)}{2 a w_0 k(a/h, \nu)} \quad (3.1)$$

Where:

- p is the indentation strength;
- w₀ is the indentation depth;
- a is the indenter radius;
- h is the thickness of the measured tissue;
- ν is Poisson’s ratio (ranging from 0.4 to 0.499 in order to ensure convergence);

- k is a scaling factor that depends on the geometry and material (values of k factors are tabulated and have been obtained for different values of the ratios a/h and v).

Choi and Zheng [81] and Lu and Zheng [82] analysed the finite deformation effect of indentation using a finite element model, according to different indenter diameters and different deformation ratios. Delalleau et al. [83], combining experimental results with a numerical FE model, proposed a new method to derive the mechanical linear elastic properties of soft tissues from the indentation test. In the similar mixed method, Avril et al. [84] characterized the soft tissue as compressible and hyperelastic, using a simple neo-Hookean strain energy function, with discrepancies of more than 35% from one area to another. Hendriks et al. [85] developed a numerical-experimental method to describe the non-linear mechanical behaviour of human dermis with Mooney characterization and achieving also a first rough value for fat tissue.

3.2.3 Interaction

Interaction between the residual limb and the prosthetic socket can be modelled as a contact problem at different levels of complexity, either considering friction or not.

Contact problem

To simulate the interaction it is necessary to consider the contact between the socket and residual limb surface. This makes the problem nonlinear, complicating it and increasing the computational cost. The solution of a contact problem starts with the identification of points on the interacting boundary surfaces and then the insertion of appropriate conditions to avoid interpenetrations [86].

Penalty method and the Lagrange multiplier method are the two main techniques for describing contact. Penalty method is the simpler technique to pair the boundary points of contact surfaces and uses gap elements. In practice, a line element links two nodes at the opposite points on two surfaces, and, by knowing the initial distance between them, subsequent behaviour can be checked so that, if contact is detected, the element possesses an artificially high stiffness. The concept is point-to-point contact pair and it can be applied to structures of any dimensionality. Penalty method with simple line elements can be considered valid for linear elements, for small sliding and for small deformation cases in terms of FEM formulation, and require conforming FE meshes [87].

An alternative approach is the use of Lagrange multiplier algorithms, which allow nodes to slide along the boundary edge/surface for a distance of several elements. With this technique, the degrees of freedom are linked just when the contact occurs; when there is no contact, the degrees of freedom are independent of one another. So, the main issue to solve consists in deciding when contact occurs. The method is suitable for large displacement. It considers both normal and shear forces to evaluate friction and allows the prediction accuracy of surface contact geometry, also when the distances between the two surfaces are considerable, without degrading the precision [87].

Contact problems can be described over a finite region or using a set of discrete points. To model different contact problems, commercial FE packages have implemented different contact elements and algorithms. Some are targeted to particular cases, such as gap contact elements, slide line contact elements, rigid surface contact elements or tube-to-tube contact elements.

The surface-to-surface contact elements perform better than the point-to-point contact pairs in simulating sliding behaviour. Zhang et al. [38] and Wu et al. [64] assert that the infinitesimal sliding formulation allows computation time to be reduced because it does not require the contact surface between slave nodes and master surface to be monitored, whilst Jia et al. [10] considered that small relative motion is less computationally expensive.

Zachariah and Sanders [74] compared an automated contact interface model with a gap element model, and evaluated the sensitivity of automated contact to the interfacial friction coefficient. They found that gap elements distort the interface stress distributions under a large slip, while automated contact methods are useful when the residuum position in the socket is not known a priori, where loads cause a large slip and design significance of local geometric features is high.

Using the same computational model of Zachariah and Sanders, Lee et al. [54] considered the prosthetic socket and residual limb as two deformable bodies in contact with different shapes and, by introducing socket donning into the socket, implemented a pre-stress simulation.

Some research groups [10, 54, 66, 74] used a contact method to simulate the interaction that automatically detects any overlap among interface nodes and imposes a non-penetration constraint condition. In particular, Lee et al. [54] considered the socket inner surface as master and the residuum surface as slave, imposing the master surface as fixed, and analysed bones and soft tissues as a single body with different mechanical properties. When the slave surface was in contact with the master one, the slave nodes were automatically forced not to penetrate into their tangent planes on the master surface. Jia et al. [10] used an automated surface-to-surface hard contact interaction with a friction penalty formulation, where the contact pressure only occurs when the clearance between the surfaces is zero.

Wu et al. [64] used a further model for comparing the Kondylen-Bettung Münster socket and the Total Surface Bearing socket. The surface-to-surface contact element was used to simulate the sliding behaviour at the residuum-socket interface, which provided a better performance than the traditional point-to-point contact pairs.

Frillici et al. [46] adopted an explicit FE code that allows adequate management of the simulation problems characterized by large deformations and difficult contact conditions. At computational level it is more efficient and faster than the implicit model. The choice of an explicit solver allows the use of models that do not require definition of the contact surfaces. In fact, this strategy is able to deal with problems where surfaces are unknown a priori, for example, the donning simulation phase.

Friction/slip conditions

In this case, friction means considering the friction coefficient between the skin and different materials. Friction/slip conditions permit to assess the shear stress and slipping at the socket-residuum interface and to estimate the shear stress contribution during load transfer.

In order to limit the computational cost, initial models consider the residuum fully connected to the socket as a single body, but with different mechanical properties [71]. This reduces model difficulty and convergence problems but, preventing any slippage at the interface, the plane stress developed on the limb surface was not quantified.

The next step was to consider the residuum and the socket as two separate bodies with the same surface shape. In this case Zachariah and Sanders [74] used a friction coefficient of 0.675. The need to consider the friction at the socket-residuum interface in the FE model was emphasized by Zhang et al. [76, 77], since it is a very sensitive parameter for determining interface pressures, shear stresses and slip. Both papers show that friction acts in supporting the body weight during walking and prevents slippage during direction changes. They noted that the growth of the coefficient of friction (COF) is directly proportional to the shear stresses and inversely proportion to the pressure and the slip. A frictionless model ignores shear stress and overstates the maximum pressure by about 100%, while a model without sliding underestimates the maximum pressure by almost 50%. Finally, they discovered how tissue damage depends on shear and normal stress values:

$$\sigma_c = \sqrt{\sigma^2 + \tau^2} \quad (3.2)$$

Where:

- σ_c is the critical stress;
- σ is the normal stress;
- τ is the shear stress.

The magnitude of COF depends on the skin condition: it is reduced if the skin is dry, greasy or very wet, and increases when it is moist. The dynamic COF is not significantly influenced by age or gender but varies considerably in the different anatomical body regions [77]. Furthermore, an appropriate choice of the friction coefficient, and thus material, can balance the stress due to the load and prevent tissue damage, such as bubbles or heat production [77].

To simulate the friction/slip condition between the liner and skin, Zhang and Roberts [65] used interface elements to connect them. However, this led to a poor match between the clinical data collected and simulations as well as underestimation of the pressures.

Lee et al. [54] and Colombo et al. [66] considered different friction coefficients in relation to the simulation phase. During the donning simulation, the friction phenomenon was neglected and so the shear stress was assumed to be zero, because the residuum tended to slide. During the loading phase, they assumed that the static and kinetic COF were the same and slippage was permitted when the shear stress exceeded the critical shear stress:

$$\tau > \tau_c = \mu P \quad (3.3)$$

Where:

- τ is the shear stress;
- τ_c is the critical shear stress;
- P is the normal stress value;
- μ is the COF equal to 0.5.

Zhang and Mak [88] investigated five materials (aluminium, nylon, silicone, cotton sock and Pelite) and found an average COF equal to 0.46 ± 0.15 ; nylon had the lowest (0.37 ± 0.09) while silicone had the highest (0.61 ± 0.21). Lacroix and Ramírez Patiño [59] consider a friction coefficient equal to 0.415, while Portnoy et al. [60-62] used a value of 0.7. Ramirez and Vélez [63] considered a friction coefficient equal to 0.415 to describe socket-residuum contact and equal to 0.3 for bone-residuum interaction.

The literature shows that the friction coefficient depends on the socket material and on skin conditions. Furthermore, it is necessary to consider the friction between the residuum and socket in order not to overestimate the pressure at the interface.

3.2.4 Boundary conditions and analysis steps

The FE model needs to specify and numerically quantify the location of the external forces acting on the structure. The load can be expressed in terms of strength and/or movement. The load is static when it only takes into account the body weight. On the other hand, if load fluctuates over time, as happens during walking, they can be evaluated quasi-dynamic when inertia forces are considered and quasi-static otherwise.

Generally, the load is applied as a concentrated force/displacement in a single node: at the knee joint centre of the bone structure or at the distal end of the socket, if the bone structure is fixed. Load magnitude is estimated according to body weight or through experimental measurements that require a survey of ground reaction forces and joint angles. To identify the magnitude of loads (forces and

moments to be applied in the knee joint), Jia et al. [53] wrote rotational and translational dynamic equations along three axes, assuming that there was no relative movement between residuum and socket during walking and only considering inertia effects in the sagittal plane (Figure 3.2).

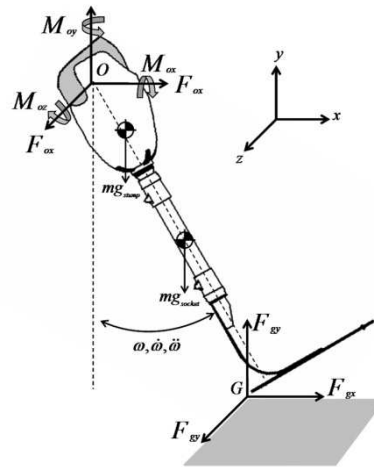


Figure 3.2 - 3D model to compute load magnitude at the knee joint [53].

A subsequent research, provided by Jia et al. [10], showed how the load location has significant effects on the interface pressure. In particular, the knee is not a simple revolute joint and the contact point between femur and tibia changes and depends on the leg posture during walking. In addition, they emphasized the substantial difference between the mean pressure and pressure peaks, which are present when inertia is considered.

The older models started the simulation with the prosthetic socket already donned because the socket shape was supposed the same of the residuum and, for this reason, load application was done in a single step. Sanders et al. [73] and Silver-Thorn and Childress [71, 72] applied loads and moments at the top of the socket and did not consider friction at the interface.

Zhang et al. [65, 76] used a socket whose inner surface did not coincide with the external residuum surface. The analysis was divided into two steps, reflecting the two different phases of soft tissue deformation. When the first step was completed, the pre-stress status on the residuum surface was due to the differences between the limb and the rectified socket shape. It was achieved by applying radial displacements to nodes on the external surface of the liner resulting from donning the socket. Keeping the pre-stresses, in the second analysis step the static forces were introduced on the proximal end of the bone in order to obtain the stresses. This framework, that consider two analysis steps, was used in successive simulations by other researchers: Jia et al. [10, 53], Lee et al. [54], Lee and Zhang [69], Frillici et al. [46] and Colombo et al. [66] (Figure 3.3).

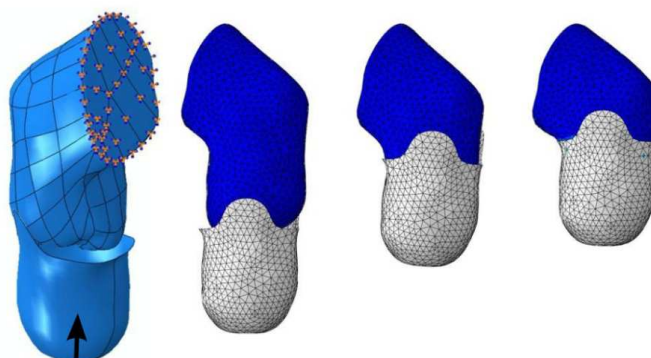


Figure 3.3 - Boundary conditions applied to an FE model (fixed region and load direction) and frames sequence of the donning simulation.

In the first step, the donning simulation was achieved by applying an axial load of 50N at the knee joint centre (Lee et al. [54]), or a load equal to half weight of the patient to the residuum (Frillici et al. [46]) or a displacement of the residual limb surface where overlaps occur with the inner socket surface [10, 53, 59, 63, 66]. To reduce the computation costs, Kovacs et al. [15] considered a thermal strain that widens the socket and, in a second time after the latter is moved over the residuum, forces it to its original shape.

In the second phase, keeping the calculated pre-stress and deformations, the loads are applied as concentrated forces on a single node; specifically, on the centre of the knee joint [53, 54], on the proximal end of the tibia [10], on the prosthetic socket [46, 59, 63] or in the vertical direction on the femur [69]. To simulate the load condition, [66, 69] imposed a force equal to the subject's weight, while Ramirez and Vélez [63] equal to half of the weight. Jia et al. [10] applied both constant concentrated force and five cases of gait cycle. Lee et al. [54] used forces and moments to simulate conditions at foot flat, mid-stance and heel off during walking, and assuming that the knee joint angle did not change at different loading cases. Frillici et al. [46] and Jia et al. [53] analysed the gait load cycle.

In other papers the authors considered the inner socket surface and external residuum surface with a different shape, but without specifying whether they considered one single step analysis or more. Goh et al. [48] replicated loading conditions at 10%, 25% and 50% of the gait cycle on the proximal end of the tibia. Wu et al. [64] simulated a static stand with half and full body weight, assigning a downward displacement of the bone until to the sum of the reactions reached a datum value. Lin et al. [37] did the same, but only considering the full body weight. Faustini et al. [47] applied quasi-static forces and moments, derived from experimental measures, to simulate some phases of the gait cycle. Furthermore, to account for the pre-stresses in the socket and stiffening of the soft tissues that occur during load bearing conditions, Young's modulus in the patellar-tendon region was increased by 25%.

Constraints are usually applied to the socket edge but, during testing, different schemes were adopted according to related simplification of the model [38]. Sanders et al. [73] assumed the bone and knee joint to have zero displacement surfaces. Zachariah and Sanders [74] presumed the tibia and fibula to be rigid. Silver-Thorn and Childress fixed bones as a single part [72] or as an internal boundary [71]. Zhang et al. [65, 76] and Goh et al. [48] assumed the socket to be rigid. Wu et al. [64] and Lee et al. [54] considered the socket or the outer liner surface, which has the same inner socket shape, as fixed. In addition, Lee and Zhang [69] considered the bones as rigid. Jia et al. [10, 53] modified the boundary conditions according to the analysis steps, simplifying the model. In the first step, the bones and the outer surface of the liner were forced as fixed elements. After the donning simulation, only the outer

surface of the liner was kept fixed, assuming that the hard socket would offer a rigid support, while the bones were free to move. External forces and moments were applied at the knee joint.

According to Zhang et al. [89], the geometries of the FE model, or rather the directions of external forces and moments, largely determine the results of the analysis: the change in residuum posture affects the accuracy of the pressure. They found out how an incorrect leg alignment, which differs by $\pm 8^\circ$, produced a change in peaks of the longitudinal shear stress in the range of $8\div 11.5\%$. This highlights the importance of having a CAD model with real and consistent alignment.

Seelen et al. [90] evaluated the effects of anteroposterior alignment of the prosthesis on pressure distribution, in both static and dynamic conditions. They found that, during gait, a wrong ankle joint alignment raises the loads in sub-patellar area and decreases those ones in tibial end region. They concluded that pressure interface obtained during stance are not predictive as that during gait; and, a better pressure distribution can be obtained by varying ankle alignment instead of reshaping the socket.

The boundary conditions, such as the definition of load regions/points or fixed nodes, allow extensive customization and usually depend on the type of analysis (e.g. static or dynamic, implicit or explicit) and the software used. However, to achieve greater convergence of the results, a simulation model has to replicate the real geometries and correct alignment, consider the prosthesis inertia and the residuum deformation undergone during the socket fitting.

3.3 Evaluation parameters

The main purpose of the prosthetic socket is to distribute loads over desired regions of the residual limb acting on the volume and shape differences between residuum and socket. Through an iterative process of adjustments, the socket shape is usually modified and optimized by the prosthetist to eliminate undercuts, minimize weight and, especially, distribute loads in the correct way. The pressure values at the socket-residuum interface is the parameter commonly used to evaluate the socket shape, and it should not exceed the pain threshold in order to be tolerated for a certain time period.

Critical areas, that are both load and off-load regions, have been identified from the literature (transfemoral case) and from the analysis of current development process (transtibial case). Figure 3.4 portrays the critical zones for transtibial case, while Figure 3.5 shows those for transfemoral case.

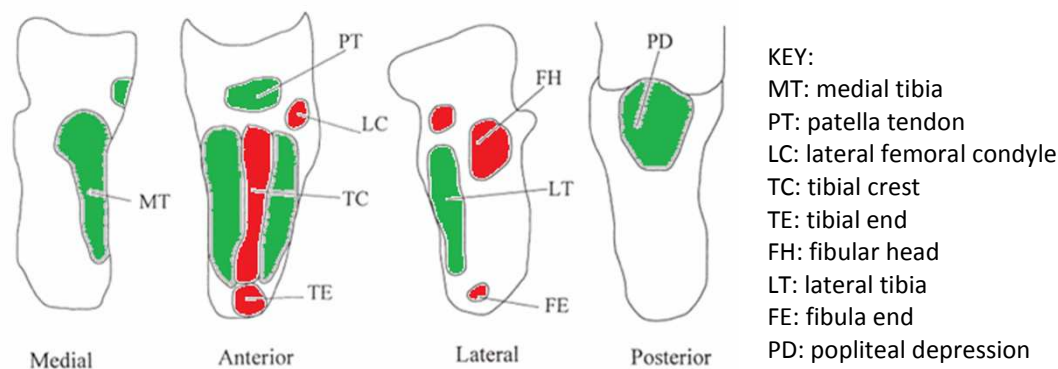


Figure 3.4 – Critical areas of transtibial residual limb (in green the load areas and red the off-load areas) [65].

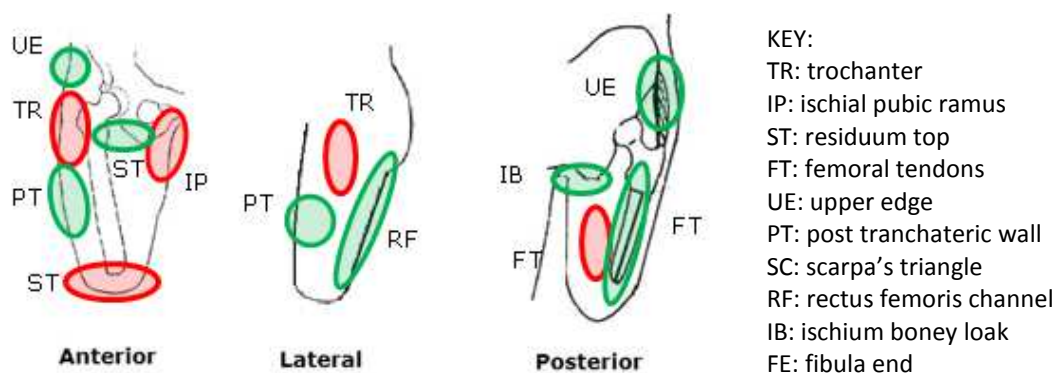


Figure 3.5 – Critical areas of transfemoral residual limb (in green the load areas and red the off-load areas).

Surface pressure transducers or force transducers are used to obtain pressure distribution over residual limb. First generation sensors only allowed pressure to be detected in a single point and, because of their size, they had to be installed outside the socket, forcing manufacture of an additional socket. Current sensors (second generation) have large sensitive areas and enable mapping of almost the entire interface surface [91-94]. Thanks to their thickness of less than 1 mm, they can be placed on the socket inner surface without significantly disturbing the interaction contact between the socket and residuum and avoiding the need to construct a further socket.

Pressures survey at the socket-residuum interface permits to evaluate the socket functionality; better understand this complex contact phenomena, examining the distribution of pressure during various phases of gait; develop more comfortable and fitting typologies of sockets. The use of pressure transducers consent to identify the values of pressure thresholds and pressure tolerances to avoid skin disease complications (e.g., pressure ulcers, blister, cysts, oedema, skin irritation and dermatitis). Moreover, investigating the real pressure distribution permits a preliminary evaluation of the numerical simulation results and enhanced implementation of a reliable numerical model.

Table 3.7 summarized the sensors technology and what areas were measured. Also in this case, literature is mainly focused on the below-knee amputation, just a few on below-knee ones.

Table 3.7 - Summary of studies involving interface pressure and shear force measurement.

Referents	Sensor Mounting	Technology	Measurement
Abu Osman et al. [95]	External	- Patellar tendon transducer; - Normal pressure/shear stress transducers (BESTs); - Entran ELFM-B1-5L load cell - Electro hydraulic pressure sensor.	Point on Anterior, posterior, medial and lateral walls
Ali et al. [96]	Internal	Tekscan F-Scan socket transducers	Map
Amali et al. [42]	External	Strain gauges	16 socket regions
Convery and Buis [97, 98]	Internal	Tekscan transducers 350 sensor cells sampling at 150 Hz	Anterior, posterior, medial and lateral walls
Dumbleton et al. [99]	Internal	Tekscan F-Scan socket transducers	Map
Dou et al. [100]	Internal	Pliance pressure distribution measuring system (Germany-Novel Electronics, Germany)	Point: PT, LT, MT, KP, PD
Goh et al. [48, 101, 102]	External	Pressure transducer assembly with Entran ELFM-B1-5L load cell (Entran International, USA)	16 pressure measurements
Krouskop et al. [103]	Internal	Pneumatic pressure transducer array	
Polliack et al. [104]	Internal	a. Rincoe SFS (force sensing Resistor embedded onto a polyvinilidyne Fluoride strip) b. F-socket systems	a. 6 strips each comprised of 10 sensors b. 96 individual sensors (16x6)
Portnoy et al. [61]	Internal	Tactilus, version 3.1.12, Sensor products co., NJ, USA Tekscan flexi force	Map & point
Rogers et al. [105]	Internal TT socket	Tekscan F-Scan Mobile system, Resistive ink transducers	Map (distal tibia and fibula head)
Sanders et al. [106]	External	Polycarbonate transducer	13 point
Sanders and Daly [73]	External	Normal and shear stresses transducer custom designed by the investigators	Point: LT, MP, PSD, ALD, PD
Seelen et al. [90]		IEE, FSR-649 linear array sensors, (International Electronics & Engineering SARL, Luxembourg)	6 sensor strips
Sengeh and Herr [107]	Internal	Tekscan F-Scan socket transducers	Map
Sewel et al. [45]	External	Electrical resistance strain gauges (ERSGs)	
Zhang et al. [77]	Internal	Tekscan transducers	Map
Zhang et al. [89]	External	The sampling frequency was set to 200 Hz during walking and 20 Hz	Point: PD, MT, LT, PT, KP, MG, LG, MS, LS
Zhang and Roberts [65]	External	Triaxial force transducers, developed by Williams et al.	Point: PD, MT, LT, KP, MG, LG, MD

KEY: MT: medial tibia, PT: patella tendon, LC: lateral femoral condyle, TC: tibial crest, TE: tibial end, FH: fibular head, LT: lateral tibia, FE: fibula end, PD: popliteal depression, KP: kick point, PSD: postero-distal, ALD: antero-lateral distal, MG: medial gastrocnemius, LG: lateral gastrocnemius, LS: lateral supracondyle, MS: medial supracondyle.

Wu et al. [64] and Lee et al. [108] obtained and compared the pain threshold (the minimum pressure that induces pain) and pain tolerance (the maximum tolerable pressure without feeling discomfort) in different regions of the residual limb by means of the indentation test (Table 3.8). Lee et al. [108] demonstrated that these two parameters depend on age and on the detection area, but are independent of the thickness of the skin layers.

Zhang et al. [76] concluded that socket rectifications have an important effect on the interface pressure, leading to an increase in pressure in key zones (such as patellar-tendon, popliteal, medial and lateral tibia), and to a reduction in sensitive areas (such as the distal part of the tibia front, the tibia crest, the fibula head and the residuum end). Furthermore, Silver-Thorn models [71] showed that an adjustment of two of the main areas - the patella tendon and popliteal area - significantly influenced the pressure in other residuum areas.

Table 3.8 - Pressure pain threshold and pain tolerance in different transtibial residuum regions [64].

Pressure (kPa)	Fibula head	Medial condyle	Popliteal depression	Distal area	Patella tendon
Pain threshold	599.6±82.6	555.2±132.2	503.2±134.2	396.3±154.5	919.6±161.7
Pain tolerance	789.8±143.0	651.0±111.1	866.6±77.3	547.6±109.1	1158.3±203.2

Zhang et al. [89] measured pressures and bi-axial shear stresses at the residuum-socket interface in five unilateral transtibial amputees during standing and walking. They recorded 320 kPa as the peak pressure over the popliteal area during walking and a maximum shear stress of 61 kPa over the medial tibia area. They observed different pressure waveforms during walking at the various points measured. According to their data, they found that a misalignment of $\pm 8^\circ$ produced a change in the peak longitudinal shear stress of between 8% and 11.5%.

Zachariah and Sanders [75] tried to understand whether standing interface stress can be considered as a prediction of walking interface stress. Their results, lower than those reported by Zhang et al. [89], showed that walking interface stress had a regional dependence and that standing stress was moderately predictive of peak walking stress (the correlation coefficients varied from 0.46 to 0.88 for pressure and from 0.30 to 0.81 for shear stress).

Convery and Buis [97] recorded dynamic pressures at the residuum/socket interface for Patellar Tendon Bearing (PTB) prosthesis during the gait of a transtibial amputee. They found average pressure per transducer during prosthetic stance was lower than 80kPa, but potentially dangerous pressure peaks (>100 kPa) has been documented, until 417kPa.

Dou et al. [100] compared the pressure distribution for the same type of socket during natural gait, walking on stairs, on slopes and uneven roads. The results revealed that pressure characteristics during natural ambulation do not seem to be highly predictive of what occurs in the other conditions.

Values of pressure distribution at the socket-residuum interface can be also derived from literature about comparative studies among different socket typologies. Goh et al. analysed dynamic and static pressure profiles of a unilateral PTB socket using a purpose-built strain gauged type pressure transducer [102]. They then compared the PTB sockets obtained by means of a hand-cast method with the TSB sockets produced from a hydrostatic cast [101]. Convery and Buis' studies [98] showed that the pressure gradients within the hydro cast socket were lower than those of the hand-cast PTB socket. This result was not later confirmed by Dumbleton et al. [99]. They found that the distribution of dynamic pressure at the limb-socket interface was slightly different: sockets produced with pressure-casting technique developed higher values than ones manufactured with hands-cast technique. To reliably measure the areas with high curvature in the patella tendon region, Abu Osman et al. [95] designed and evaluated two new external transducers able to record normal and shear stress and

quantify the three components of force applied during an amputee walking trial. In a similar way, Commean et al. [109] and, recently, Papaioannou et al. [110] focused on residuum slippage and residual limb deformations. They performed measurements using magnetic resonance imaging of the residuum slippage inside the socket to evaluate the socket fit and function and prevent discomfort or skin ulcers.

The Rehabilitation Engineering Division (RED) and King's Centre for the Assessment of Radiological Equipment (KCARE) [111] carried out in-depth analysis of the factors that influence the fit of artificial lower limb sockets, taking into consideration: socket design, different components (liners, pylons, feet, etc.), limb alignment, the manufacturing process and rectification techniques, as well as the checking process. Their appendix clearly and comprehensively summarizes the studies involving interface pressure and shear force measurement, specifying the objectives, the measurement method and what was found for each research carried out.

Further studies are necessary to understand pressure and friction effects on the residuum/socket interface and to create statistical database. Moreover, new techniques for load distribution could be considered to improve the quality of the socket fit.

3.3.1 Numerical model validation

Validation of the finite element model can be done by comparing the pressure values from the FEM analysis with those empirically measured directly at the socket-residuum interface, as carried out by Sanders and Daly [73], Zhang and Roberts [65] and Goh et al. [48].

Sanders and Daly [73] compared the normal and shear stresses during walking. The FE model results differed in terms of stress intensity and shear directions with experimental measurements obtained using custom-built strain-gauge transducers.

Zhang and Roberts [65] found that FE-predicted pressures during standing and walking were, on average, 11% lower than those measured by triaxial force transducers placed on a PTB socket wall. The estimated stresses were of the same order of magnitude but without a one-by-one match.

Goh et al. [48] compared predicted FEA stress with experimental data and attested that the average percentage error was 12% (the maximum absolute error was 30.3 kPa). They used 16 pressure transducers (ELFM-B1-5L, Entran International) distributed uniformly along the socket length in the 4-quadrant.

3.4 Discussion

During last fifteen years significant improvements have been made mainly thanks to hardware and software developments. Best acquisition techniques, more computational power, more sophisticated finite element codes have increased the performances and allowed more reliable results, allowing to their diffusion within new research areas.

The core of this chapter concerned the numerical models, performed over the last twenty years, to investigate the interactions between the socket and the residuum in lower limb prosthesis. The finite element method offers great potential for developing well-fitting and comfortable prosthetic sockets, especially when it supports the prosthetist tasks without being stand-alone system, but integrates with other tools. Current commercial CAD-CAM systems do not offer any integration with numerical simulation tools. An integrated CAD-CAE framework, included in a knowledge-based system, remains confined to the academic field [8, 46, 55, 66]. This approach tries to replicate what the

orthopaedic technicians usually do manually, suggesting rules and procedures. The integration with FEA tools should allow an optimal socket shape to be achieved, which means best load distribution over the residuum surface, without exceeding the pressure threshold [64]. Moreover, 3D virtual model of the socket can be used to produce the physical socket with rapid prototyping techniques, as reported by some study about the feasibility of direct manufacturing technologies [32, 55, 105, 112]. This will permit to reduce development time, to automate the manufacturing process and to have a closer control on the design parameters.

The accuracy of the FEM model depends on many factors: geometries simplification, size and type of grid, properties of elements, material modelling and characteristics, details and numbers of the interaction between the parts involved, loads and boundary conditions. The computational time is usually correlated to the size problem: more realistic models increase the computational time significantly. Therefore, the implementation of an embedded system to support the design activities of prosthetic technicians necessarily requires an optimization, limiting the amount of freedom of the model without losing precious information about socket-residuum interaction. By analyzing every single step, it is possible to identify various simplifications and assumptions that characterize realization of the finite element model and then to understand the critical aspects that could be improved.

Performing a FE analysis including all the parts involved (socket, liner, soft tissues and bones), with accurate shape geometry and good alignment between the residuum, bones and prosthetic socket, has a strong influence on the results of the analysis. CAD systems offer specific tools to manipulate the acquired shapes, and they can be used to prepare and to fix the geometries for the FE analysis.

The new acquisition techniques permit to overcome these problems by providing parts with detailed and properly aligned geometry. Laser scanning, Computer Tomography and Magnetic Resonance Imaging seem to be the best technologies for reconstructing the whole 3D residuum model, but the choice should be done according to availability of the system and the patient's characteristics. For internal parts, except for the technical specifications discussed above, it is difficult to indicate *a priori* the “best solution” between CT and MRI because the high cost of both systems presents availability problems. Orthopaedic centres cannot afford their purchase costs and not all hospitals have both. MRI seems to be better than CT because it does not expose the amputee to radiation, but this is not true in all cases. For example, it is contraindicated when the patient has metallic foreign bodies or medical implants. As reported by Kovacs et al. [15], CT images are in general more accurate than MRI and because of the correlation between Hounsfield Units (HU) and tissue density allow an automatic segmentation using thresholding. With MRI images, it is more difficult because the grey values do not correlate to HU and tissue density. Therefore, the different tissues need to be identified and segmented by hand in general and this is a very time consuming process. A good solution could be acquiring simultaneously external surface by laser scanning and internal parts by MRI and/or CT.

Regarding socket and residual limb meshing, automatic generator algorithms simplify this phase. The new algorithms allow good quality mesh elements to be obtained. Furthermore, the accuracy of the FE simulation results is related to the mesh size, element shape and geometric order used.

As previously mentioned, the material characterization of soft tissues is one of the main parameters the FE results are sensitive to. Most FE models still chose Hookean's law, specifying the Young's modulus and Poisson's ratio. The main limitation of a linear model, ill conditioning the whole analysis, is due to a single stiffness constant, which does not consider different behaviours at the small or large strains, unlike what hyperelastic or viscoelastic models could do. Perhaps, the main problem regarding diffusion of non-linear models remains the lack of clear information about them and the excessive computational costs. Further studies should be done to better clarify values, which describe soft tissues, whether these are linear with a double step, hyperelastic or viscoelastic, according to the

region considered and the patient's condition. In fact, a highly detailed geometric model that provides the main distinction of tissues, such as bones, tendons, cartilage, muscle and epidermal tissues needs to be characterized by specific behaviour. Also the role of the skin and socket needs to be better understood because some simplifications were made: for example, skin was assimilated to soft tissue and the socket was considered rigid. Parallel computing, by using multiple processors, could drastically reduce the computational time to achieve the simulation of socket-residuum interaction, avoiding any material simplifications or allowing considering highly detailed geometric model.

As described before, the socket-residuum interaction implies the presence of contact phenomenon, which can be modelled by contact elements or by contact algorithms. The contact elements are no longer used to describe the interaction and are replaced with contact surfaces, computationally more complex, but able to describe large slippage because they are not structure elements. FE solvers automatically detect the contacts between two surfaces when these are expressed as potential contact surfaces in the model.

The importance of friction has been demonstrated and all the latest FE models consider the friction between the interface surfaces, only allowing slippage during the donning simulation. The friction coefficient needs to be estimated every time according to the interface materials and skin condition because the reference range is wide and the stresses and strains are sensitive to its values.

The pre-strain due to the prosthetic socket rectifications, which reduce and change the shape with respect to that of the residuum, is a consolidated approach. Its effects involve two aspects: soft tissue behaviour and socket alignment with regard to the residuum and bones. There are two different ways to apply a pre-strain to the residual limb: one is to force a radial displacement and the other one is to simulate socket donning. The latter replicates the real procedure. The displacements are not imposed *a priori*, but follow the socket movements.

Loads are related to boundary conditions, while the directions and amplitude are correlated to the assumption and simplification of the model, but they should reflect real and consistent alignment. In any case, load directions are quite important because they can produce considerable changes in shear and normal stress, while amplitude is specified on the basis of the choice of analysis, static or dynamic.

To conclude, implementation of reliable FE models need further improvements, especially in relation to material characterization, socket-residuum interface and load conditions that mainly determine the FE results. If performed in a systematic way, experimental tests, associated with FE models, will be the final step towards achieving better matched results in FE models. Model development should be closely monitored, evaluated and validated so that it can be considered consistent and reliable. More research is required to obtain qualitative and quantitative parameters that allow the analysis results to be verified, and the FE model set-up must be refined and how the pressure threshold depends on age, skin characteristics and pathology must be explained. For future developments, it is essential to obtain experimental data about pressure and shear stresses, which are not influenced by the shape of the acquisition area, residuum-socket slippage and large strains. Thinner and more precise pressure-stress sensors might be incorporated between the socket-residuum interface, allowing measurements without substantial environmental effects.

4

Tools and Methods

As previously stated, it is crucial understand if the socket shape is comfortable and well fit on the residual limb before manufacturing it. This task can be performed to analysing the contact interaction between prosthetic socket and residual limb. This chapter introduces the tools and methods adopted to develop the embedded simulation module.

First, the modelling tools have been considered since they are used to create the residual limb and the socket models necessary for the FE analysis and the whole prosthesis model indispensable for the gait analysis. Then, the focus has been paid on the FE solvers through the implementation of some FE models; both commercial and open source solvers have been considered and evaluated. Finally, the Digital Human Modelling system has been adopted to perform gait simulation of the patient's avatar and get the forces applied to the socket.

4.1 Modelling tools

4.1.1 Socket Modelling Assistant

To numerically analyse the interaction between socket and residual limb is necessary to have the geometric models of these two parts. Within the PVL, Socket Modelling Assistant has been considered in order to provide the aligned geometric models to the FE model.

The Socket Modelling Assistant – SMA is module specifically developed to model the socket, both transtibial and transfemoral prosthesis, directly on the digital model of the residual limb. The socket design is performed according to the patient's characteristics, in correlation to the implicit experts' knowledge and the process rules implemented into the system. The system, when possible, executes automatically some design operations while in other cases it supports step by step each phase of the modelling, providing suggestions that guide the task execution.

Four main steps are necessary to complete the socket design within the SMA: the specification of the patient's information, the preliminary modelling, the customized modelling and finalization modelling.

The design process starts acquiring patient's information traditionally considered by the technician (such as weight, muscles tonicity, skin conditions and residual limb stability) and importing the

residuum digital model. This geometric model is reconstructed from the MRI images by the use of GEOMETRIC module. During this phase, the prosthetist sets the critical zones that will require specific manipulations by using the Marker Tool (Figure 4.1).

Then, the SMA generates a preliminary geometric model of the socket onto which other specific modifications will be applied to reach a functional shape. Following operations, performed in automatic way according to patient's characteristics, regards: the scaling of residual limb model, the generation of socket reference surface and the socket top optimization. Circumferences Scaling Tool (Figure 4.1) automatically applies the appropriate range for reduction percentage to the residual limb reference circumferences. The SMA creates the socket reference surface as an offset with constant distance from the scaled residual limb model (Figure 4.2); this surface constitutes the socket inner surface and represents the starting point for the customized modelling. Then, the system automatically levels and rounds the surface at top of the residual limb, that has an irregular shape due to bone protuberances and scars (Figure 4.2).

The customized modelling of the socket is reached by an interactive shape manipulation through the use of Sculpt Tool and Section Tool. The first permits the technician to modify the critical surface area, pushing or pulling the socket surface (Figure 4.3). The second tool allows checking and modifying the model surfaces working directly on the shape sections and on each single surface control point.

The final phase allows finalizing the upper edge of the socket model by using the Surface Tool (Figure 4.3). This tool is similar to the Section Tool, but it has the advantage of working on both horizontal and vertical sections. In addition, it allows the user to modify in detail and in a homogenous way the socket shape using surface control points.

Once completing the socket design, the SMA generates the .IGES files of the geometric models: the socket, the bone, and the residual limb. This phase is fundamental for the FE model because it allows obtaining the geometric models completely aligned, that adopt the same coordinate system.

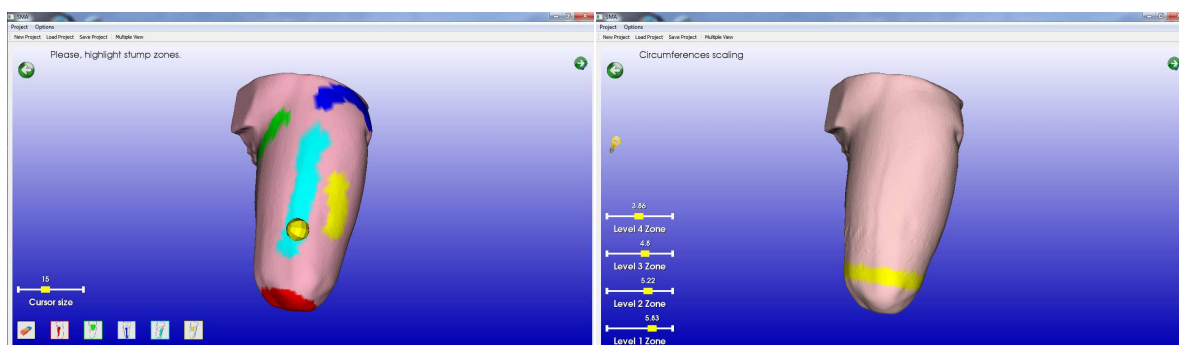


Figure 4.1 - Example of Marker Tool functionalities with highlighting the critical zones (left) and Circumferences Scaling Tool (right).

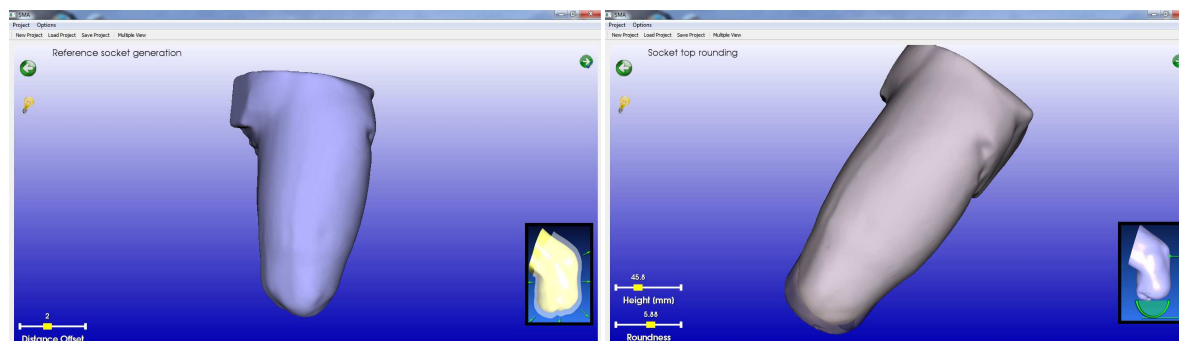


Figure 4.2 - Example of the creation of the reference socket surface (left) and the socket top rounding (right).

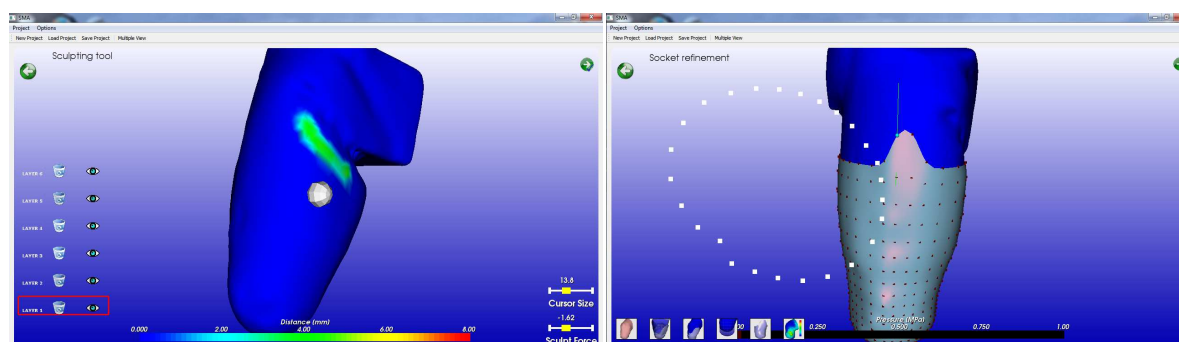


Figure 4.3 - Examples of Sculpt Tool functionality (left) and the use of the Section Tool for moving the surface control point in green (right).

4.1.2 Prosthesis configuration and assembly

In order to perform a virtual gait analysis of the patient's avatar it is necessary to configure and assembly a complete prosthesis.

Within the PML, a commercial 3D CAD system (SolidEdge) has been integrated in order to select standard components and create the final assembly (as portrayed in Figure 4.4). The prosthetist, guided by system, chooses the most appropriate standard components for the patient; then, the system proposes possible configurations of the whole prosthesis according to patient's characteristics. For prosthesis configuration, the lower limb prosthesis has been divided into five main modules; they are (Figure 4.4):

- Socket module (liner, socket and socket adapters).
- Double adapter (double male or female pyramid adapters).
- Knee module (prosthetic knee and knee adapters, only for transfemoral amputee).
- Tube module (connecting pylon and tube adapters).
- Foot module (prosthetic foot, foot adapters and heel).

The rules necessary to size and select the standard components have been derived from technicians' know-how and extrapolated from commercial catalogues provided by main prosthetic brand. 3D models of the standard components are included in a library as parametric model in order to size each component according to the patient's characteristics (such as the weight and the height).

The system automatically assembles all the possible combinations of the selected different parts, and provides to the prosthetist all the related BOMs. At this point, the user selects the most suitable prosthesis and changes, if necessary, some components according to patient's needs. While

assembling the final components, the system ensures that the alignment of the prosthesis is similar to the skeletal structure of the other leg. Finally, the system exports the 3D model of prosthesis using the Parasolid that is used by LifeMOD to perform the virtual gait analysis of the patient's avatar.

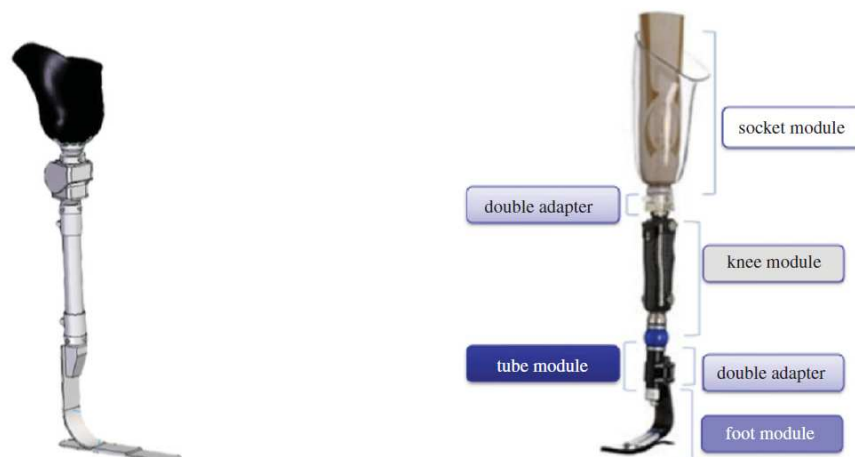


Figure 4.4 - Example of an assembly of transfemoral prosthesis (left) and prosthesis modules (right).

4.2 FE solvers

Finite element modelling and analysis to evaluate the socket-residuum interaction has been performed since the 1990s [11, 38-41]; most of researches considered transtibial socket, only few transfemoral. Anyway, none of them tried to integrate and/or automate the analysis within a CAD framework and mainly focused on the fulfilment of the model itself. Differently, the goal of the thesis has been to implement an automatic simulation procedure to make the prosthetic able to run automatically FE analysis.

From the analysis of the state of the art, it was possible to identify the commercial and general-purpose FEA systems commonly adopted (see Table 3.4). Among them, Abaqus package V 6.9 (Dassault Systemes S.A.) has been considered because it is widely used and it permits to bypass the graphical user interface and communicate directly with the kernel through a script. The Abaqus kernel interprets the script commands and automatically creates an internal representation of the model.

Furthermore, open-source solvers have been taken into accounts. The choice of the open-source solvers has been made considering software packages that have stable versions and are supported by developers. Some examples are: ELMER, CODE_ASTER, CalculiX, and Z88. Table 4.1 lists considered open source solvers and their main characteristics. Among them, CalculiX has been chosen because it satisfies all the requirements: (i) it permits to solve contact algorithm with or without friction, (ii) it runs linear and non-linear (material, geometric) static and dynamic analysis, (iii) it permits to include linear elastic and hyperelastic material model. In particular the bConverged Open Engineering Suite includes CAD exchange software (STEP, IGES and BREP translations to STEP, IGES, BREP, VRML, STL and partial translation to FBD) and a graphical user interface.

In order to select the FE solver, identify the simulation rules and the procedure for the simulation module, preliminary tests have been performed with Abaqus and CalculiX. To this end, a unilateral transfemoral male amputee, 49 years old, 175 cm height, and 80 kg weight has been considered as test case.

For the definition of the FE model with both solvers, the key issues identified from the analysis of the state of art have been considered. They are: acquisition and definition of the residuum and socket geometries, mesh generation, material characterization, analysis steps and boundary conditions.

Table 4.1 – Open-source finite element software specifications.

Software	ELMER	CODE_ASTER	CalculiX	Z88
License	Open source - GPL	GPL	GPL	Freeware GNU GLP
Contact Simulation	No	Yes	Yes	No
Scripting	Python language	Python language	Yes	Yes
Type of analysis	Multi-physical	Structural and thermo-mechanical Linear and non-linear (material, geometric) static and dynamic analysis	Structural and thermo-mechanical Linear and non-linear (material, geometric) static and dynamic analysis	Structural and thermo-mechanical Linear static analysis
Geometry	STL, Gmsh,	ACIS, BREP, STEP, IGES, ProEngineer, SolidWorks, Nx, SolidEdge, Parasolid, and CATIA V4	BREP, STEP, IGES, STL (ASCII and binary format), geometry file (*.geo, *.in2d)	STEP, STL (ASCII and binary format), and Autocad
File compatibility	None	None	Partially compatible with Abaqus	Nastran, Abaqus, Ansys, and Cosmos
Pre/post processor	Embedded, Tetgen, Netgen	SALOME	Embedded, Gmsh, Netgen	Embedded

4.2.1 Abaqus FE model

Geometries

The finite element model consists of three parts the soft tissues (that includes skin) the bones and the socket; the liner was not considered.

To achieve a geometric model with reasonable accuracy, the soft tissues and the residual bones have been acquired using MRI system. The detailed 3D model of soft tissues and residual femur were reconstructed using GEOMETRIC, the integrated module within the SMA. The 3D digital representation of the prosthetic socket was achieved by using our *ad-hoc* software, the Socket Modelling Assistant – SMA [8].

The alignment of bone and soft tissues was guaranteed since the 3D models derive from the MRI images; while, the socket-residuum alignment was guaranteed because the socket was modelled on the residuum outer surface within the SMA. The SMA generates the geometric models providing the same coordinate system to the models, kept also during the FE model definition.

The socket is imported in Abaqus was 3D deformable shell, because socket thickness is considerably smaller than the other two dimensions, while bony structure and soft tissues as 3D deformable solids. Within Abaqus software, bones and soft tissues were merged by Boolean operation of union to form a single part, the 3D virtual model of the residuum, without geometric discontinuity but characterized by two different models material. This Boolean operation allows reducing the degrees of freedom of the FE model and the number of surfaces in contact. Figure 4.5 portrays the geometric models for the numerical analysis.

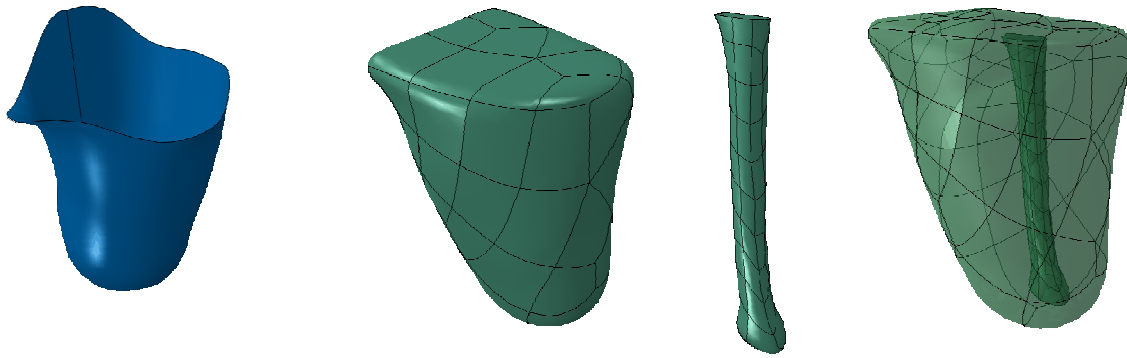


Figure 4.5 - Three-dimensional models of the socket; the residual limb and the femur; and, finally, the results of the Boolean operation of union of residuum and bone.

Mesh

A free auto meshing technique has been adopted to mesh the involved parts (Figure 4.6), considering triangular (S3R) and tetrahedral (C3D4) elements for a better discretization of the non-linear geometries. The seed values, summarized in Table 4.2, has been chosen performing a preliminary sensitive analysis, following the conformity requirements of tetrahedral and triangular elements of the involved parts and without dramatically increasing analysis time.

Table 4.2 - Mesh characteristics: seed value, node number and elements number.

	Residuum	Socket	Whole model
Seed value [mm]	6.3	8	-
Nodes	12176	920	13096
Elements	62279	1763	64042

Material properties

The material properties of the residuum (or rather bone and soft tissues) and the socket were considered as linear elastic, homogeneous and isotropic, as assumed by other authors [10, 47, 48, 53, 54, 64, 65, 69]. Table 4.3 lists the mechanical properties used for the materials characterization, according to Jia et al. [10, 53] and Lee et al. [54]; while Table 4.3 displays the meshed parts.

Some researches [65, 69] evaluated negligible the deformations of the bones and the socket because their Young's modulus is five orders of magnitude greater than soft tissue ones. According this observation, the socket and bone were considered as rigid body without losing crucial information about the pressure interface. Soft tissues stiffening, due to the pre-stresses and the load bearing, has not been taken into account, unlike [47, 65].

Table 4.3 – Material properties.

Part	Density [Kg/dm ³]	Young's modulus [MPa]	Poisson's ratio
Socket	7.8	15000	0.3
Bone	2.0	10000	0.3
Soft tissues	1.48	0.2	0.49

Analysis steps and boundary conditions

The simulation was performed in three phases corresponding to the deformation stages of soft tissues using explicit simulation. The first step replicates the donning of residual limb into the socket and it

imposes a pre-stress on the residuum, [65, 76]. Then, the adjustment step follows to reach a better repositioning of the socket around the residuum and to obtain maximum comfort. In the third and final step, the static full weight of the patient on a single leg is applied as load to the centre of mass of the socket in vertical direction.

Boundary conditions (Figure 4.6) and loads have been defined according to the simulation step. The donning simulation (in Figure 4.7) is carried out fixing the upper residuum surface and moving the socket proportionally to the residual limb length, causing the pre-stress on the external tissues. I chose to move the socket because relative adaptive movements are not known a priori and it limits computational costs. In the adjustment step, the upper residual limb surface is still fixed; the socket is free to translate and rotate in all directions with the exception of the vertical one, which is kept locked until the load phase to prevent elastic spring back due to fitting. During these first two steps, no external load is applied. Socket translation and patient's weight are not applied instantly, but gradually during the analysis step to avoid excessive acceleration and then high mass inertia.

To model the interaction between residuum and socket, the automated surface-to-surface contact element was adopted since it is better than the traditional point-to-point contact pairs, as reported by Wu et al. [64]. According to the master-slave contact formulation and hard contact relationship used in Abaqus, donning and adjustment steps are friction-free, while during loading the friction coefficient is equal to 0.4, within the range of value documented by Zhang and Mak [88].

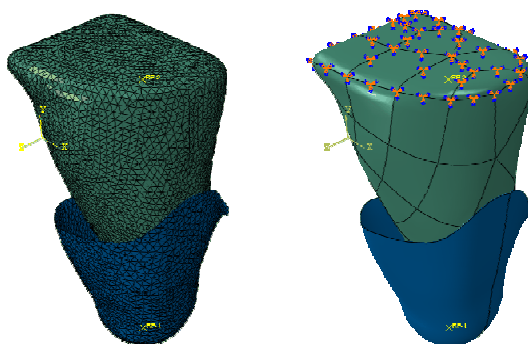


Figure 4.6 - Meshed models of the socket and residuum with initial over-closure (left) and FE model boundary condition relative to the fixed nodes of the residuum (right).

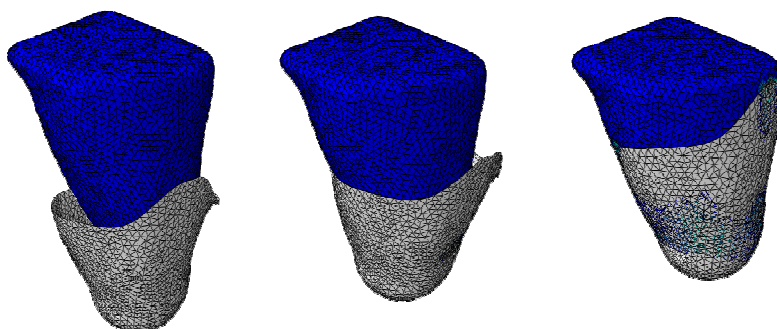


Figure 4.7 - Donning simulation of a transfemoral socket.

Preliminary results

The pressure distribution on the residuum surface is portrayed in Figure 4.8. Pressure values, expressed in MPa, are associated to a range of values from 0 to the maximum pressure values

computed during the analysis and the colour scale is from blue to red. The pressure distribution obtained with Abaqus is well distributed and homogeneous without exceeding 100 kPa in most areas of the residual limb. The exception of external trochanter area and the inguinal area are the only area overstressed with pressure values close to the maximum values equal to 167 kPa.

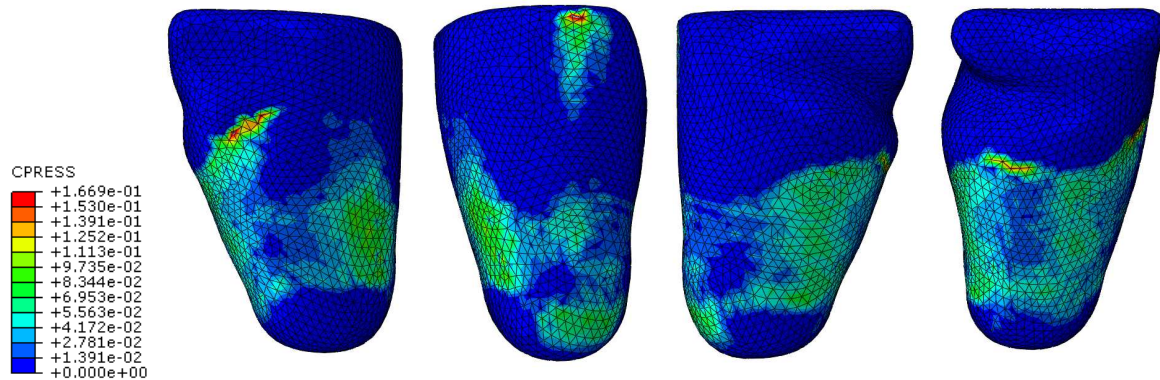


Figure 4.8 - Pressure distribution on residuum surface after loading simulation performed with Abaqus.

4.2.2 CalculiX FE model

Geometries

The geometric models of bone and soft tissues are the same aligned model adopted to implement the preliminary FE model in Abaqus. In this case, the socket model, achieved by using the SMA module, has the same shape of the external surface of residual limb with the rounded socket top.

Before using soft tissue and residual femur models in numerical analysis, the femur volume was removed from the soft tissues model through a Boolean operation in order to reduce the degrees of freedom of the FE model. The task was accomplished using a commercial CAD system (Solid Edge). At this point, the FE model consists of two parts (see Figure 4.9): the residuum (residual limb without residual femur) as 3D deformable solids and the socket as 3D deformable shell, since socket thickness is considerably smaller than the other two dimensions.

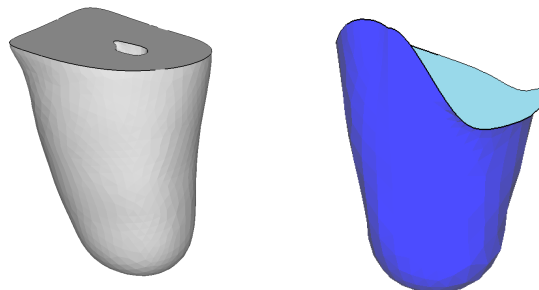


Figure 4.9 - Residual limb without residual femur and prosthetic socket used for the FE analysis.

Mesh

Socket and residuum were meshed using Netgen V4.9.12. A free auto meshing technique was adopted due to the geometries complexity of the parts and the impossibility to automatically build a structured mesh. 4-nodes tetrahedral (C3D4) and 3-nodes triangular (S3) elements are respectively used for the residual limb and for the socket. Before starting the FE analysis, CalculiX automatically expands the shell elements into three-dimensional wedge elements.

The mesh size, summarized in Table 4.4, has been chosen on the bases of Abaqus FE model, and following the conformity requirements of tetrahedral and triangular elements of the involved parts.

Table 4.4 - Mesh characteristics: size, node number and elements number.

	Residuum	Socket
Size [max, min, grading]	[10;5;0.3]	[12;5;0.3]
Nodes	60446	414
Elements	12756	772

Material properties

The material properties of the residuum (or rather the soft tissues) and the socket were considered as linear elastic, homogeneous and isotropic (Table 4.3). The socket has been considered as rigid body, as previously, and the external surface of the bony structures was considered fixed. Neither soft tissues stiffening nor soft tissue non-linear characterization have been taken into account.

Analysis steps and boundary conditions

To study the interaction between socket and residuum I considered two phases: the donning simulation of the socket over the residuum and the loading phase.

CalculiX does not manage big sliding, so the socket has been considered already donned. To avoid the overlap between socket and residuum and to introduce a pre-stress status on the residuum surface, a thermal analysis has been performed. Due to thermal contraction, the residuum reduces the volume and its shape becomes smaller than the socket one. Then, contact algorithm is activated and the temperature increases to the reference temperature expanding the residuum. The load was applied to the socket nodes in terms of nodes displacements, derived from previous Abaqus FE analysis.

The boundary conditions change according to the analysis steps. The nodes of the residuum upper surface and the residuum-bone surface, obtained by Boolean operation with the bone, were fixed (Figure 4.10): in other words the displacement along the three degrees of freedom were avoid. During the thermal contraction and then expansion the socket was fixed; only after, it was subjected to a vertical translation along vertical direction according to the imposed amplitude function.

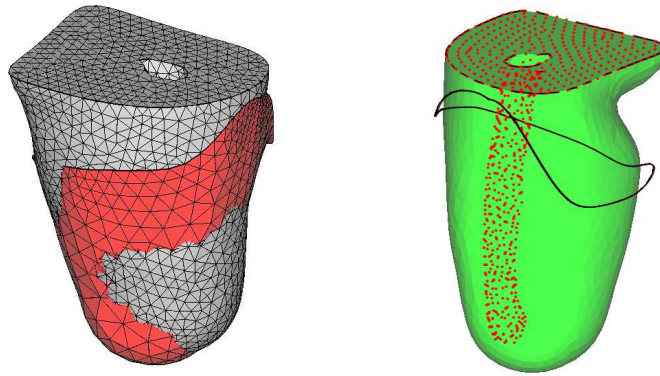


Figure 4.10 - Discretization of the socket and residuum with initial over-closure (left) and FE model boundary condition relative to the fixed nodes of the residuum (right).

Contact problems are a strongly nonlinear type of boundary conditions and avoid bodies to penetrate each other. The contact definition implemented in CalculiX is a node-to-surface penalty method based on a pairwise interaction of surfaces [113]. Due to large sliding, the pairing of the dependent nodes (residuum nodes surface) with the independent faces (socket inner surface) is checked every iteration during the numerical analysis. A linear pressure-overclosure relationship has been considered and friction has been neglected due to convergence problems.

Preliminary results

Figure 4.11 shows the pressure distribution on the residuum surface, expressed in MPa. The pressures are associated to the colour scale from violet to red and to the range of values from 0 to the maximum pressure values computed during the analysis. The pressure distribution obtained with CalculiX is well uniform and consistent. The maximum pressure value computed during the analysis is less than 3.2 kPa, that is far from the results that commonly found in the literature [38]. The area with the highest contact pressure is that around the top of the residuum since the socket has the same shape of the residuum model with the exception of the top, which was rounded using the dedicated tool within the SMA. The choice of this shape is due to the fact that I was not able to complete the contact analysis using the same socket model used in Abaqus FE model. During the loading simulation the solver crashed due to the large deformation that occurred.

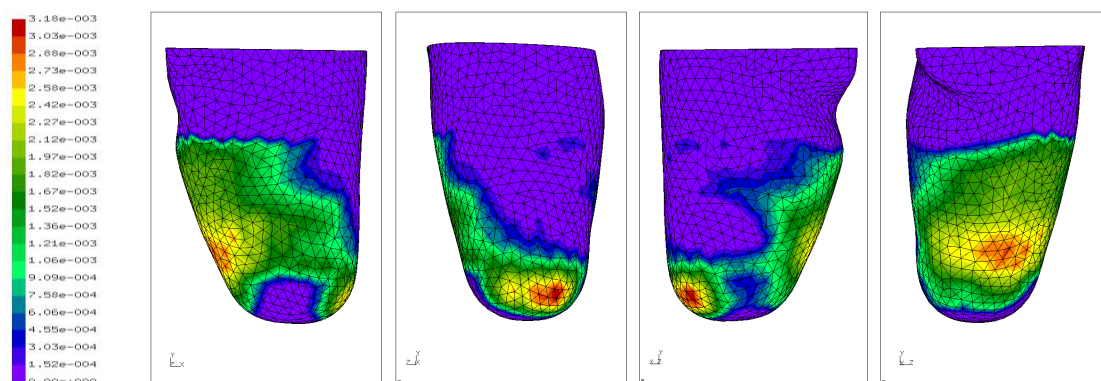


Figure 4.11 - Pressure distribution on residuum surface after loading simulation performed with CalculiX.

4.2.3 Discussion

According to the analysis of the results and considering the limitations that were occurred during the implementation of the CalculiX FE model, Abaqus solver proved to be the best choice to simulate the socket- residuum interaction. Follow the motivations related to this choice:

- Pressure values obtained with Abaqus are similar to those one founded by Hong [114] and have the same order of magnitude of other research summarized in [38], while the pressure values computed in CalculiX are almost two order of magnitude lower.
- CalculiX doesn't allow to properly perform donning simulation because the solver is not able to manage the contact interaction when big sliding occurs, as is during this phase. It requires to introduce a thermal analysis in order to avoid the initially overlap of the socket on the residual limb. This limit causes the impossibility to consider a valid pre-stress status on the residuum before loading simulation.
- CalculiX allows completing the simulation that considers a socket with the same shape of the residual limb, making useless the analysis. This aspect is crucial to allow the prosthetist to assess the shape of the designed socket. Moreover, also friction has been neglected because of convergence problems. So, to implement a running model with CalculiX it is necessary to significantly customize the source code and this task is time consuming.

4.3 Digital Human Modelling

Digital Human Modelling (DHM) tool is used to generate the virtual avatar of the patient and simulate the gait. First DHM tools appeared in late 60's, mainly in aeronautics and automotive industries. At present various systems, both commercial and academic, are available: virtual human/actors for entertainment, mannequins for clothing, virtual humans for ergonomic analysis, and models for biomechanical simulation. The latter category is the best suited for prosthetic field because it permits to understand human physiology and to study the human body movement, also considering different pathological conditions or disabilities.

Finite Element Analysis can increase the quality of the simulation results thanks to the interaction with Virtual Human Modelling system because the latter could retrieve loads acting on the socket in a posture or during different gait conditions. In particular, it could be possible to obtain the pressure distribution over the residual limb surface during each moment of a gait step.

In this thesis work, LifeMOD is the Digital Human Modelling system that has been taken into account. In the following sections, the steps necessary to implement the patient's avatar and perform the gait simulation are briefly introduced.

4.3.1 Patient's avatar implementation

The process to achieve a customized virtual human model starts with the creation of the patient's avatar through the use of LifeMOD, a biomechanical modelling package based on MSC ADAMS system. It permits to create a detailed biomechanical model of a human body using rigid links connected through joints to simulate the skeleton and flexible elements to represent muscles, tendons and ligaments.

The patient's avatar wearing the prosthesis is created in two steps. Starting from the LifeMOD standard model of the human being, the customized virtual model of the amputee is generated

according to his/her anthropometric measures and replacing the limb with 3D model of the residual limb (femur and soft tissues), as showed in Figure 4.12 (left). The residual bone segment is linked to the avatar's hip and then soft tissues are properly placed. In the second step the 3D prosthesis is imported using Parasolid format and the correct positioning is obtained taking into account the prosthesis height and foot rotation respect to the vertical line. In particular, the prosthetic foot has to be aligned to the other one and the socket has to hold entirely the residual limb Figure 4.12 (right).

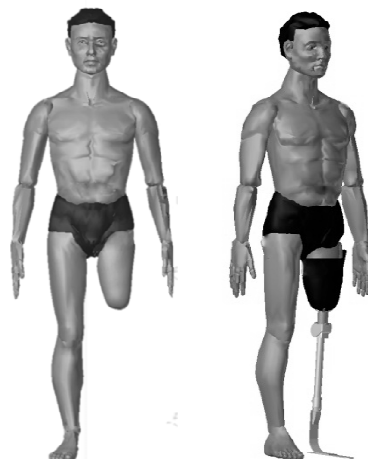


Figure 4.12 - Patient's avatar (left); avatar wearing the prosthesis (right).

4.3.2 Avatar simulation

Once created the patient's avatar, the patient's walking has been simulated using motion laws deduced from experimental tests performed with a marker less Motion Capture (MoCap) equipment, implemented with four Sony-eye webcams. The motion law is described by "Motion agents" that drive the skeleton joints and teach to patient's avatar how to move through an inverse dynamic simulation. Once segments angulations and muscles contractions of the avatar are known and traced, LifeMOD proceeds with the direct dynamics simulation.

In this case, to replicate the functionality of the residual limb, "augmented motion agents" linked to the prosthesis segments have been inserted: three associated to the prosthetic foot, one to tube below-knee representing the lower part of the leg, one to the knee and another one to the socket.

Main goal of the simulation is to get necessary data to evaluate the system residuum-socket-prosthesis during walking on a flat ground, i.e., to calculate the corresponding loads acting on the socket. The attention focused on the first step, which goes from initial loading response to terminal stance. Each force component, whose magnitude fluctuates over the time, has been exported separately in a text file in order to create the specific motion law associated to the force components.

Figure 4.13 shows the graph of numerical result in terms of the force (components and magnitude) acting on the socket during walking and over the stance phase; the three components refer to inertial frame of reference respect to the socket.

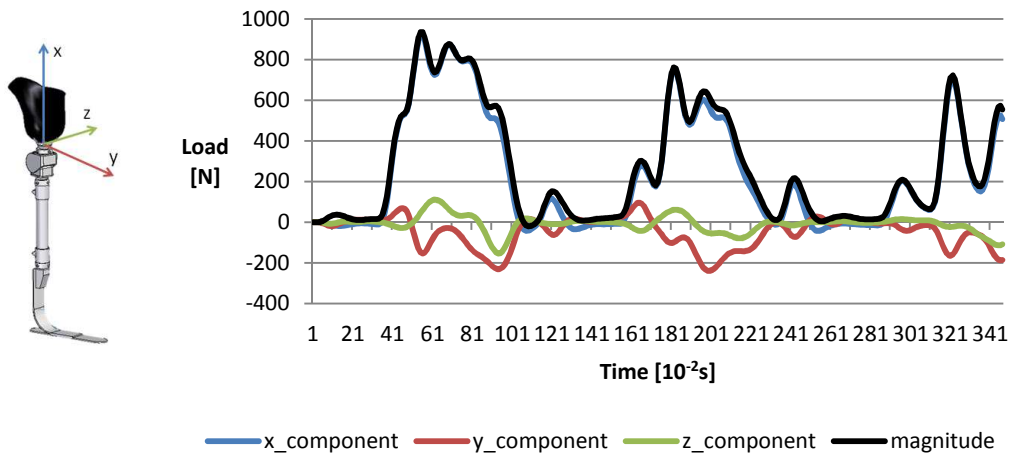


Figure 4.13 - Load components acting on the socket during walking.

5

Embedded Simulation Module

This chapter focuses on the embedded simulation module, developed to evaluate the socket shape with the design process. It permits to automatically analyse the contact interaction between the socket and the residual limb, without the interactions of the user. This last aspect is fundamental to allow the prosthetist to use numerical simulation tools in orthopaedic laboratory.

First, the architecture of the FEA module is exposed and the attention is centred on the simulation phases, the involved players, the definition of the simulation rules and the interaction with SMA and LifeMOD. The definitive architecture of the FEA module has been identified according to the consideration made on the state of the art, the investigated numerical simulation models and the interaction with the SMA and the DHM system. Then, according to the considerations derived from the state of the art and from preliminary FE model, the simulation rules characterizing the FE model are defined and reported. Finally, the implementation of the embed module by the use the Python script is exposed.

5.1 FEA module architecture

The automation of the simulation process requires the analysis of the problem from different points of view and the formalization of the procedure, the rules and the results evaluation. Simulation rules, embedded within the system, permit to support the end-users applying in automatic or semi-automatic way simulation procedures (e.g., mesh generation) and design rules (e.g., analysis of simulation data).

To this end, it was necessary to analyse strategies and parameters to automate the steps that characterize the simulation process, i.e., pre-processing, solving and post-processing. Generally, an approach based on an embedded simulation has to follow some basic steps:

1. Automatic definition of the geometric models involved in the numerical simulation;
2. Pre-processing phase managed in automatic mode through the application of specific rules;
3. Calculation phase performed by one or more solvers depending of the problem under investigation;
4. Post-processing phase automatically managed through a knowledge-based approach;
5. Iterative automatic or semi-automatic modifications of geometric models (if necessary).

Figure 5.1 shows the logic schema of the proposed approach. The user provides data to model the product and perform the simulation. The user models the 3D model of the socket and the PML generates in automatic or semi-automatic way the data and the geometric models for the simulation. The simulation tool generates the proper model and run the analysis. Output data are imported and

visualized within the PML environment for carrying out the post-processing phase. If results are acceptable the simulation is stopped and the PML goes ahead, otherwise, changes are applied until the optimal solution is reached.

Therefore, three main players with different roles can be identified:

- *End user (prosthetist)*. S/he provides all the necessary inputs for the prosthesis design and the numerical simulation. S/he evaluates the simulation outcomes with the support of the system, which suggests rules and guidelines to re-design or optimize the part.
- *PML environment*. It controls the whole simulation process. Starting from the input, it generates data and model for the analysis, activates the simulation process, imports and visualizes the results and, according to codified knowledge, evaluates the critical parameters. If pressure values are acceptable it closes the simulation, otherwise the socket shape is modified by the user or automatically by the system and runs a new simulation. The PML environment is composed by ad-hoc modules that perform the specific tasks. In particular, GEOMETRIC module reconstructs the residual limb from MRI and the SMA module allows modelling 3D socket geometry. Moreover, SMA creates the files with the aligned geometric models and launches the simulation. The visualization of numerical results is done within the SMA; so, the socket shape modifications of critical areas are performed according to the pressure distribution.
- *Simulation tool*. Based on characterization parameters and a pre-compiled script, it creates the simulation model, bypassing the graphical user interface, and resolves: it's simply a calculus slave. Presently, Abaqus FE system is the simulation tool that executes the FE simulation and sends results, when required, to PML.

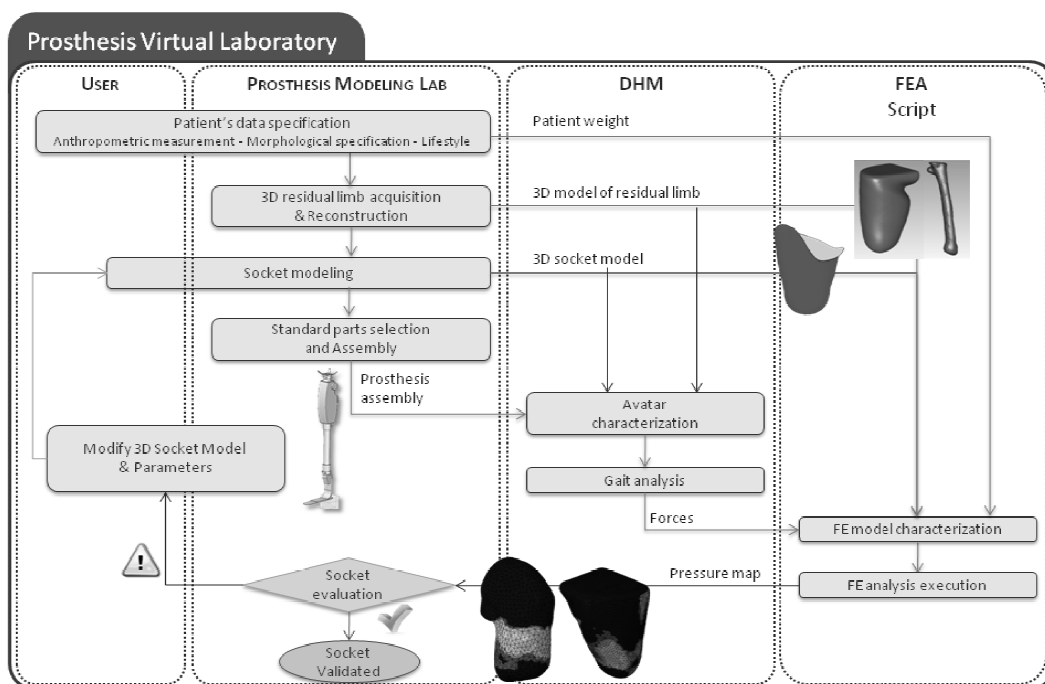


Figure 5.1 - Logic schema of the framework: socket design process integrated with the FEA module and the DHM module.

To automate and integrate FE analysis process within design platform (see Figure 5.2), the parameters guiding the process and simulations rules have been defined:

- *Inputs to simulation.* This data that should provide by the users or generated by the PML system to perform the following steps. In socket design process, the information necessary for the simulation concern patient’s characteristics, such as weight and residual limb’s length, friction between residual limb and socket and forces and moments due to walking (if the patient’s gait analysis has been performed).
- *Geometric models.* The FE model requires two parts: the residual limb and the socket. The SMA has to provide the .IGES files of these parts already aligned. Soft tissues and bones are supposed to consider as 3D deformable solids while the socket as 3D deformable shell, since socket thickness is significantly smaller than the other two dimensions. In order to reduce computational costs, bones and soft tissues should be merged to create a unique part without geometric discontinuity and with zones characterized by different material properties.
- *FE model.* Definition of the rules to implement and characterize the numerical model, such as mesh, material model, load and boundary conditions, constraints and analysis steps.
- *Evaluation rules and parameters* to assess simulation results and therefore to support the end-users applying in automatic or semi-automatic way the necessary model modifications to adopt. Every model change has to be evaluated again and so new simulation runs are necessary. The meaningful parameter recognized to evaluate the socket shape is the contact pressure between socket and residual limb during patient’s walking, since it allows taking into account the whole residuum’s morphology. From literature analysis [64, 108], it was possible to identify the pain threshold, i.e., the minimum pressure that induces pain, and the pain tolerance, the maximum tolerable pressure without feeling discomfort, associated to specific zones of the residuum.

In the following section, the simulation rules and the implemented procedure are described.

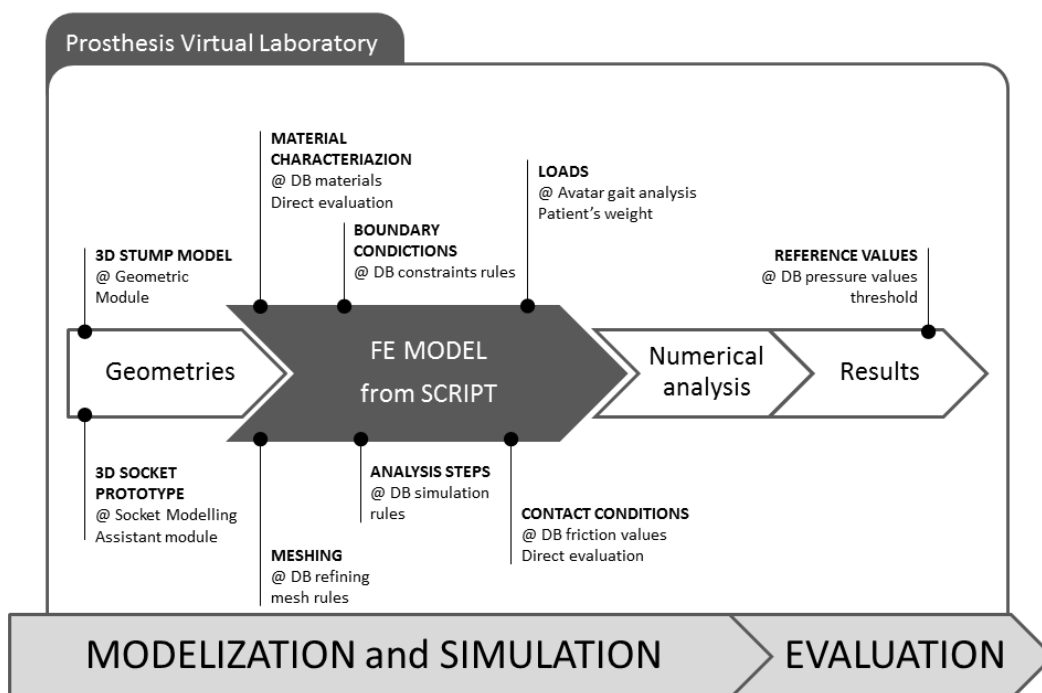


Figure 5.2 - Integrated FE analysis procedure within the design platform.

5.2 Simulation rules

The definitive Abaqus FE model has been identified according to different numerical simulation aspects emerged from the state of the art, during the experimentation of the FE solvers. At this point, all the simulation rules to characterize a running FE model have been defined in order to create the default simulation model able to analyse the contact interaction between socket and residual limb.

5.2.1 Geometric model

Rules. 3D geometric models of the residual limb (soft tissues and bone) and the socket in .IGES format.

As mentioned before, for the acquisition of the patient's residual limb morphology, MRI has been selected since it is the less invasive technique for the patient. GEOMETRIC module is used to reconstruct the residuum 3D model and the SMA to create the 3D model of the socket around the residual limb. The alignment of the parts is guaranteed by the SMA, which generates the geometric models providing the same coordinate system.

The models are imported and assembled into Abaqus using .IGES format: soft tissues and bones as 3D deformable solids while the socket as 3D deformable shell. Bones and soft tissues are merged to create a unique part without geometric discontinuity, despite the different parts that compose it, and taking into account the real distribution of rigidity. This solution permit to simplify the real problem and consider the residual limb as a continuum that is characterized by two models of different materials. It also prevents to specify the type of interaction existing between bones and muscles.

5.2.2 Mesh properties

Rules. Socket: S3R elements with seed equal to 8. Residuum: C3D4 elements with seed equal to 6.3.

The automatic procedure forces to adopt a free auto meshing technique, in particular triangular and tetrahedral elements are adopted to better discretize the non-linear geometries. I have considered 3-node triangular elements (S3R) elements for the socket and 4-node tetrahedral elements (C3D4) for the residual limb, which increase their size in the internal regions.

The discretization of the continuum influences the model size and consequently the computational time, the results quality and the geometrical quality of the elements, which have to fulfil the conformity requirements such as aspect ratio. A sensitive analysis, summarized in Table 5.1, has been performed to select the seed values. The FE model is loaded with a static force along to vertical direction, equal to 800N, without constraints in planar directions; soft tissues was characterized with the linear model ($E = 0.2$; $\nu = 0.49$), while bones and socket are considered as rigid parts.

Table 5.1 - Mesh characteristics and simulation times for transfemoral model according to seed values.

Seed [residuum; socket]	3; 5	3; 8	4; 7	5; 8	6; 8	6.3; 8	7; 8	8; 8
Elements	317537	312445	172353	106409	74398	65557	53273	41911
Nods	63405	60836	34521	21700	15536	13096	11508	9290
Variables	202965	187551	110049	70143	51651	64042	39567	32913
Simulation time	49h35'	47h 58'	20h 50'	9h 33'	5h 40'	3h 36'	2h 37'	1h 46'

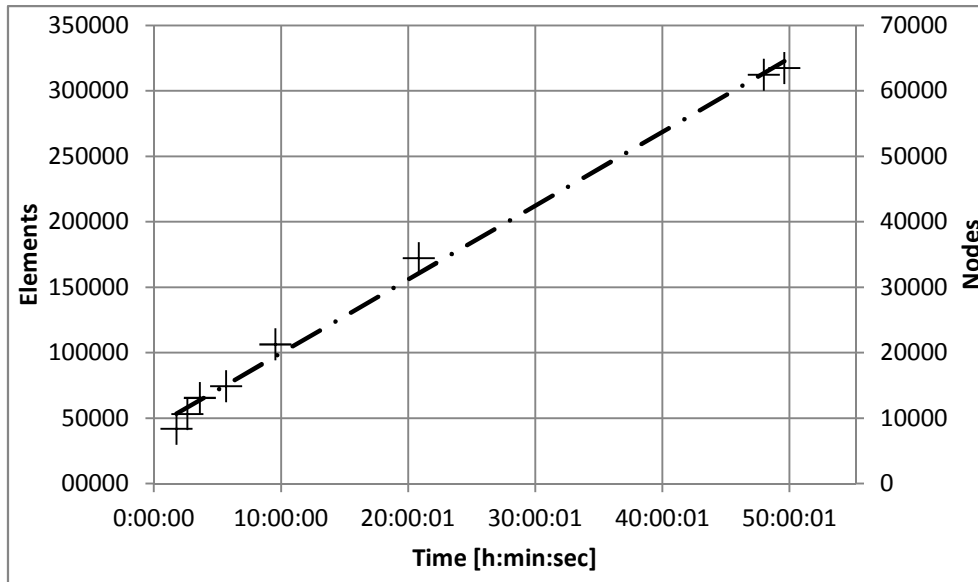


Figure 5.3 - Graphic correlation between model size and computational time (dot-dashed line refers to linear trendline).

Figure 5.4 and Figure 5.5 display the pressure maps achieved with the simulation. The analysis of the results shows a good uniformity of the pressures and no trend in the maximum values. The socket prototype stresses the inguinal area, independently from the mesh size; and, when seed mesh of the residuum is bigger than 6, the outer part of the hip is overstressed with pressures values above 150 KPa. The residuum mesh with seed equal to 8 leads to results that differ significantly from the rest of the simulations. Finer mesh (residuum seed that goes from 3 to 5) seems to have a similarity in results but they emphasize a non-uniform contact between socket and residuum in numerical simulation.

After the considerations exposed above and thanking into account the simulation runtimes (see Table 5.1), it was decided to do adopt S3R elements with seed equal to 8 for the socket and C3D4 elements with seed equal to 6.3 for the residual limb (bones and residual limb)

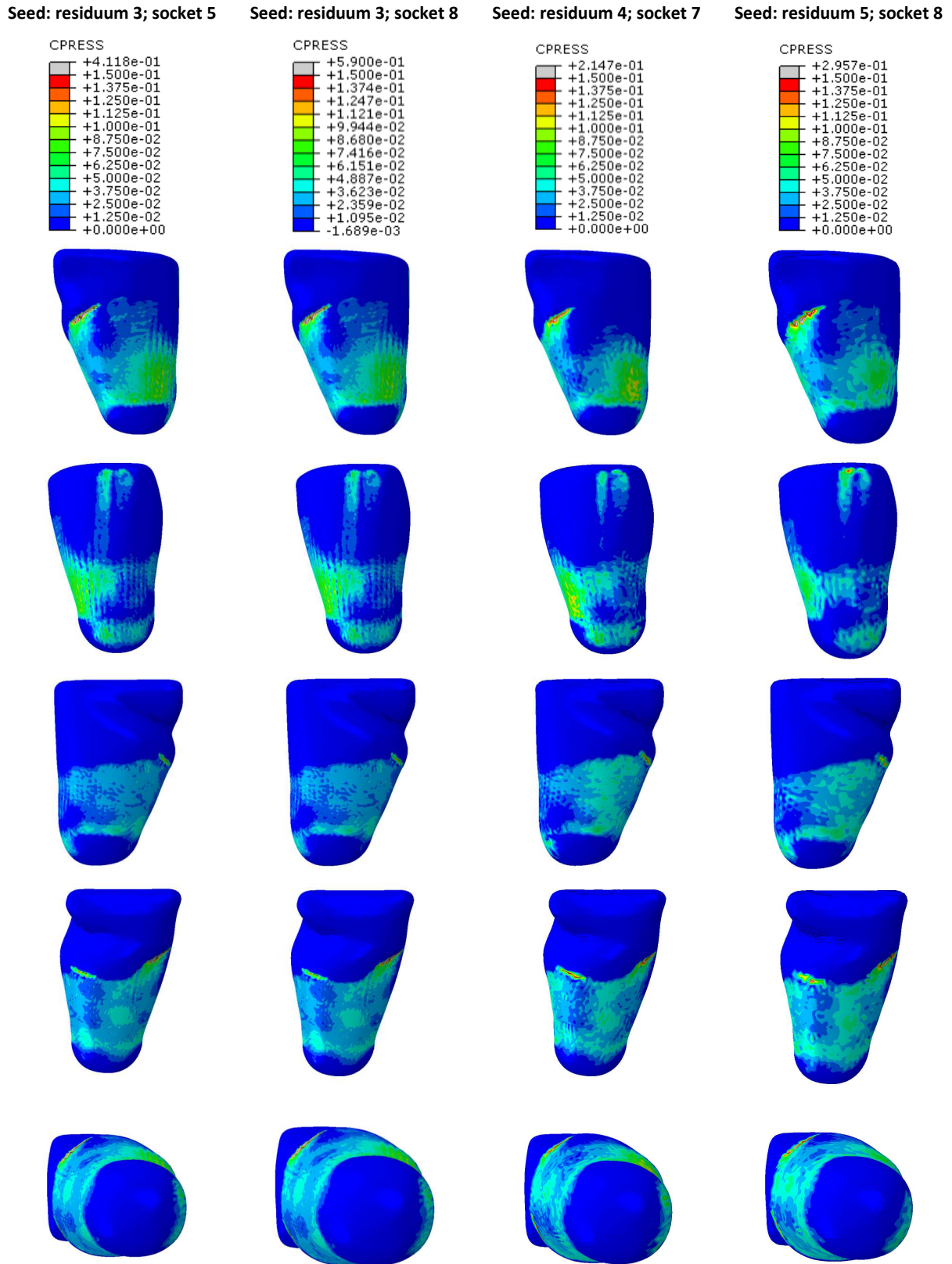


Figure 5.4 - Simulation results with different mesh size (from 3 to 5): legenda (first row), yx view (second row), zy view (third row), xy view (fourth row),yz view (fifth row), zx view (sixth row).

Seed: residuum 6; socket 8 Seed: residuum 6.4; socket8 Seed: residuum 7; socket 8 Seed: residuum 8; socket 8

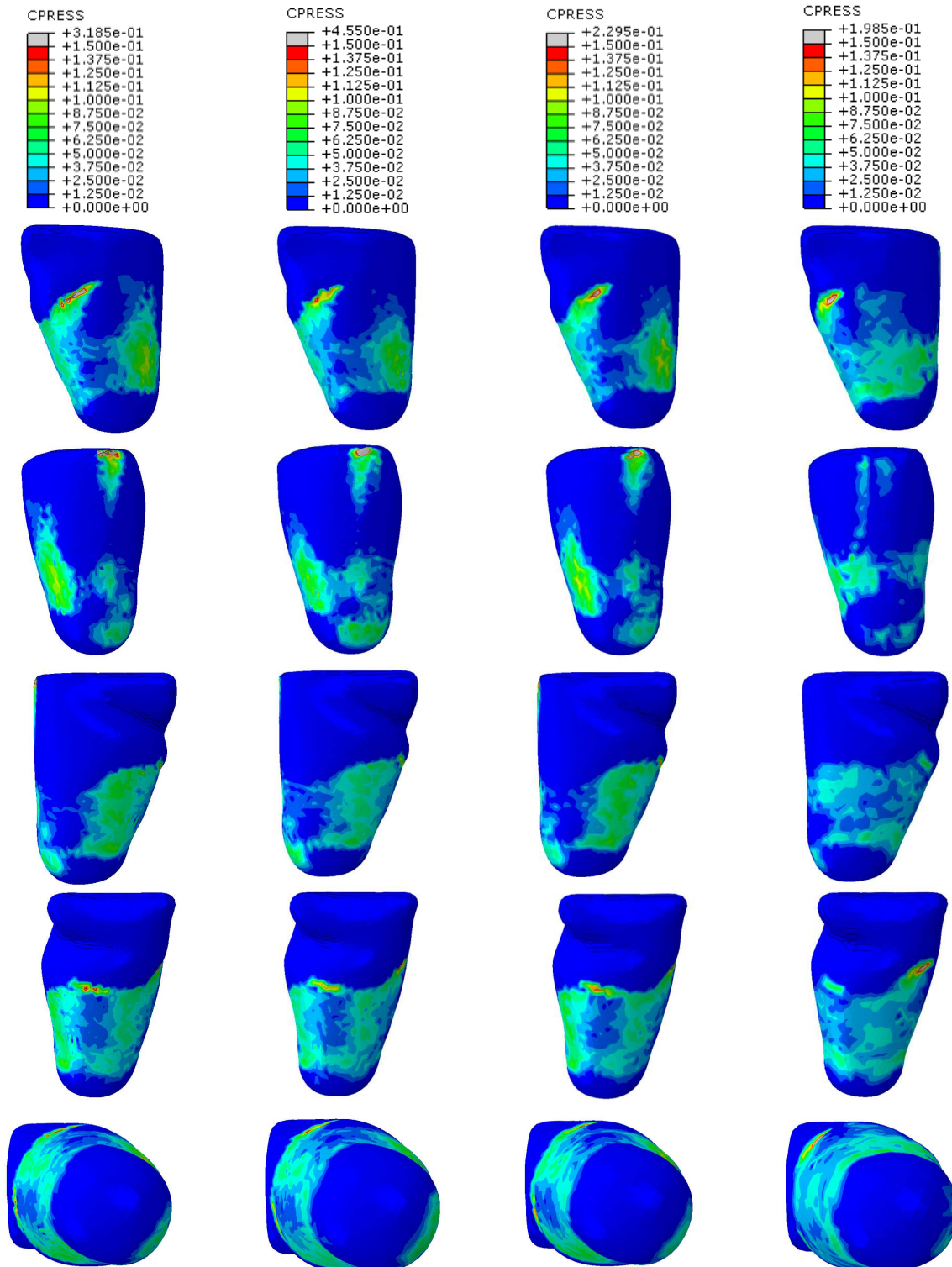


Figure 5.5 - Simulation results with different mesh size (from 6 to 8): legenda (first row), yx view (second row), zy view (third row), xy view (fourth row),yz view (fifth row), zx view (sixth row)

5.2.3 Material properties

Rules. Soft tissue ($\rho=1.48 \text{ Kg/dm}^3$; $E=0.2 \text{ MPa}$; $\nu= 0.49$). Bones ($\rho=2.0 \text{ Kg/dm}^3$; Rigid body). Socket ($\rho=7.8 \text{ Kg/dm}^3$; Rigid body).

Material characterization of soft tissues is one of the main parameters that influence FE model results. The preliminary FE model considered the soft tissues with a linear elastic behaviour, limiting in such a way the computational time. Table 5.2 summarizes linear mechanical properties adopted to characterize socket, bone, and soft tissues (i.e., density, Young's modulus, and Poisson's ratio), according to Jia et al. [10, 53] and Lee et al. [54]. On the basis of these values, socket prototype and bony structures have been considered as rigid bodies, as also supposed by other researches [69, 71, 73]. In fact, the deformations of the socket and the bones can be neglected without losing crucial information about the pressure interface, because Young's modulus of these parts is five orders of magnitude greater than soft tissue ones [69].

The state of the art emphasized that non-linear elastic description should permit a better approximation of soft tissue behaviour. So, in order to understand advantage and disadvantage, this characterization has been investigated. Different non-linear models have been considered: Kovacs' model [15], Portnoy's model [70] and nonLINEARmaterial model.

Table 5.3 reports the second order coefficients of Mooney-Rivlin hyperelastic characterizations.

Table 5.4 summarizes the simulation runtime and Figure 5.6 portrays the pressure distribution on the residuum after the simulation of loading phase.

Table 5.2 - Mechanical properties for linear characterization.

Part	Density [Kg/dm^3]	Young's modulus [MPa]	Poisson's ratio
Socket	7.8	15000	0.3
Bones	2.0	10000	0.3
Soft tissue	1.48	0.2	0.49

Table 5.3 - Second order coefficients of Mooney-Rivlin hyperelastic model used for the characterization of soft tissues.

Referents	C_{01} [MPa]	C_{10} [MPa]	D_1 [MPa^{-1}]
Kovacs et al. [15]	0.003	0.001	0.1667
Portnoy et al. [70]	0.00425	0	2.36
nonLINEARmaterial	0.0167	0.0167	0.6

nonLINEARmaterial coefficients are obtained from the formulas suggested by Simulia Italy:

$$C_{01} = C_{10} = \frac{E}{8(1 + \nu)} ; D_1 = \frac{6(1 - 2\nu)}{E}$$

Table 5.4 - Simulation time for the entire process according to material characterization.

Material model	linearMATERIAL	Kovacs et al.	Portnoy et al.	nonLINEARmaterial
[h min]	3h 36'	107h 50'	31h 27'	33h 08'

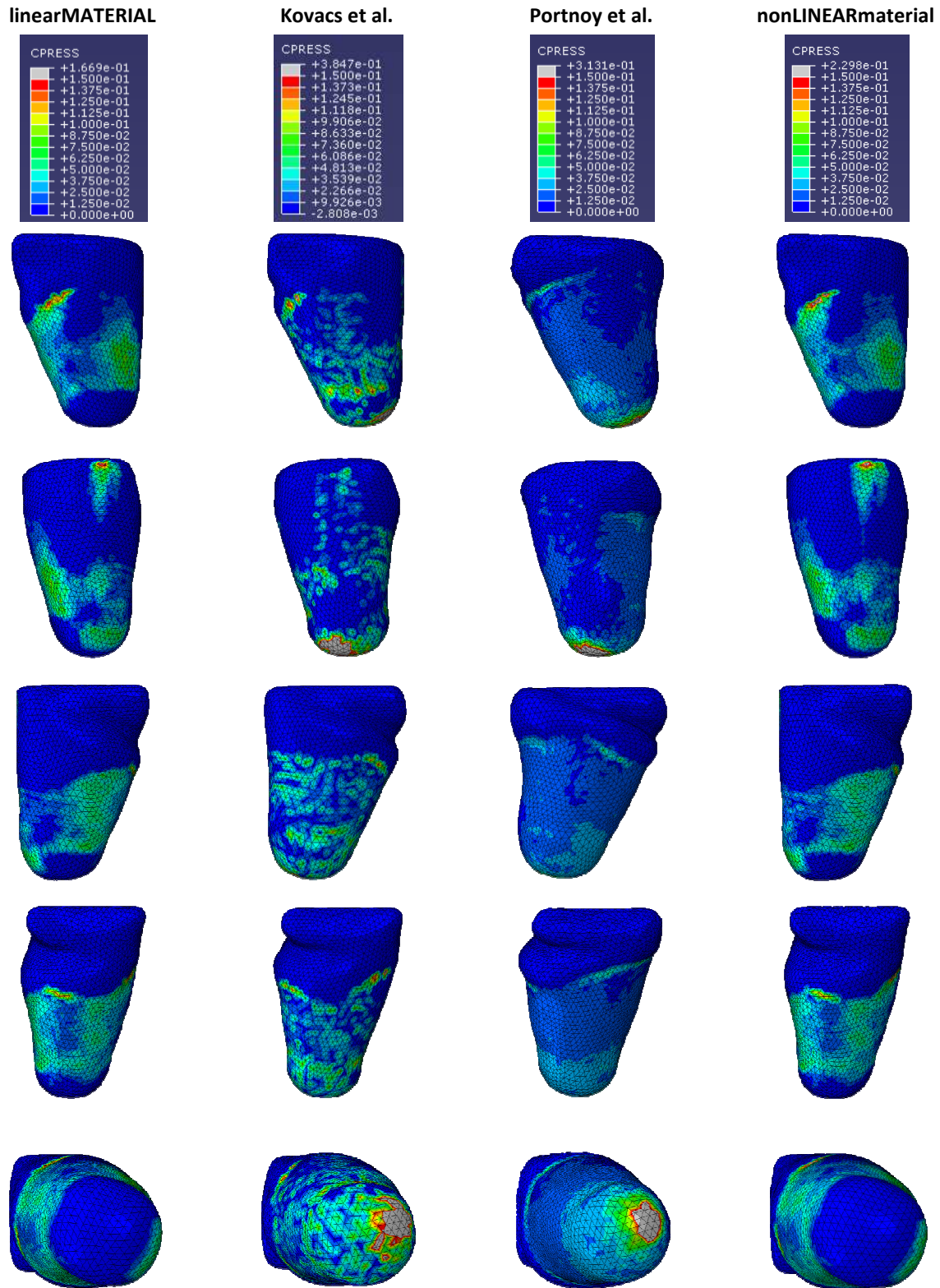


Figure 5.6 - Simulation results with different model material: legenda (first row), yx view (second row), zy view (third row), xy view (fourth row), yz view (fifth row), zx view (sixth row).

A first analysis of the results based on the maps of pressure (Figure 5.6), you may notice that the pressures values remain well below 500kPa, a critical threshold identified for the transtibial cases, but some differences can be highlighted.

The nonlinear model of Kovacs presents computational time exorbitant (reported in Table 5.4) and the inconsistent pressure distribution might suggest convergence problems of the results.

The Portnoy's nonlinear model presents a uniform distribution of pressure contact, but far beneath the expected values. The excessive deformation of the residuum causes an overstress area at the final part of the residuum that should remain off-load. Furthermore, the parameters that characterize the model are questionable due to the fact that one of the terms is assumed to be zero, making the characterization more linear than non-linear.

The pressures distribution in linearMATERIAL and nonLINEARmaterial is similar and this is presumably related to the fact that the non-linear model is derived from the linear one. Thus, the results similarity suggest that the derived nonlinear model is computational inconvenient.

Non-linear models were confirmed computationally disadvantageous. The tested coefficients of Mooney-Rivlin characterization have not proved to improve the results accuracy, requiring further investigations. According to these considerations, the soft tissues model is characterized with linear elastic, homogeneous and isotropic properties.

5.2.4 Boundary conditions and analysis steps

Rules. Explicit analysis of the contact interaction during the donning and the loading (static or dynamic) phases. Residuum fixed in the upper area, translations and loads applied to the socket. Friction considered just during the loading phase and equal to 0.4.

The simulation is performed in three phases corresponding to the deformation stages of soft tissues using explicit simulation (Figure 5.7). The first step replicates the donning of residual limb into the socket and it imposes a pre-stress on the residuum. Then, the adjustment step follows to reach a better repositioning of the socket around the residuum and to obtain maximum comfort. In the third and final step, static or dynamic loads are applied to the centre of mass of the socket. In dynamic load, the forces, computed by gait analysis, permit to simulate the single-leg stance over the phase from Initial Loading Response to Terminal Stance. The interaction with the DHM system is not indispensable, it is possible to consider the static load, equivalent to the patient's body weight on a single leg, applied as concentrated load in vertical direction.

Boundary conditions and loads have been defined according to the simulation step. The donning simulation is carried out fixing the upper residuum surface and moving the socket proportionally to the residual limb length, causing the pre-stress on the external tissues. This choice is due to limit computational costs and because the socket relative adaptive movements are not known a priori. In the adjustment step, the upper residual limb surface is still fixed; the socket is free to translate and rotate in all directions with the exception of the vertical one, which is kept locked until the load phase to prevent elastic spring back due to fitting. During these first two steps, no external load is applied. Socket translation and patient's weight are not applied instantly, but gradually during the analysis step to avoid excessive acceleration and then high mass inertia.

To model the interaction between residuum and socket, the automated surface-to-surface contact element was adopted since it is better than the traditional point-to point contact pairs, as reported by Wu et al. [64]. According to the master-slave contact formulation and hard contact relationship used in

Abaqus, donning and adjustment steps are friction-free, while during loading the friction coefficient is equal to 0.4, within the range of value documented by Zhang and Mak [88].

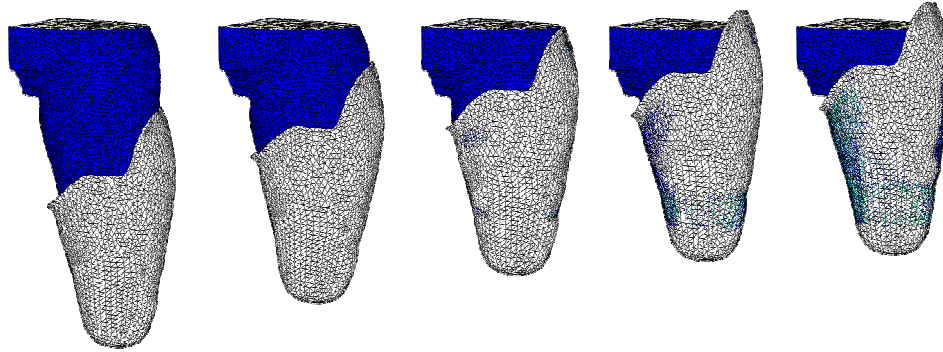


Figure 5.7 - Example of the simulation steps: from the initial position to the end of phase static load.

5.2.5 Evaluation parameters

Parameters. Pressure values on the residuum surface according to the critical area (Figure 5.8 and Figure 5.9) and pressure thresholds (Table 5.6).

The pressure distribution at the socket-residuum interface is the adopted parameter to evaluate the socket shape, and it should not exceed the pain threshold in order to be tolerated for a certain time period. From the analysis of the state of the art, a map of the critical areas both for transtibial and transfemoral has been identified (Figure 5.8 and Figure 5.9); in addition, pressure values of pain thresholds and pain tolerance have been found for the transtibial case (Table 5.6).

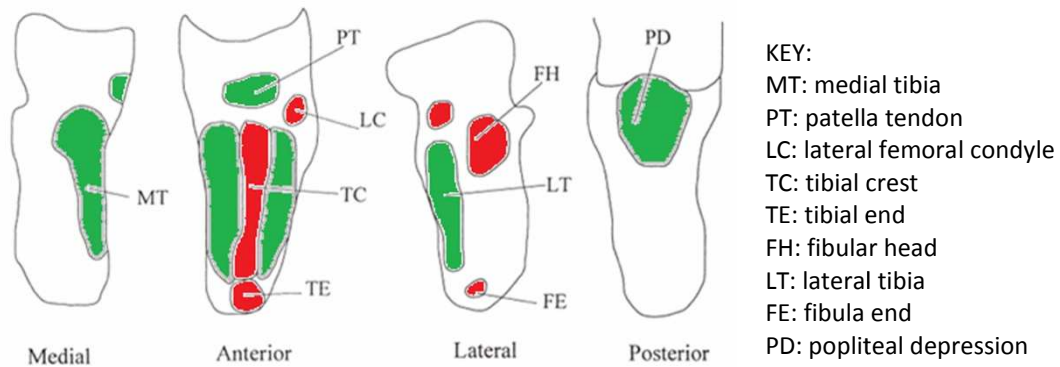


Figure 5.8 – Critical areas of transtibial residual limb (in green the load areas and red the off-load areas) [65].

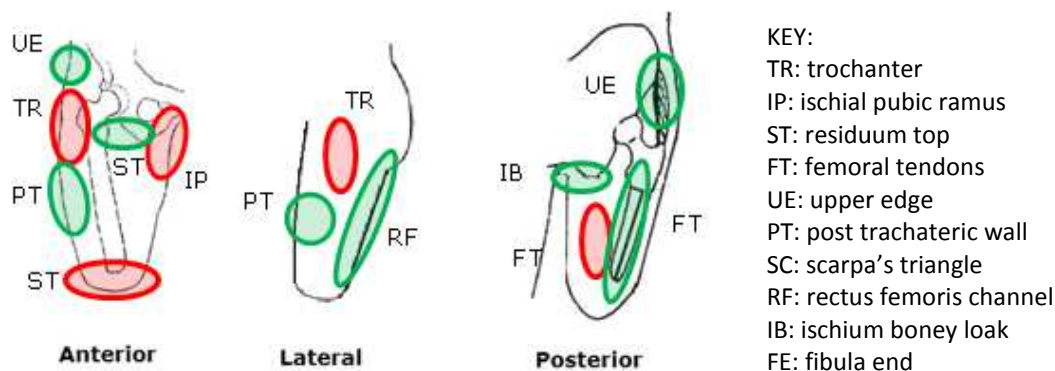


Figure 5.9 – Critical areas of transfemoral residual limb (in green the load areas and red the off-load areas).

Table 5.5 - Pressure pain threshold and pain tolerance in different transtibial residuum regions [64].

Pressure (kPa)	Fibula head	Medial condyle	Popliteal depression	Distal area	Patella tendon
Pain threshold	599.6±82.6	555.2±132.2	503.2±134.2	396.3±154.5	919.6±161.7
Pain tolerance	789.8±143.0	651.0±111.1	866.6±77.3	547.6±109.1	1158.3±203.2

5.3 Module Implementation

In order to integrate the finite element analysis within the Virtual Testing Lab, it is necessary to implement a set of instructions embedded within the systems to create automatically the FE model and to execute the analysis. This operation can be done using a scripting code, a programming language written for a specific run-time environment that permits to automate tasks. Abaqus consents to interpret, compile, and execute these set of commands stored inside the script. Specifically, Abaqus script is an extension of the popular object-oriented language called Python.

The Abaqus Scripting Interface allows you to bypass the graphical user interface (GUI) and to communicate directly with the kernel by a script file that contains the commands, as illustrated in Figure 5.10. These commands allow setting automatically the FE model in the same way the model is created along with the options and settings selectable from each dialog box of the GUI. Afterwards, the kernel interprets the commands and it uses the options and settings to create an internal representation of your model.

In the following, the script that implements the simulation rules is described.

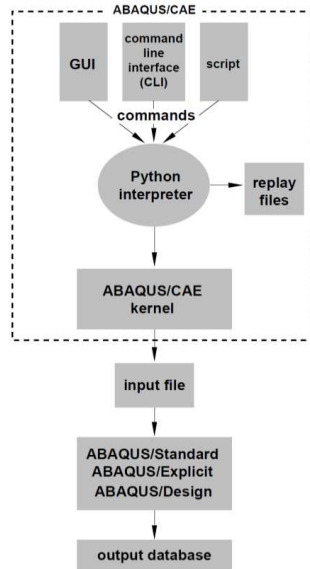


Figure 5.10 - Abaqus Scripting Interface commands and Abaqus/CAE.

Model definition and parts import

The script begins by defining the model name and all the modules that has to be imported before starting the analysis in Abaqus.

Once created the model and defined the necessary modules, the involved parts are individually imported, following default parameters related to the import settings. Socket has been defined as three-dimensional shell, while soft tissues and bone as three-dimensional solid. Vertices and edges of bone and soft tissues part are repaired in order to improve geometry precision and its validity, and to prevent any possible geometric problem during the meshing phase.

```
# PART IMPORT
# socket
mdb.openIGES('C:/... /socket.igs', msbo=True,
    scaleFromFile=OFF, topology=SHELL, trimCurve=DEFAULT)
myModel.PartFromGeometryFile(combine=False, convertToAnalytical=1,
    dimensionality=THREE_D, geometryFile=mdb.acis, name='socket_shell',
    stitchAfterCombine=False, stitchEdges=1, stitchTolerance=1.0,
    topology=SHELL, type=DEFORMABLE_BODY)
...
mdb.openIGES('C:/... /TFsoftTISSUE.igs', msbo=True, scaleFromFile=OFF,
    trimCurve=DEFAULT)
myModel.PartFromGeometryFile(combine=False, convertToAnalytical=1,
    dimensionality=THREE_D, geometryFile=mdb.acis, name='softTISSUE',
    stitchAfterCombine=False, stitchEdges=1, stitchTolerance=1.0,
    type=DEFORMABLE_BODY)
# geometry repair of soft tissue
myModel.parts['softTISSUE'].RepairInvalidEdges(edgeList=
    myModel.parts['softTISSUE'].edges)
myModel.parts['softTISSUE'].RemoveRedundantEntities(vertexList=
    myModel.parts['softTISSUE'].vertices)
...
```

Material properties

Mechanical characteristics of socket, bone and soft tissue were considered as linear elastic, homogeneous and isotropic. Table 5.6 lists the default mechanical properties used for the materials characterization. Density, Young's modulus and the Poisson's ratio are read from a file text that specifies these characteristics. If necessary, it is possible to modify the material behaviour, according to the feature of each patient, simply releasing a new text file. Every defined material is associated to a section which is assigned to the relative part.

Table 5.6 - Material properties.

Part	Density [Kg/dm ³]	Young's modulus [MPa]	Poisson's ratio
Socket	7.8	15000	0.3
Bone	2.0	10000	0.3
Soft tissues	1.48	0.2	0.49

```
# reading material txt file
fid=open("C:/... /tab_material.txt","r")
text = fid.readlines()
fid.close()

myModel.Material(name='MsoftTISSUE')
D= float(text[9])
YM= float (text[10])
PR= float (text[11])
myModel.materials['MsoftTISSUE'].Density(table=((D, ), ))
myModel.materials['MsoftTISSUE'].Elastic(table=((YM,PR), ))
...
# softTISSUE section creation and assignment
myModel.HomogeneousSolidSection(material='MsoftTISSUE', name='Section-
softTISSUE', thickness=None)
region = (myModel.parts['softTISSUE'].cells,)
myModel.parts[0].SectionAssignment( region=region,
sectionName='Section-softTISSUE')
...
```

Geometries assembly and analysis steps

After defining the coordinate system, every instance is added to the assembly.

Once included, the socket has to be translated along vertical direction, since it is already fitted on the soft tissues, and the respective value is read from a text file. This is because the socket is modelled directly on the outer surface of the residual limb within the SMA, which provides the same coordinate system to the bone, the soft tissues and the socket.

Follow the Boolean operation of merge about the geometries of soft tissues and bone, which allows creating a single domain, called *Residuum*, characterized by two different mechanical properties. In this case, the original instances are deleted.

Finally, the three analysis steps are defined: *Step-donning*, *Step-adjustment* and *Step-loading*; that come after the Initial step. The time period of each step has been assigned on the basis of convergence complexity.

```
# MODEL ASSEMBLY
# set of coordinate system
myModel.rootAssembly.Instance(dependent=ON, name='bone-1',
part=myModel.parts['bone'])
myModel.rootAssembly.Instance(dependent=ON, name='softTISSUE-1',
part=myModel.parts['softTISSUE'])
```



```

# socket vertical translation
fid=open("C:/... /lenght.txt","r")
value = fid.read()
fid.close()
length = float(value)
myModel.rootAssembly.translate(instanceList=('socket_shell-1', ),
    vector=(0.0, -length, 0.0))
# bone & soft tissue merge
myModel.rootAssembly.InstanceFromBooleanMerge(domain=GEOMETRY,
    instances=(myModel.rootAssembly.instances['softTISSUE-1'],
    myModel.rootAssembly.instances['bones-1']), keepIntersections=ON,
    name='Residuum-1', originalInstances=SUPPRESS)

# STEPS DEFINITON
myModel.ExplicitDynamicsStep(name='Step-donning', previous='Initial',
    timePeriod=4.0)

```

Model interactions

It starts with the definition of the rigid bodies, in this case bone and socket, which expects to enter the geometric region and the point of reference. The identification of the reference points is required exclusively for the characterization of rigid bodies. It is possible to specify any nodes of the part because the reference point is subsequently moved to the centre of mass of the body to which it assigned at the start of the analysis. Furthermore, the socket region is selected considering all the faces, while for defining the bone as rigid body it is necessary specify cells that compose the part by the mask command.

The *IntProp-frictionLESS* contact property characterizes the contact model without friction during the donning and arrangement steps; while the *IntProp-friction* throughout the loading phase and its value is read from a text file (default value is equal to 0.4). In both cases, normal behaviour of default is set as hard contact, which is the surfaces transmit no contact pressure unless the nodes of the slave surface contact the master surface, no penetration is allowed at each constraint location and there is no limit to the magnitude of contact pressure that can be transmitted when the surfaces are in contact.

The next step is to select the surfaces that become in contact during the analysis. The properties of the contact model changes during the simulation according to the step analysis.

The contact is a surface-to-surface type, its mechanical constraint formulation is described with a penalty contact method and the sliding formulation is finite. The contact model sets the socket as master surface, because it a rigid body, while the outer residuum surface as slave.

```

# INTERACION
# SOCKET rigid body
myModel.rootAssembly.ReferencePoint(point=
    myModel.rootAssembly.instances['socket_shell-1'].vertices[0])
r1 = myModel.rootAssembly.referencePoints
refPoints1=(r1[10], )
region1=regionToolset.Region(referencePoints=refPoints1)
faces1 = myModel.rootAssembly.instances['socket_shell-1'].faces
region2=regionToolset.Region(faces=faces1)
myModel.RigidBody(name='Constraint-socket', refPointRegion=region1,
    bodyRegion=region2, refPointAtCOM=ON)
...
# CONTACT MODELS
# reading friction values txt file
fid=open("C:/... /friction.txt","r")
value = fid.read()
fid.close()
frictionvalue=float(value)

```

```

myModel.ContactProperty('IntProp-friction')
myModel.interactionProperties['IntProp-friction'].
  NormalBehaviour(allowSeparation=ON,
  constraintEnforcementMethod=DEFAULT, pressureOverclosure=HARD)
myModel.interactionProperties['IntProp-friction'].
  TangentialBehaviour(dependencies=0, directionality=ISOTROPIC,
  elasticSlipStiffness=None, formulation=PENALTY, fraction=0.005,
  maximumElasticSlip=FRACTION, pressureDependency=OFF,
  shearStressLimit=None, slipRateDependency=OFF,
  table=((frictionvalue, ), ), temperatureDependency=OFF)

# SURFACE CONTACT DEFINITION
myModel.interactions['CP-1-Residuum-1-socket_shell-1'].setValues(
  clearanceRegion=None, datumAxis=None, initialClearance=OMIT,
  interactionProperty='IntProp-frictionLESS',
  mechanicalConstraint=PENALTY, sliding=FINITE)
myModel.interactions['CP-1-Residuum-1-socket_shell-1'].
  setValuesInStep(interactionProperty='IntProp-friction',
  stepName='Step-carico')

```

Boundary conditions

Boundary conditions (BCs) are related to the analysis steps and could change during the whole simulation. To set boundary conditions is necessary to select element surfaces and then to assign geometric constraints or load values.

During the whole analysis, movements of the upper surfaces of the residuum and the bone are not allowed (in Abaqus language they are “encastres”).

The socket boundary conditions are set in order to simulate the donning, the arrangement and, finally, the possibility to apply loads. In the first step, the socket translation is the same used in the assembly phase but it is accomplished following a motion law (amplitude), called *Amp-donning*, in order to avoid high inertia forces. The further steps leave the socket free to move but avoiding elastic return caused by residuum deformation. The BCs through the loading step is set according to the load type, static or dynamic.

```

# BOUNDARY CONDITIONS
# SOCKET
# socket-donning
myModel.SmoothStepAmplitude(data=((0.0, 0.0), (4.0, 1.0)), name='Amp-
  donning', timeSpan=STEP)
a = myModel.rootAssembly
r1 = a.referencePoints
refPoints1=(r1[10], )
region = regionToolset.Region(referencePoints=refPoints1)
myModel.DisplacementBC(name='calzata', createStepName='Step-donning',
  region=region, u1=0, u2=lenght, u3=0, ur1=UNSET, ur2=UNSET,
  ur3=UNSET, amplitude='Amp-donning', fixed=OFF,
  distributionType=UNIFORM, fieldName='', localCsys=None)

```

The loads definition depends on the analysis scenario, it is possible simulate the patient’s weight on the socket (static load) or during the stance phase of the gait (dynamic load). Once chosen the type of simulation, the other is automatically excluded. In both cases the load values are read from text file, for the stance phase of the gaits each component is stored in a single text file.

In static load, the patient’s weight is set as load and it is applied according to a smooth motion law and starting from the 25% of the total weight. While, in stance simulation, the read values define the specific motion law, one for each direction, which is respectively applied to a unitary force.

```
# FORCES
# static weight
fid=open("C:/... /load.txt","r")
value = fid.read()
fid.close()
L = float(value)

myModel.SmoothStepAmplitude(data=((0.0, 0.25), (2.0, 1.0)), name='Amp-
loading', timeSpan=STEP)
a = myModel.rootAssembly
r1 = a.referencePoints
refPoints1=(r1[10], )
region = regionToolset.Region(referencePoints=refPoints1)
myModel.ConcentratedForce(amplitude='Amp-loading', cf2=L,
createStepName='Step-loading', distributionType=UNIFORM,
localCsys=None , name='load', region=region)
...
# dynamic weight
fid=open("C:/... /load-x.txt","r")
text = fid.read()
fid.close()
myModel.TabularAmplitude(data=((text) ), name='Amp-x', timeSpan=STEP)

a = myModel.rootAssembly
r1 = a.referencePoints
refPoints1=(r1[10], )
region = regionToolset.Region(referencePoints=refPoints1)
myModel.ConcentratedForce(amplitude='Amp-x', cf1=1,
createStepName='Step-loading', distributionType=UNIFORM,
localCsys=None , name='load_X', region=region)
```

Mesh

The meshing process follows an automatic technique due to the strong non-linearity of the geometries. Every part has a specific shape and type of element, and the discretization parameters: size, deviation factor and minimum size factor. These values, summarized in Table 5.7, are saved in a text file, but can be modified according to the user specifications or if non-conforming elements invalidate the analysis.

Table 5.7 - Mesh characteristics: element type, seed value, deviation factor and minimum size factor

	Residuum	Socket
Element type	Tetrahedral (C3D4)	Triangular (S3R)
Seed value [mm]	6.4	8
Deviation factor	0.3	0.1
Minimum size factor	0.5	0.1

```
# reading mesh txt file
fid=open("C:/... /mesh.txt","r")
text = fid.readlines()
fid.close()

S_residuum= float(text[4])
```

```

dF_residuum= float (text[5])
mSF_residuum= float (text[6])

# residuum
myModel.parts['residuum-1'].seedPart(deviationFactor=S_residuum,
    minSizeFactor=mSF_residuum, size=S_residuum)
pickedRegions = myModel.parts['residuum-1'].cells
myModel.parts['residuum-1'].setMeshControls(elemShape=TET,
    regions=pickedRegions, sizeGrowth=MODERATE, technique=FREE)
elemType = mesh.ElemType(elemCode=C3D4, elemLibrary=STANDARD,
    distortionControl=DEFAULT)
pickedRegions = (myModel.parts['residuum-1'].cells,)
myModel.parts['residuum-1'].generateMesh()
myModel.rootAssembly.regenerate()

```

Study definition

Once completed the whole FE model, the settings of the study, called Job in Abaqus, are defined such as to the accuracy of the output and the CPU number to achieve the numerical simulation. The analysis is submitted and, when finished, it creates the output file with the results and a series of documents that contain the data analysis in input.

```

#JOB DEFINITION
fid=open("C:/... /patient.txt","r")
jobName = fid.readlines()
fid.close()
mdb.Job(atTime=None, contactPrint=OFF, description='', echoPrint=OFF,
    explicitPrecision=DOUBLE, getMemoryFromAnalysis=True,
    historyPrint=OFF, memory=90, memoryUnits=PERCENTAGE,
    model=modelName, modelPrint=OFF, multiprocessingMode=DEFAULT,
    name=jobName, nodalOutputPrecision=FULL, numCpus=1, numDomains=1,
    parallelizationMethodExplicit=DOMAIN, queue=None, scratch='',
    type=ANALYSIS, userSubroutine='', waitHours=0, waitMinutes=0)
mdb.jobs[jobName].submit()

```

6

Case Study

Through the adoption of a case study, a unilateral male transfemoral amputee, the new virtual process to design the prosthetic socket has been tested, from the patient's data acquisitions to the release of the socket. The patient is 51 years old, 174 cm tall, 76 kg mass; he is a very active patient and usually uses his prosthetic limb for his job as house mover and for all his daily activities.

The main objectives of this phase have been: test the whole design procedure, verify the data exchange among different integrated modules, and confirm the automatic execution of the numerical simulation.

In the following sections each step of the new design process is described: specification of the patient's case history, 3D reconstruction of the residual limb, prosthesis design (socket modelling and standard parts selection), gait analysis of the patient's avatar and numerical simulation of the socket-residuum contact interaction.

6.1 Patient's case history

The backbone of the whole system are the patient's characteristics, therefore the first step of the process consists in collecting them. The patient's characteristics are necessary for the next stages to apply rules and/or suggest the most appropriate procedures to the user during each step of the prosthesis design process.

In particular, for the case study the main characteristics can be summarized as follow:

- Excellent general health conditions.
- Residual limb has a uniform skin surface and a conical shape and excellent stability.
- Residual limb does not present pathology, bone protuberance or high skin sensibility.
- Tonicity of muscle is very good also thank to great dynamism of the patient.

Figure 6.1 portrays an example of the patient's data definition within the PML.

The screenshot shows a software window titled 'New Project' with several sections for data entry:

- Patient evaluation:** Includes fields for Name (Patient Name), Age (age), Surname (Patient Surname), Sex (MALE), Patient force (Low), Life-style (K3), and Pathologies (Yes).
- Stump evaluation:** Includes Amputation type (TT), Amputation side (Left), Stump stability (Yes), Shape (Conical), Bones protuberance (On top), Skin conditions (Normal), and Tonicity (Normal).
- Anthropometric measures:** A table of measurements:

Weight [Kg]	70
Height [mm]	1800
A) Tronchanter height [mm]	1200
B) Tronchanter-knee distance [mm]	600
C) Dist. knee joint-stump top [mm]	120
D) Knee joint height [mm]	600
E) Foot lenght [mm]	320
- Project initialization:** Includes fields for Path STL bones, Path STL stump, Path MAT bones, Path MAT stump, MRI Volume Folder, and Project path (C:/).

On the right side, there is a diagram of a human figure with various anatomical points labeled: TRH (Tronchanter height), KS (Knee joint-stump top), KH (Knee joint height), TH (Tronchanter-knee distance), FL (Foot lenght), and H (Height).

Figure 6.1 - Example of definition of the patient's characteristics.

6.2 3D reconstruction of the residual limb

As mentioned in the previous chapter, the detailed models of soft tissues and residual femur have been reconstructed from medical images acquired using MRI technique. The MRI scan parameters adopted for the case study were: T2 weighted MRI, $288 \times 288 \times 150$ voxel matrix (resolution and number of slices), pixel spacing 0.729×0.729 mm and slice thickness 2.0 mm. During the scan, the patient was laid down in supine position, and he wore the prosthesis liner.

The 3D models were generated using GEOMETRIC module, integrated in SMA. The reconstruction procedure starts with the pre-process of MRI images in order to reduce noise and digital artefacts. Then, the voxels segmentation allows identifying and generating two voxel clusters that represent the geometry of bone and of residuum external surface. Finally, the 3D geometric models are created using NURBS surfaces, whose control points are placed on the external perimeter of the cluster.

Once the geometric models are created, the module can export a standard IGES or an STL file after triangulating the NURBS surface. In particular, the geometric models for the finite element analysis are provided in IGES format because it is a neutral data format that allows data exchanged among CAD systems.

6.3 Prosthesis design

After reconstructing the 3D models of the residual limb, the virtual prosthesis has been designed according to the patient's characteristics, in correlation to the implicit experts' knowledge and the process rules implemented into the system.

By using the Socket Modelling Assistant, socket has been created following the design procedure exposed in Chapter 4.1.1. Modelling task has been performed shaping and modifying the socket silhouette using the specific tools (e.g., Sculpt Tool, Surface Tool). Once completed, the SMA exports the socket and the residuum geometric models in .IGES format and releases the text files with the characteristics to implement automatically the FE model. This step is fundamental to provide the aligned geometric models for the FE model.

Then, through the commercial 3D CAD system, the most appropriate standard components for the patient have been selected and the final assembly is created and exported. The exported files are needed to create the patient's avatar within LifeMOD and perform a virtual gait analysis.

Figure 6.2 shows the socket model at the end of the design process and the whole assembled prosthetic device.

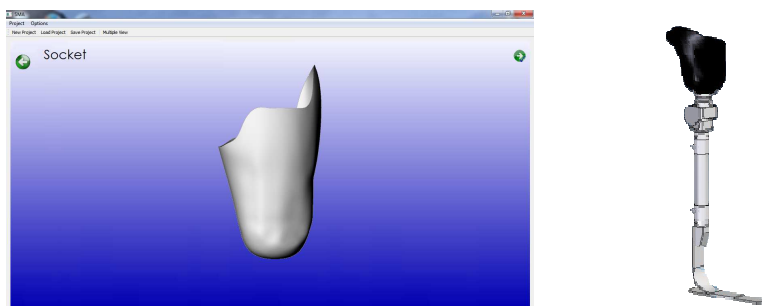


Figure 6.2 - Socket model within the SMA and complete prosthetic device.

6.4 Gait analysis

The process to perform the gait analysis of the patient's avatar follows the procedure reported in Chapter 4.3. By using LifeMOD, a detailed biomechanical model of the patient has been created also considering the whole prosthesis model. The latter is imported within the avatar model and the correct positioning is obtained taking into account the prosthesis height and the foot rotation respect to the vertical line. Once created the patient's avatar, the patient's walking has been simulated using motion laws deduced from experimental tests performed with a marker less Motion Capture equipment.

From the analysis results, the forces acting on the socket has been selected and exported separately in a text file in order to create the specific motion law associated to the force components that will be used in the FE analysis. In particular, the exported forces (portrayed in Figure 6.3) are related to the first step of the gait, which goes from initial loading response to terminal stance.

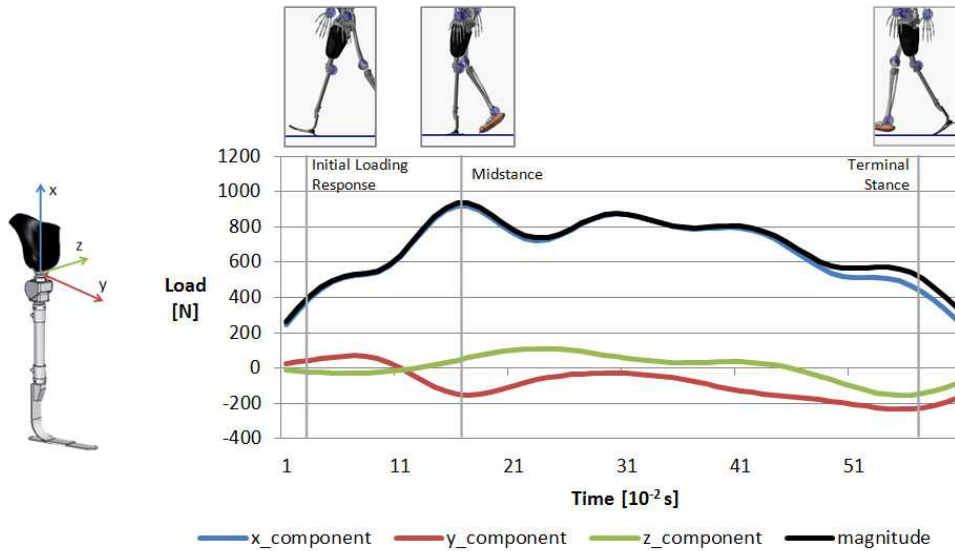


Figure 6.3 - Load components acting on the socket during stance phase: Initial Loading Response, Midstance, and Terminal Stance.

6.5 Finite element analysis

Once the digital model of the patient’s residual limb and the prosthetic socket have been created, the SMA exports the geometric models and releases the text files with the numerical model characteristics, and then it launches the script. The script automatically creates the FE model for analysing the socket-residuuum interaction, according to the implemented simulation rules, and runs the simulation. These characterization files, set by the prosthetic technician, contain the parameters that the script reads to create and to parameterize the numerical model on the basis of the patient’s characteristics. The parameters of the simulation (summarized in the Table 6.1) are:

- Patient’s weight: retrieved automatically from initial acquisition of patient’s data.
- Dynamic loads: computed by gait analysis and related to the first step from initial loading response to terminal stance.
- Material mechanical properties: selected from a database of standard values.
- Coefficient of friction: selected from a database of standard values.
- Translation values of the socket: values are computed automatically according to the size of the residual limb.

Table 6.1 - Numerical values of simulation parameters.

Patient’s weight	Coefficient of friction	Translation values
760 [N]	0.4	(0; 100; 0) [mm]

Part	Density [Kg/dm ³]	Young’s modulus [MPa]	Poisson’s ratio
Socket	7.8	Rigid body	
Bones	2.0	Rigid body	
Soft tissue	1.48	0.2	0.49

Figure 6.4 portrays the geometric models for the numerical analysis; Figure 6.5 shows the socket and the residual limb meshed; and Figure 6.6 illustrates the assemble model and the socket fixed region.

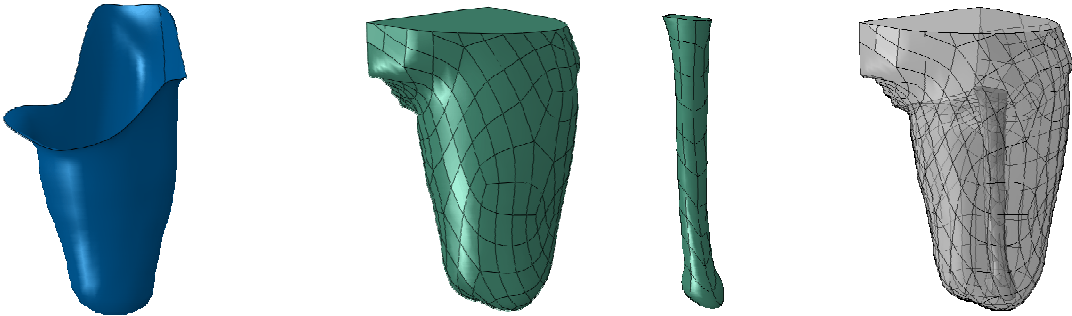


Figure 6.4 - Three-dimensional models of the socket; the residual limb and the femur; and, finally, the results of the Boolean operation of union of residuum and bone.

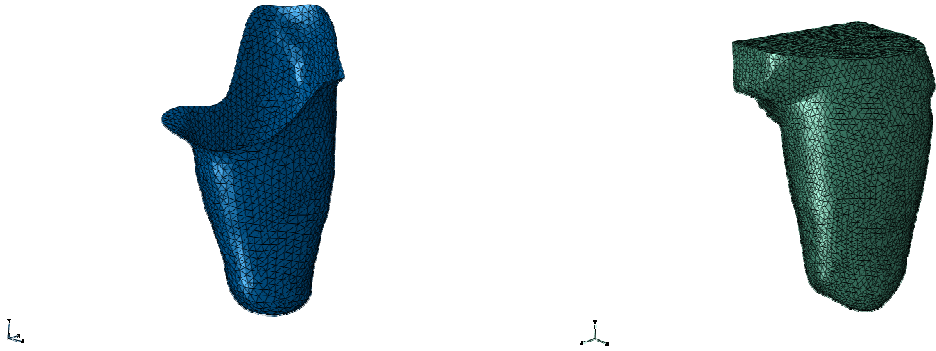


Figure 6.5 - Socket and residual limb meshed.

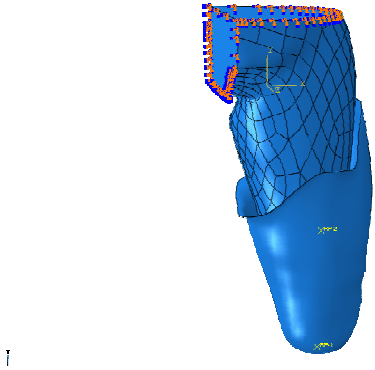


Figure 6.6 - Complete assembled model with the fixed surface contoured in orange.

6.6 Results

The results have been automatically visualized within SMA (Figure 6.7).

Figure 6.8 shows the pressure distribution over the residual limb after the simulation of the donning and the loading phases. Pressure values are associated to a colour map from blue to red with a scale of fixed values ranging from 0 to 100 kPa; the areas that exceed the maximum are coloured in gray. The pressure distribution is uniform and consistent, with the exception of post trochanteric area where during the loading phase the area increases the pressure from 116 to 178 kPa.

To decrease the pressure in post trochanteric area (a “load” region), the geometric model of the socket has been modified with the SMA (Figure 6.7) and the simulation has been re-executed. The new results, compared in Figure 6.9 with the old one, show a significant decrease of the pressure on post trochanteric wall area (111 kPa) and a pressure reduction distribution over entire stamp surface.

Finally, Figure 6.10 shows a comparison of pressure distribution during loading step in three different stance phases (Initial Loading Response, Mid-stance, and Terminal Stance) using the re-shaped socket. The pressure distribution is well distributed and homogeneous, with the exception of external trochanter area, which seems to be overstressed. During the loading step the pressure distribution increases, as it should be, without exceeding 100 kPa in most areas of the residual limb. Similar data can be found in literature, as described by Hong in [9].

According to the pressure map achieved considering both the static full weight of the patient and the single stance over the phase from Initial Loading Response to Terminal Stance, the socket shape can be validated and the prosthetic socket manufactured.

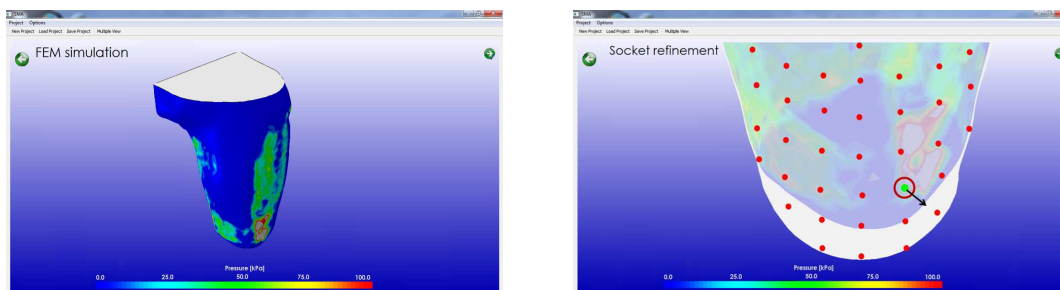


Figure 6.7 - Simulation results visualized in SMA (left) and Socket shape modification (right).

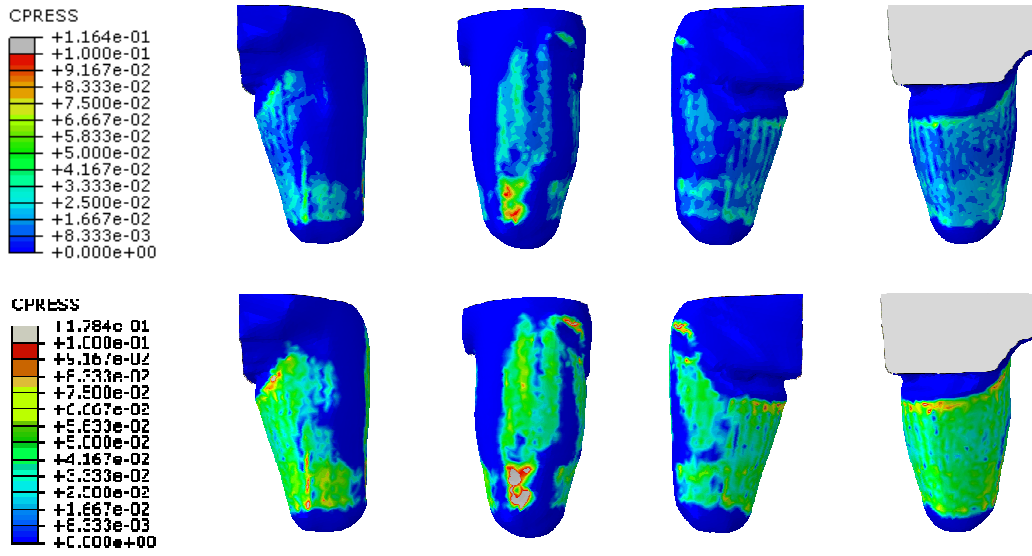


Figure 6.8 - Donning and loading simulation: front, back and side views.

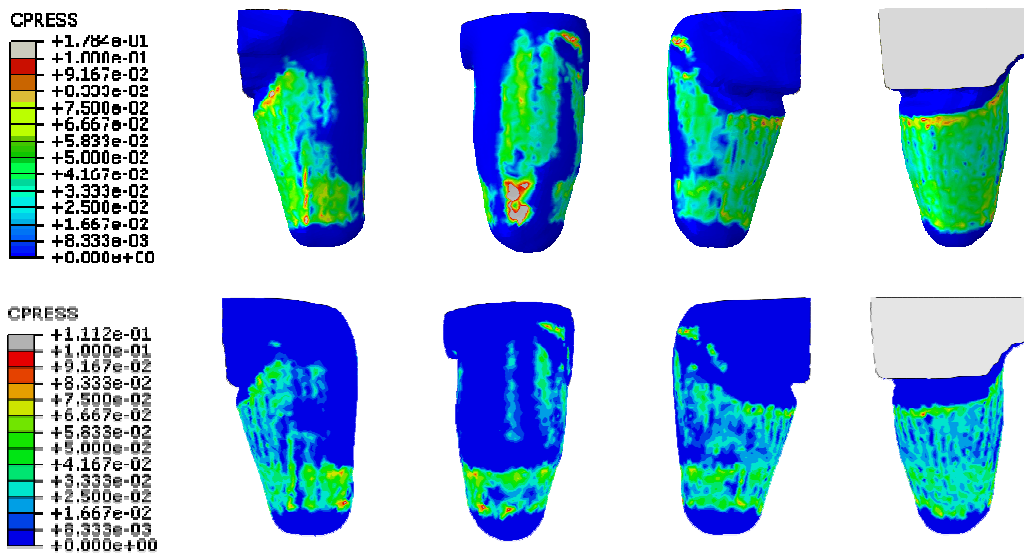


Figure 6.9 - Comparison of the pressure maps obtained with FE analysis between the preliminary socket model (first row) and the refined socket model (second row).

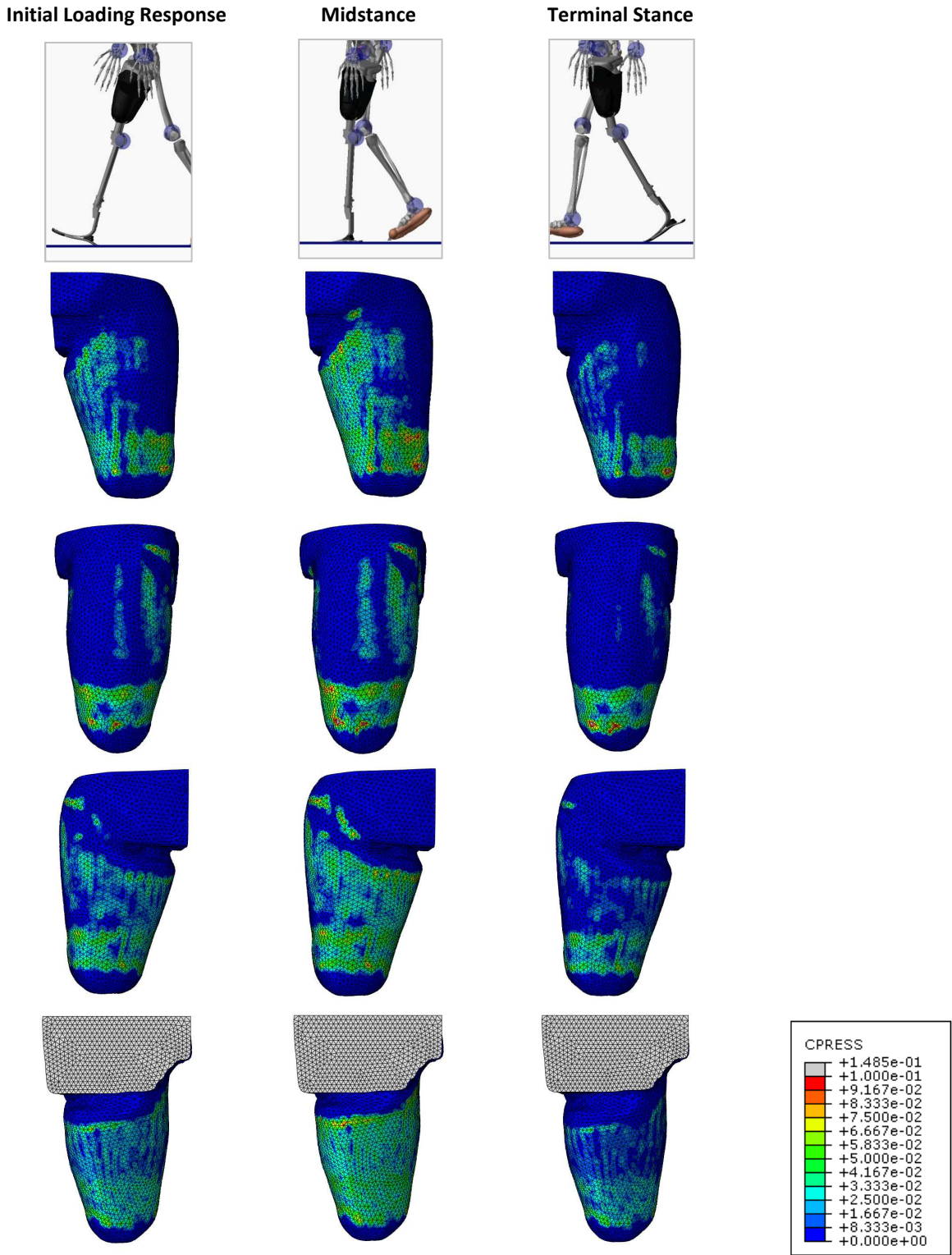


Figure 6.10 - Pressure distribution on residuum surface during loading step in three different stance phases.

To conclude, according to the analysis of the tested procedure and the obtained results, the objectives, previously mentioned, has been achieved. The whole design process proved to be adequate to design and test the socket. The data exchange among different integrated modules has been positively verified, no problems has occurred during these phases. The automatic execution of the numerical simulation has been confirmed, the script allows implementing the FE model without the user intervention.

The pressure distribution obtained with the FE analysis is comparable with the data found in literature, but the FE model should be further evaluated. In the next chapter, the issues related to FE model assessment are discussed comparing the pressures distribution over the residuum surface experimentally measured by means of pressure sensors with numerical simulation. To accomplish this task, a real prosthetic socket, designed by an expert prosthetist, has been considered.

Future tests concern the manufacturing of the socket prototype designed within new platform in order to compare its shapes with that one designed by prosthetist. The comparison will be completed considering the pressure distribution measured with pressure sensors and taking into account the viewpoint of the amputee.

7

FEA Model Assessment

As stated in the previous chapter, the FE model needs to be validated. This chapter concerns the preliminary assessment of the FEA model through the comparison of the pressures distribution over the residuum surface obtained with numerical simulation with experimental data from the pressure transducer measurements. The real socket, worn by the amputee and designed by the prosthetist of the Ortopedia Panini, has been taken into account.

First the choice of the pressure transducers system is reported. The experimental acquisition of pressures distribution is described focusing the attention on the technical specifications of the transducers, the acquisition protocol, and the calibration method. Then the FE models implementation, to numerically simulate the socket-residuum interaction, is exposed. Finally, the comparison of pressure maps from numerical analysis and from experimental measurement concludes the chapter.

7.1 Pressure sensors systems

The acquisition of the pressures distribution at the socket-residuum interface is carried out by the use of commercial pressure transducers. The choice was made after fulfilling and analysing the state of the art about commercial pressure sensors systems, that allow examining the distribution of pressure in transtibial and transfemoral sockets in non-invasive way. Thanks to their reduced thickness, these sensors can be placed inside the socket, directly in contact with the skin (or the liner), without excessively influencing the pressure measurements and, especially, without damaging the amputee's socket.

In this section the commercial sensors solutions are classified and analysed. The attention has been paid on the second-generation sensors, in particular on those specifically developed for prosthetic purposes. Both complete sensor systems and stand-alone transducers have been investigated.

Commercial sensors employ different technologies (capacitive, resistive or piezoelectric), sizes and loads ranges, sometimes customized by the user. Resistive sensors, based on the variation of the electric resistance of an element, are the most common and they are often combined with Wheatstone bridges [115]. Piezoelectric devices are based on the physical principle that a piezoelectric material induce a change or develops a voltage across itself when it is deformed by stress; they allow wide operating temperature range (up to 300°C) and high operating frequency range (up to 100kHz), but they can suffer from offset and temperature dependent operation when used in the frequency range below 5Hz [116]. Finally, capacitive sensors measure the capacitance between two or more conductors

in a dielectric environment. Capacitive pressure sensors have no turn-on temperature drift, high sensitivity and robust structure, and are less sensitive to side stress and other environmental effects [117].

The main characteristics of the compared mapping systems are summarized in Table 7.1, then, follows a description of the most interesting sensor systems, specifically developed for prosthetic use, available on market.

Table 7.1 - Commercial pressure sensors and systems.

Company	System Components	Sensor Technology	Scan rate [Hz]	Pressure Ranges [kPa]	Sensing Area [mm x mm]	Thickness	# of sensels	Sensels Density [cm ²]
Tekscan	F-Socket system (Sensor 9811E)	Resistive	160	172÷517	203.2x76.2	0.1mm	96	0.62
Tekscan	ELF 4200 Flexiforce	Piezoresistive	200	0÷62300	∅ 9.53mm	0.13mm		
Novel	Pliance®-RLS prosthesis system	Capacitive	20k	20÷600	Different sizes	<1mm		1
SensorTech	ZEBRA Thermoforming System	Resistive (Conductive polymer)	1k	0÷10300	304.8 x 16 or 29 stripes	<1mm	256-841	0.28-0.9
SensorTech	ZEBRA System	Resistive (Conductive polymer)	4	7÷698	127x127	0.2	144	0.89
SensorTech	SensorSpot Force/Pressure Sensor	Resistive (Conductive polymer)	4	0÷138 Custom Ranges	∅ 12.7÷38.1	0.76		
Vista	Prosthetic System			0÷207				
Xsensor	PX100:36.36.02 Seat	Capacitive pressure imaging		0.6÷27.6	45.7x45.7	1-1.6mm		1.7
I-CubeX	Single component	zero-travel force sensitive resistor	1k	0.4÷981	Different sizes	0.5mm		
Pressure Profile Systems	Conformable TactArray Pressure Sensor	Capacitive (Conductive cloth)	5k	0÷1400	304x304	1mm	Up to 10240	
Sensor Products Inc.	Tactilus® Stretch	Piezoresistive / Resistive	1k	0÷207	430x290	0.7mm	1024	1.6
Sensor Products Inc.	Tactilus Free Form®	Resistive	1k	0÷1380	4x44	0.36mm		

7.1.1 Novel Prosthesis System

Novel GMBH has developed Pliance®-RLS prosthesis system, portrayed in Figure 7.1, for socket evaluation and fit. It provides a quantification of the level of pressure at the residual limb/socket interface during static and dynamic movements. A maximum of 16 sensors can be attached simultaneously to the pliance socket sensor system.

Pliance®-RLS sensors are flexible and elastic and have the ability to conform very well around highly contoured sites. This is particularly advantageous in prosthetics because of the highly irregular surface and geometry of the residual limb and the shape of the socket.

The general Pliance data acquisition software operates in Windows environment and contains many tools for data collection and scientific analysis of dynamic pressure. Features include: calibrated pressure values for each individual sensor element, Center of Pressure, 2D, 3D and isobar displays; force, pressure and area-time graphs.

The company optionally offers a calibration device that allows regulating simultaneously each single sensor with homogeneous air pressure on a flat plain.



Figure 7.1 - Novel Prosthesis System: Pliance-RLS system, RLS sensors with different standard shapes.

7.1.2 SensorTech Zebra™ 3D System

SensorTech develop Zebra™ 3D System, displayed in Figure 7.2, is designed for many applications, but it fits well for prosthetic field. Differently from the previous sensors, Zebra sensor is a sheet that has to be thermoformed over the residual limb mold. After thermoforming, the sensor is placed into the socket for 3D pressure distribution measurement and the data are transmitted wirelessly, in real time, to the computer. This characteristic allows a best fitting of lower limb prosthesis and a more precise pressure mapping (i.e. determining the distribution and degree of pressure across multiple locations) of complex 3D dimensions be measured. Since sensors sheet is thermoformed, it cannot be used to acquire the pressure distribution of other patients and this increases the costs. The SensorTech offers thermoforming jig and a calibration system as optional elements.



Figure 7.2 - Zebra™ 3D System: Zebra sheet sensors and thermoformed sensors within the prosthetic socket.

7.1.3 Tekscan F-Socket™ System

F-Socket Pressure System, portrayed in Figure 7.3, consists of scanning electronics, software and patented thin-film sensors. The sensors are thin paper with high-resolution sensor placed within the socket that can be trimmed into freely floating fingers to closely approximate the curvature of the socket interface.

The F-Socket system is available with the following hardware choices: Tethered Wireless, and Datalogger. Tethered device connect the sensor and scanning electronics on the subject to the computer via USB port. Wireless tool transmutes data in real time directly from the subject to the computer, up to 100 meters away from the computer; while, datalogger allows to collect and to store sensor data in its internal memory for upload to a computer at a later time.

F-Socket Software characteristics are: 2-D and 3-D display, both real-time and recorded data; contact area, average and peak pressures; Center of Pressure and its trajectory; frame by frame data view; side-by-side comparisons of pre- and post-treatment conditions; measure distance between two points; analyse isolate and specific regions; import and export subject movie files.

A full line of equilibration devices are sold as optional by Tekscan. These devices apply a uniform pressure load across the sensor surface that is placed on a flat plain. This process electronically compensates for any variation or uneven output across individual sensing elements (sensels) caused by manufacturing or repeated use of the sensor. Equilibration devices are useful to perform quality assurance checks on the sensor and confirm uniform output by the sensor.



Figure 7.3 - F-Socket Pressure System: scanning electronics (left), software (middle) and patented thin-film sensors (right).

7.1.4 Selection of the system

Tekscan F-Socket System has been chosen according to the technical specifications of the sensors and the need to have a system ready to use. In fact, the system permits to determine contact area and dynamic stress due to the interaction of the residuum with the socket both during single stance and in various phases of gait. Moreover, the gain experience of the company on the pressure acquisition in the prosthetic socket field and the extended literature that analyses the technical performances and adopts this sensors system were crucial in this choice [96, 107, 118-120].

7.2 Pressures distribution acquisition

The pressure acquisition has been performed with the patient wearing the real socket. In particular, a copy of his socket, made by CEMPLEX (Figure 7.4), has been used. This choice has been done to avoid damages that eventually may occur during the acquisition.

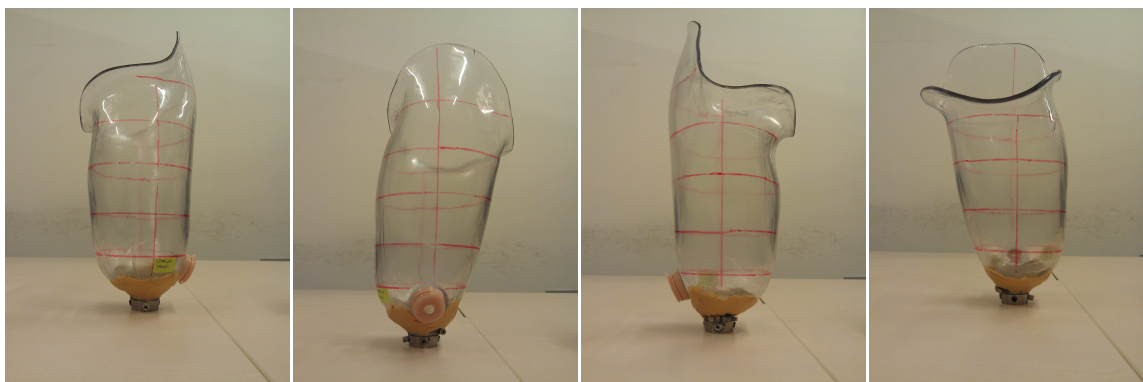


Figure 7.4 - Socket made by CEMPLEX from different views.

7.2.1 Sensors specifications

Tekscan pressure transducer is a sandwich of two sheets of plastic. The used sensors were Tekscan 9811E with an operating pressure range between 0 and 517 kPa. The sensors dimensions are 76.2 mm width, 203.2 mm length, and the thickness is 0.1mm; the sensors have 96 sensels each, placed in 6 columns and 16 rows, with a spatial resolution of the 0.62 sensels/cm². Each sensel is a force sensitive variable resistor, whose impedance changes according to the force that is applied to the sensor. The analogue to digital converter assigns a digital value between 0 and 255 (8 bit) to each sensel, depending on its impedance value, and the correlation between digital output and to engineering units (such as force or pressure) is performed through calibration process.

7.2.2 Acquisition protocol

In this section, the acquisition of the pressure distribution at the socket-residuum interface has been accomplished according to the acquisition protocol that has been defined as follows:

1. *Sensor preparation.* To achieve a better placement on complex curves of the socket surface, it is recommended to trim the sensors along specific lines not to disconnect the sensors (Figure 7.5).
2. *Sensor application.* Sensors have to be attached temporarily to the inner socket surface using an adhesive tape, in order to be removed after the acquisition. The number of the sensors is proportional to the acquisition area. It is recommended to place the sensors in an orderly manner avoiding overlaps. The application of the sensors has to be performed one strip at a time. Specifically, six sensors were adopted to cover the whole upper area of the socket surface (Figure 7.5).
3. *Preparing the patient.* The patient wears the instrumented socket being careful not to damage or mode the sensors. Since the socket was not assembled with the standards parts, it was necessary to support the patient with a trestle, whose height was set according to the amputee's leg (Figure 7.6).
4. *Conditioning sensor.* Before starting the acquisition, sensors have to be conditioned in order to give the subject an opportunity to become accustomed to the equipment and to exercise the sensors to the load. Since the patient was supported with a trestle, this operation was performed loading and unloading the residuum using just the body weight for one minute.
5. *Acquisition.* Once the sensors are connected to the system it is possible to start the acquisition. The acquisition was done in RAW format, considering a full scale range equal to 255 units. The pressures are measured during single-leg standing for 5 seconds. The conversion of pressures maps from RAW data into kPa pressure units is made after through the calibration process. This sequence permits to take into account the pressure values reached during the measurement and identify the better calibration, improving the quality of the results.

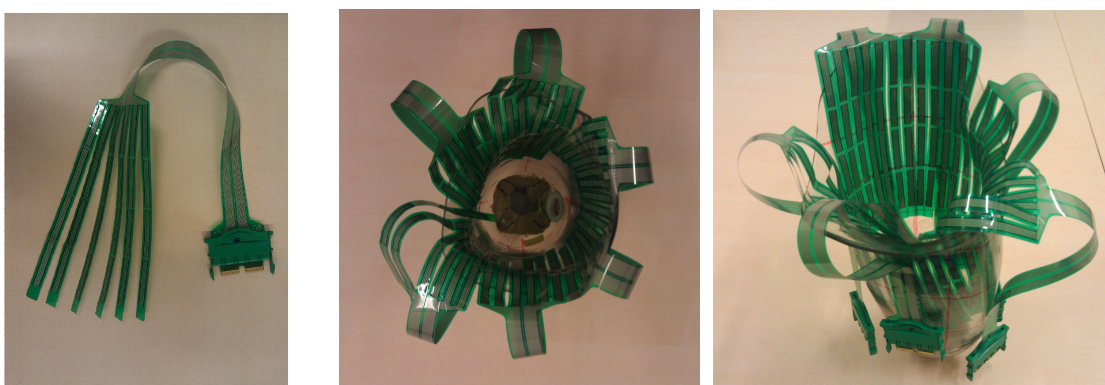


Figure 7.5 - Example of trimmed sensor (left) and sensors positioning within the socket (middle and right).



Figure 7.6 – Patient wearing the instrumented socket (left and middle) and patient with the prosthetic socket positioned on the trestle for the acquisition phase (right).

7.2.3 Calibration method

Calibration process is the method by which the raw digital output of the sensor is correlated to pressure units or in terms of force. Calibration is a sensitive and delicate process since an error in the calibration converts into an error of the measured load. The overall system accuracy is generally $\pm 10\%$ of the full scale and do not exceed 15% of the applied load [121]. Anyway, to achieve accurate calibration and to minimize errors, it is necessary to perform the calibration process in similar conditions to those that are found inside the socket, both in terms of involved materials and of pressure values.

To perform a good calibration, it is essential to operate in the conditions close to test conditions. Actually, the material stiffness strongly influences the way in which the load is applied on the sensels. Materials with low values of stiffness, like foams, distribute part of the load also on the gap existing between two consecutive sensels, reducing the stress on the sensels; while, materials with highest stiffness distribute the load mainly on the sensels. Figure 7.7 portrays the material behaviour at the sensor-interface on the basis of the material stiffness.

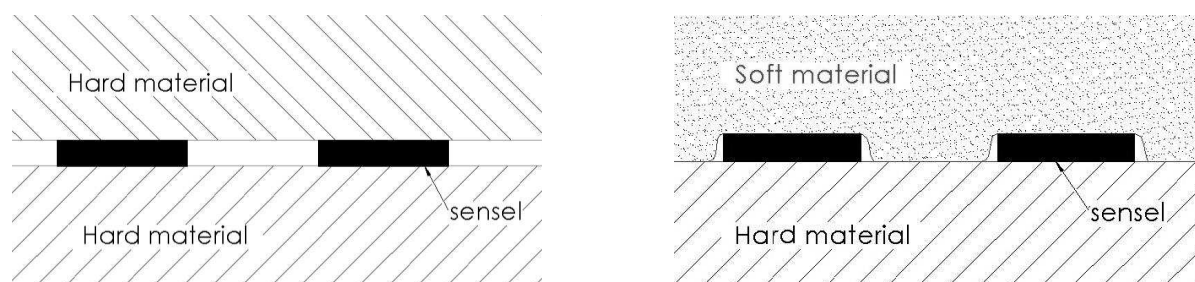


Figure 7.7 - Examples of the material behaviour at the sensor-interface according to the material stiffness: hard material (left) soft material (right).

Taking into account the pressure values developed during measurement, it is possible to know indicatively the pressure that characterizes specific socket-residuum interaction so as to adjust the calibration in order to achieve better results. Single point calibration has been adopted to calibrate linearly the pressure sensors. This means that a straight line between the two points (zero point and the calibration point) describes the behaviour of the sensor. The sensor has zero output with zero applied load and the calibration point is defined by the user applying a known force.

The calibration, to convert the RAW data into kPa, was done using a flat plate of Plexiglas with dimensions similar to the sensor (Figure 7.8). The plate stresses the sensors for 40 seconds with a known load, providing the same pressure condition of the experimentation. Each sensor has a specific calibration that is identified according to the measured RAW values. The Plexiglas support allows covering most of the sensor during calibration in order to achieve statistically representative data. In order to obtain conditions similar to the skin-sensor-socket interface, the sensors calibration was performed on a flat table (simulating the socket-sensor interaction) and using a piece of pork skin with the same size of the support to reproduce the human skin contact interaction on the sensor.

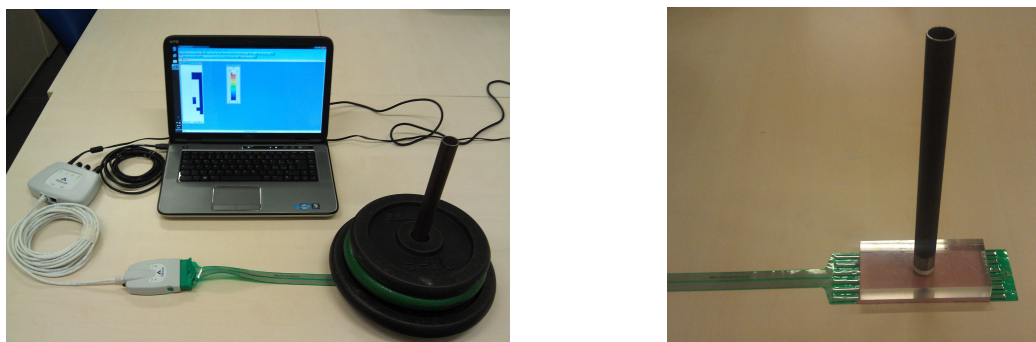


Figure 7.8 - Examples of calibration system and flat plane of Plexiglas.

The acquisition has been done in RAW format, considering a full scale range equal to 255 units, and then the calibration has been applied to each sensor according to the maximum pressure values considered in RAW format. reports the number of the acquisition associated to the sensor and the related calibration load.

Table 7.2 reports the number of the acquisition associated to the sensor and the related calibration load.

Table 7.2 - Numerical values of sensors calibration.

Area	Inner thigh	Gluteal fold	Anterior Region Thing	Femoral Triangle	Upper Antero-Trochan.	Upper Postero-Trochan.	Lower Antero-Trochan.	Lower Postero-Trochan.
Acquisition number	N03	N04	N05	N06	N07	N08	N09	N10
# sensor	3	4	5	6	1	2	1	2
Calibration load [Kg]	11	21	21	21	41	61	41	61

7.3 Finite element analysis

This section focuses the attention on the implementation of the numerical model to analyse the interaction between the residual limb and the CEMPLEX socket.

The 3D virtual model of a real socket was acquired and reconstructed by the use of the 3D scanning. Two different geometric models of the patient's residuum (soft tissues and bone) were adopted: the first is the same used for testing the design process (Chapter 6); the second is virtualized by the use of the 3D scanning, as for the CEMPLEX socket. The choice of considering two models was due to the

need to better investigate how acquisition techniques influence the simulation results and to identify the limits associated to the acquisition techniques, in particular covering MRI and 3D scanning.

7.3.1 Geometric models acquisition and reconstruction

The acquisition of the CEMPLEX socket geometry and the patient's residual limb has been done using a low cost 3D scanning system, which adopts a depth camera (Kinect for Windows) and a software tool (Skanect), in order to create 3D meshes of the product.

The process to scan the scene is quite simple and fast (Figure 7.9). Once established the dimension of the scenario and selected the predefined scanning settings, Skanect acquires dense 3D information about a scene just moving around the Kinect sensor to capture a full set of viewpoint, with a scanning rate up to 30 frames per second. After the acquisition, the system elaborates the data and it allows exporting the rough model in poly-line file format. Since the CEMPLEX socket is transparent, the inner and the outer socket surface were painted green before scanning.

The editing of the digital model of the CEMPLEX socket and the patient's residuum were done starting from a poly-line file by means of Geomagic (Figure 7.10). The software was adopted to select the points forming the inner socket surface and to reconstruct the missing areas that the acquisition system was not able to detect due to geometry, such as undercut. The entire task within Geomagic was performed manually and the final geometric models are exported in .IGES format (Figure 7.11).

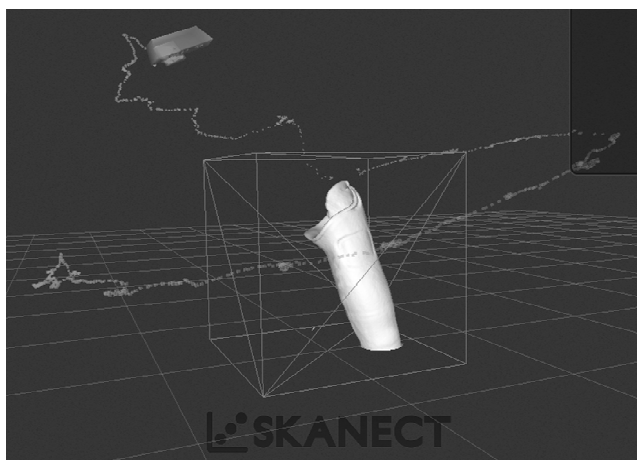


Figure 7.9 - Examples of the reconstruction phase within the Skanect.

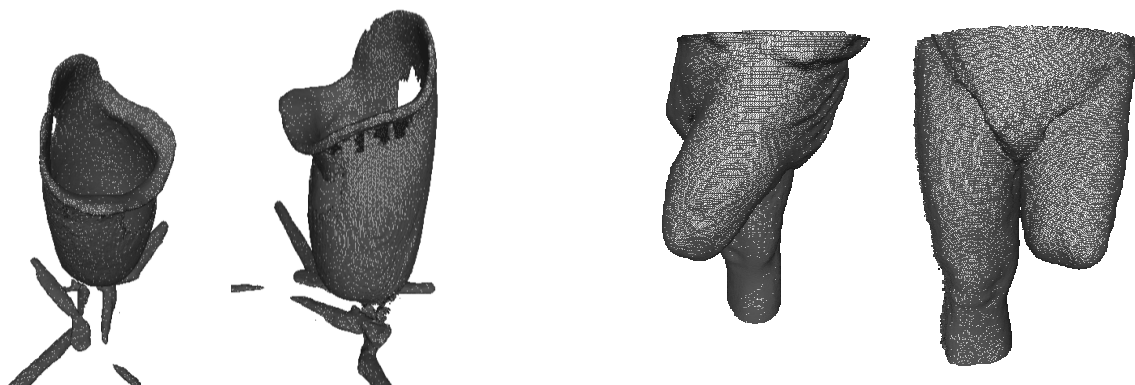


Figure 7.10 - Points cloud of the CEMPLEX socket (left) and the patient's residual limb (right) before editing phase from different views.

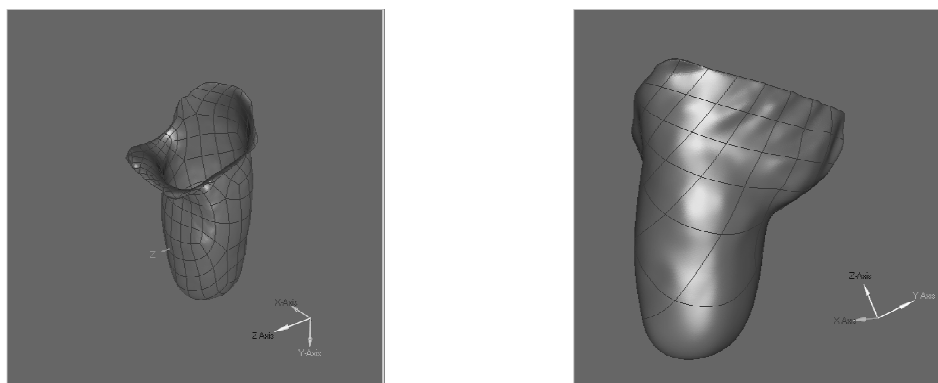


Figure 7.11 - Three-dimensional models of the CEMPLEX socket and the residuum.

7.3.2 FE analysis

The creation of the FE models was performed in two steps. The first phase concerns the identification of the correct socket alignment with the geometric model of the residual limb, the same that was used previously to test the virtual socket design process, and subsequently the magnitude and the directions of the translations to apply to the socket during the donning simulation. In the second phase, the FE model implementation was accomplished using the script file, but defining manually the numerical values of the characterization parameters (Table 7.3).

Table 7.3 - Numerical values of simulation parameters.

Patient's weight	Coefficient of friction	Translation values
760 [N]	0.4	(-10; 280; 0)* [mm] (0; 240; 0)** [mm]
		*residuum model from MRI; **residuum model from 3D scanning

Figure 7.12 shows the socket and the residual limb meshed, in Figure 7.13 the boundary conditions applied to the residuum are illustrated, and Figure 7.14 displays some steps of the analysis from the initial position to the end of static load phase.

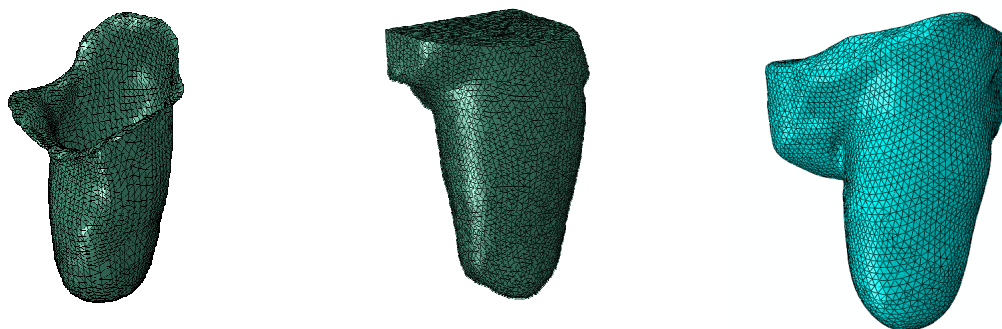


Figure 7.12 - The meshed models of the socket (left), the residual limb from MRI (middle) and the residual limb acquired with Kinect (right).

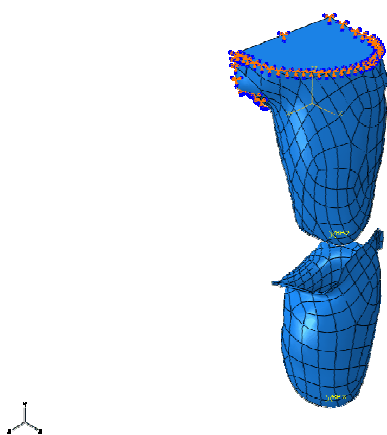


Figure 7.13 - Complete assembled model with the fixed surface contoured in orange.

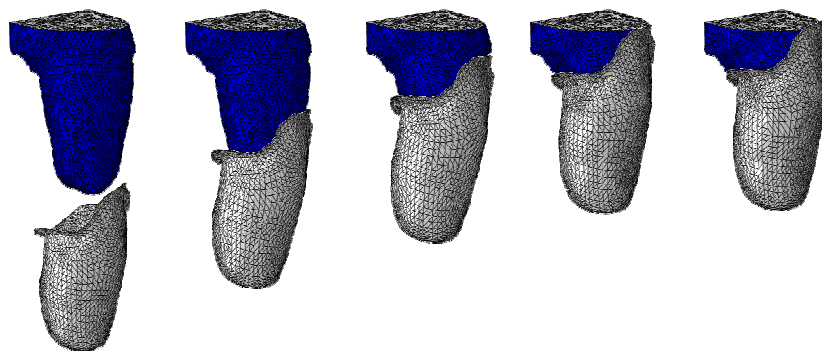


Figure 7.14 - Simulation steps of the numerical analysis from the initial position to the end of static load phase.

7.4 Comparison of the results

In this section the finite element analysis model is assessed comparing the pressure map predicted by the FE models with the one measured experimentally. The pressure values at the socket-residuum interface were measured using the Tekscan F-Socket systems, inserting the pressure transducers at the interface between socket and residuum. Thanks to the improvement in pressure transducers, the comparison has been performed in a wide areas and no longer in a limited number of points.

The pressure acquisitions consider only the full body weight on a single-leg stance. Figure 7.15 shows the pressure map whose values are associated to a colour scale from blue to red and covering a range of fixed values ranging from 0 to 240 kPa. The upper limit was chosen according to the maximum value measured by the pressure transducers. In the colour map representing the FE results, the areas that exceed the maximum value are coloured in grey. For the experimental measurements, the white colour means that the acting pressure does not exceed the operating threshold of the single transducer.

Figure 7.15 portrays the measured pressure distribution and it can be evaluated according to the load/off-load zones described in Figure 5.9. Trochanter upper area is partially unloaded, while the pressure is extended on the upper edge containment and the rectus femoral area, as it should be. The posterior areas is generally uniformly loaded except the ischium area that is quite load. The inner thigh is stressed both in the inguinal canal and the Scapa triangle areas.

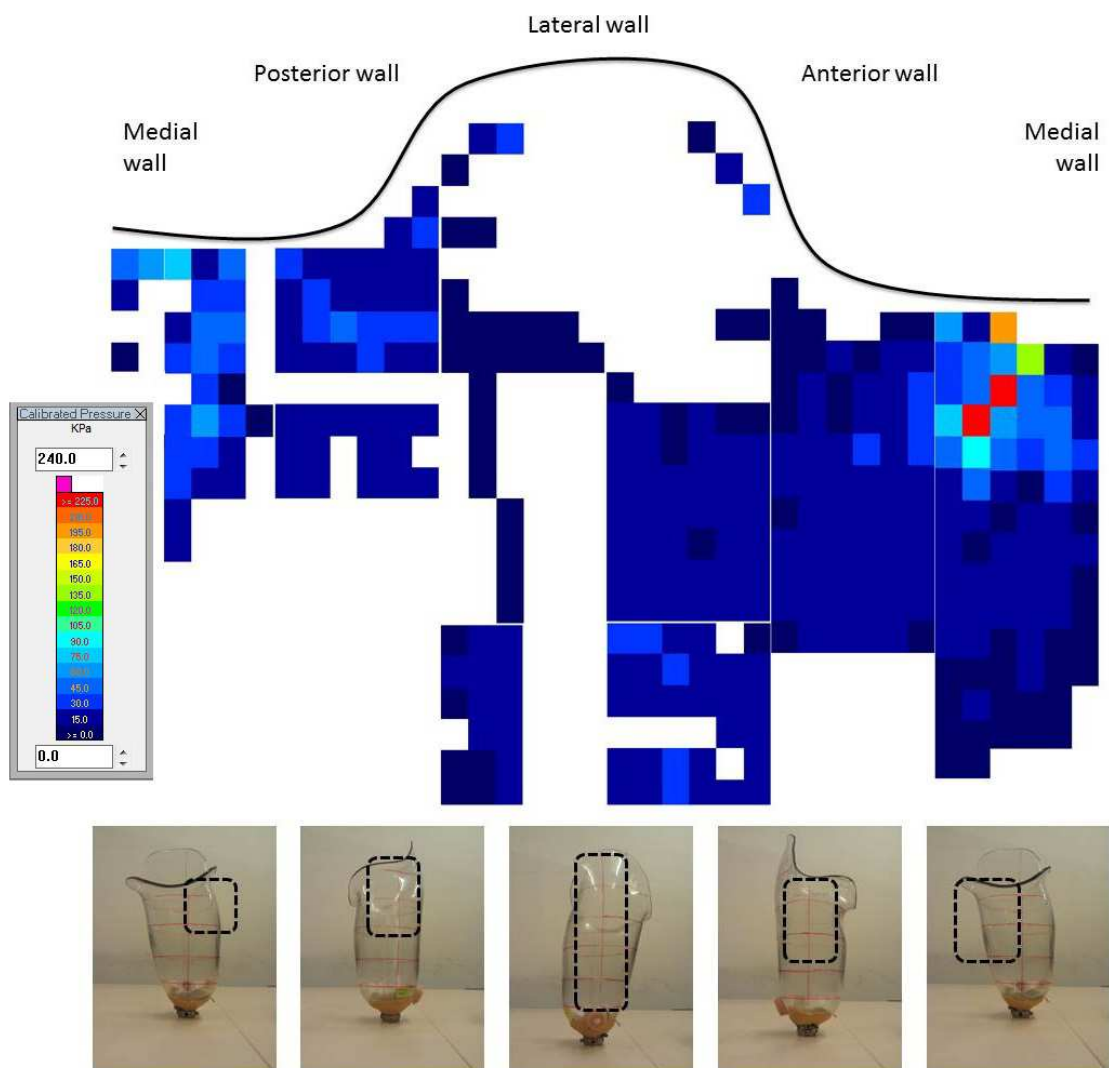


Figure 7.15 - Pressure map on the socket inner surface.

Figure 7.16 and Figure 7.17 represent the pressure map obtained with FEA simulation. Figure 7.16 refers to the residuum model acquired by the 3D scanning, while Figure 7.17 considers the residual limb model reconstructed from MRI. The load areas have similar appearance: the inguinal area and the inner thigh area are the most overloaded, also the trochanter region and the lower part of the external thigh is quite stressed.

The correlation between the pressure values predicted by the FE model with those measured experimentally confirmed the results have been the same order of magnitude; nonetheless, one-to-one correspondence has not been achieved. The predicted resultant stresses were higher than the experimental values, approximately twice.

The preliminary FE model evaluation can be considered positive, but further studies are necessary. The causes of the gap between pressure measured and pressure computed can be attributed to the geometric model of the residual limb. In both cases, residuum reconstructed from MRI and residuum reconstructed from 3D scanning, some minor geometric problems have influenced the pressure distribution on the residual surface. For example, the geometric model obtained from MRI presents a deformation on inner thigh area due to the supine position assumed during the acquisition. During the scan, the patient wore the prosthesis liner in order to reduce the residuum flatter, but it was not completely eliminated.

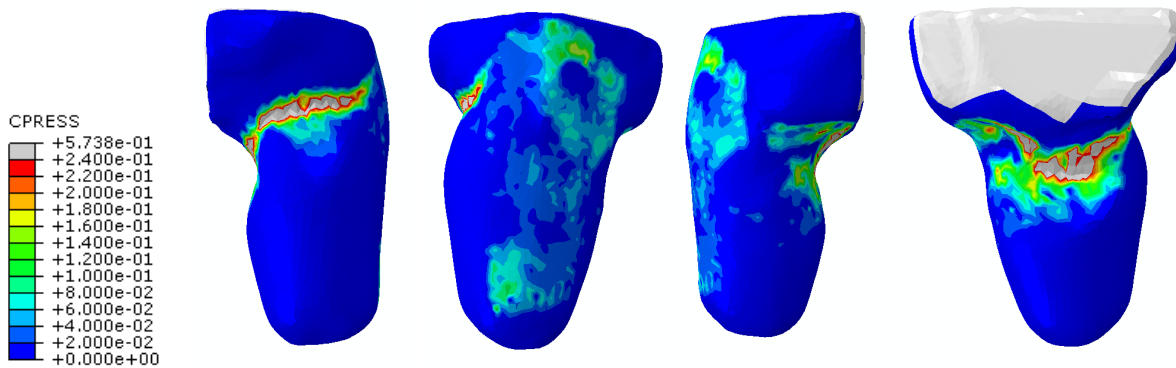


Figure 7.16 - Pressure map after the loading phase using the residuum model acquired with Kinect.

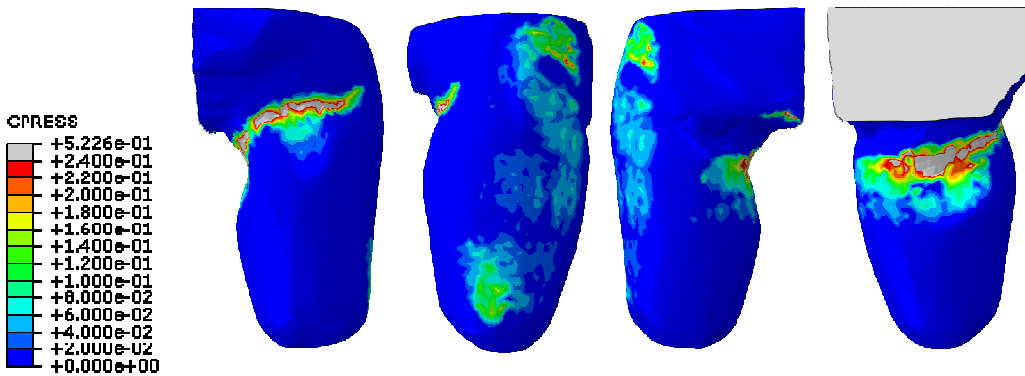


Figure 7.17 - Pressure map after the loading phase using the residuum model reconstructed from MRI.

The pressure distribution obtained with numerical simulation, considering the designed socket model, is well distributed and homogeneous (Figure 7.18). The pressure values are more similar with those measured with the pressure transducers, with the exception of the inguinal area. This result is significant and means that the design procedures and rules within the Socket Modelling Assistant can be considered adequate to model the socket shape. Actually, the socket is modelled directly on the outer residuum surface and the initial deformation is included with the final socket model, without negatively influencing the numerical analysis.

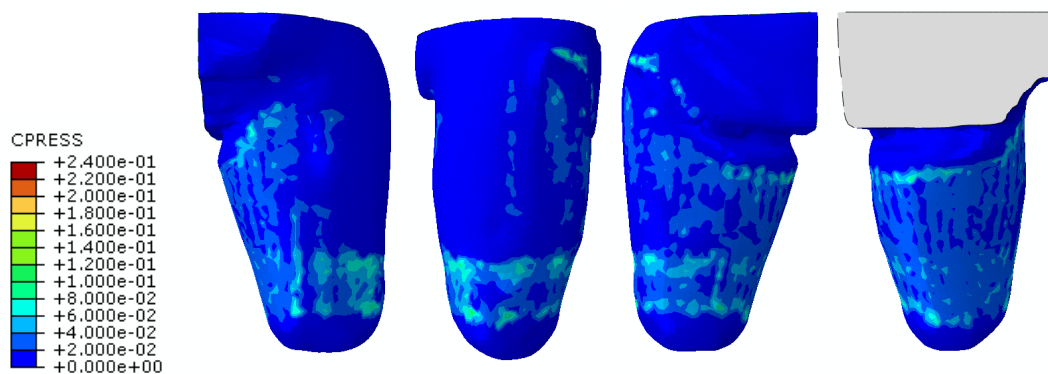


Figure 7.18 - Pressure map obtained with FE analysis considering the designed socket.

The material behaviour has a strong influence on the final results. The better way to improve the characterization of soft tissues was adopted by Silver-Thorn and Childress [72] in order to validate their results. They measured the local soft tissue properties, the local interface pressures and the load state by mounting tissue indenter and pressure transducers into the socket wall. Then, they used these parameters as input conditions into the FEA model. In this way it is possible to refine the material model in order to estimate the correct parameters. Secondly, further features could be considered to increase the FEA model; such as the identification of the specific contact conditions between the residuum-socket interface, considering also the shear stresses; the improvement of the boundary conditions; the increase of the density of discretization elements in areas where high pressures are expected and make the soft tissue parameters non-linear.

As described, the experimentation has been carried out considering a unilateral transfemoral amputee. A massive experimental campaign involving different orthopaedic labs and patients will be planned to fully validate the design platform, the FE model and the adopted acquisition techniques. Testing with different case studies will increase the quality of the process since it will allow taking into account aspects not yet considered, such as different residual limb morphologies, lifestyles and patients' needs. Finally, further acquisition of pressure distribution with Tekscan equipment will be performed and the results will be compared with those of numerical simulations as done in the preliminary step.

Conclusions

This thesis work has led to the implementation of an embedded simulation module to study the socket-residual limb interaction without the involvement of the prosthetist, thus permitting to realise a full virtual environment to design lower limb.

Starting from an extensive analysis of the state of the art about the simulation of the socket-residuum interaction, two FE models have been implemented using a commercial solver (Abaqus) and an open-source solver (CalculiX). This permitted to identify the simulation rules and the best practice procedures, select the adequate solver, and, then, define the architecture of the automatic simulation module implemented using the Python language. Furthermore, different non-linear material characterizations of soft tissues have been investigated and sensitive analysis has been performed in order to refine the FE model and reach better results.

The embedded simulation module has been integrated with the socket modelling system, namely SMA, to get the required geometric models and with LifeMOD, the DHM used to simulate and analyse the gait of the virtual patient wearing the prosthesis, to obtain the forces applied to the socket during patient's walking

The simulation procedure has been tested with a transfemoral case study. The experimental phase has been carried out to test the developed approach and procedures starting from patient's data acquisition (e.g., residuum morphology, anthropometric measures) to the release of the final socket model. The real socket of the patient has been also acquired with reverse engineering and simulated the interaction. Simulation results have been compared with those measured by pressure sensors.

From the analysis of the results some conclusive considerations have been drawn. Data exchange among the three systems (e.g., SMA, simulation module and LifeMOD) is carried out successfully and automatically. Some difficulties have been detected, such as the amputee's posture during the MRI acquisition, the creation of upper rounded edge of the socket, and the surfaces selection within the FE model. Since the real experimentation is at an early stage, simulation results have been considered positively, but further studies are required. For example, some geometric inconsistencies, occurred during the acquisition of the residual limb, have reduced the accuracy of the final results. To complete the evaluation of the FE model, a new residuum geometric model is needed and a refinement of the material model characterization is desirable.

In the following, future developments are drawn.

Future development

On the basis of the tests and mentioned problems, future activities have been identified with regards to: geometric model of the residual limb, FE model and solvers and experimental tests.

Geometric model of the residual limb

A detailed geometric model of the residual limb is a crucial issue for the whole design process and for the simulation task. It also influences the possibility to adequately evaluate the FE model, since correlation between experimental and simulation values can correctly occur only without inconsistencies in residuum geometric model. At present, the MRI acquisition requires the patient lay down in supine position, causing an alteration of the residual limb shape. This position induces a deformation around the inner thigh area, which tends to enlarge. The use of the prosthesis liner is suitable to reduce the shape distortion but it is not enough. MRI upright scanner systems, acquiring the patient in vertical position, could avoid this problem, but they are still not widespread. The 3D scanning can represent a possible solution to solve the deformations, being careful to introduce proper reference points in order to keep the alignment between bonny structure and soft tissues as demonstrated in [55, 56]. In addition, low-cost techniques are now available and have been already tested to acquire the external shape of the residuum.

FE model and solvers

A key problem concerns the surfaces selection to specify the contact regions or the boundary conditions on the residual limb. Usually the user selects interested regions through the graphical user interface. However, a different approach is required in scripting mode, i.e., the solver (Abaqus in our case) should be able to pick out automatically these areas. This problem is due to the fact that the geometric model of the residual limb is extremely different in shape and size, non-uniform and hard to standardize. Therefore, a pre-processing step is necessary to provide a model of the part with residual limb regions already defined and subdivided.

Another issue concern material characterisation. The mechanical characteristics of material, in particular the soft tissues, have been derived from literature and corresponds to a linear behaviour. Results reached so far have been considered adequate (see literature review) but to get more precise results also non-linear material characterization should be considered as well as indentation tests to determine the specific behaviour of the anatomical district. Obviously, this has an impact on the computational costs and attention must be paid since one of the overall objectives is to allow the prosthetist to get results with reasonable time. Preliminary tests and experience found in literature showed a significant increase of computational time [51, 52]. To face this problem parallel computing techniques can be employed.

Another issue concerns the contact model. At present it is assumed frictionless during the donning of the socket and adopts an average friction coefficient during the loading phase. The coefficient can significantly vary and it depends on the type of material used for the socket manufacturing, as well as from the condition of the skin. Since it influences the simulation results, it could be useful to plan an experimentation campaign to identify such behaviour.

Finally, further studies on open-source solvers are necessary to implement a design platform totally independent from commercial tools

Test campaign

As described, the experimentation has been carried out considering a unilateral transfemoral amputee. A massive experimental campaign involving different orthopaedic labs and patients will be planned to fully validate the design platform and the FE model. Testing with different case studies will increase the quality of the process since it will allow taking into account aspects not yet considered, such as different residual limb morphologies, lifestyles and patients' needs. Finally, further acquisition of pressure distribution with Tekscan equipment will be performed and the results will be compared with those of numerical simulations as done in the preliminary step.

Bibliography

1. Seymour, R., *Prosthetics and orthotics: lower limb and spinal*. 2002: Wolters Kluwer Health.
2. Ziegler-Graham, K., E.J. MacKenzie, P.L. Ephraim, T.G. Trivison, and R. Brookmeyer, *Estimating the prevalence of limb loss in the United States: 2005 to 2050*. Archives of Physical Medicine and Rehabilitation, 2008. 89(3): p. 422-429.
3. Gabbiadini, S., *Knowledge-based design of lower limb prosthesis*. 2011.
4. Shuxian, Z., Z. Wanhua, and L. Bingheng, *3D reconstruction of the structure of a residual limb for customising the design of a prosthetic socket*. Medical Engineering & Physics, 2005. 27(1): p. 67-74.
5. Smith, D.G., J.W. Michael, J.H. Bowker, and A.A.o.O. Surgeons, *Atlas of amputations and limb deficiencies: surgical, prosthetic, and rehabilitation principles*. 2004: American Academy of Orthopaedic Surgeons Rosemont, IL.
6. Bowker J.H., G.B., Poonekar P.D., *Atlas of Limb Prosthetics: Surgical, Prosthetic, and Rehabilitation Principles*.
7. Buzzi, M., G. Colombo, G. Facchetti, S. Gabbiadini, and C. Rizzi, *3D modelling and knowledge: Tools to automate prosthesis development process*. International Journal on Interactive Design and Manufacturing, 2012. 6(1): p. 41-53.
8. Facchetti, G., S. Gabbiadini, G. Colombo, and C. Rizzi, *Knowledge-based system for guided modeling of sockets for lower limb prostheses*. Computer-Aided Design and Applications, 2010. 7(5): p. 723-737.
9. Colombo, G., G. Facchetti, C. Rizzi, A. Vitali, and A. Zanello, *Automatic 3D Reconstruction of Transfemoral Residual Limb from MRI Images*, in *Digital Human Modeling and Applications in Health, Safety, Ergonomics, and Risk Management. Human Body Modeling and Ergonomics*, V. Duffy, Editor. 2013, Springer Berlin Heidelberg. p. 324-332.
10. Jia, X.H., M. Zhang, X.B. Li, and W.C.C. Lee, *A quasi-dynamic nonlinear finite element model to investigate prosthetic interface stresses during walking for trans-tibial amputees*. Clinical Biomechanics, 2005. 20(6): p. 630-635.
11. Zheng, Y.P., A.F.T. Mak, and A.K.L. Leung, *State-of-the-art methods for geometric and biomechanical assessments of residual limbs: A review*. Journal of Rehabilitation Research and Development, 2001. 38(5): p. 487-504.
12. Webb, S., *The physics of medical imaging*. 1988, Taylor & Francis.
13. Commean, P.K., K.E. Smith, J.M. Cheverud, and M.W. Vannier, *Precision of surface measurements for below-knee residua*. Archives of Physical Medicine and Rehabilitation, 1996. 77(5): p. 477-486.

14. Madsen, M., J. Haller, P. Commean, and W. Vannier, *A device for applying static loads prosthetic limbs of transtibial amputees during spiral examination*. Journal of Rehabilitation Research and Development, 2000. 37(4): p. 383-387.
15. Kovacs, L., M. Eder, S. Volf, S. Raith, M. Pecher, H. Pathak, C. Müller, and F. Gottinger. *Patient-Specific Optimization of Prosthetic Socket Construction and Fabrication Using Innovative Manufacturing Processes: A Project in Progress*. in *Materialise World Conference 2010*. Leuven, Belgium.
16. Bui, A.A.T. and R.K. Taira, *Medical imaging informatics*. 2009, Springer Verlag.
17. Kalender, W.A., *Principles and applications of spiral CT*. Nuclear medicine and biology, 1994. 21(5): p. 693-699.
18. Bui, A.A. and R.K. Taira, *Medical imaging informatics*. 2010: Springer.
19. Alberini, J.L., V. Edeline, A.L. Giraudet, L. Champion, B. Paulmier, O. Madar, A. Poinsignon, D. Bellet, and A.P. Pecking, *Single Photon Emission Tomography/Computed Tomography (SPET/CT) and Positron Emission Tomography/Computed Tomography (PET/CT) to Image Cancer*. Journal of Surgical Oncology, 2011. 103(6): p. 602-606.
20. Dougherty, G., *Digital image processing for medical applications*. 2009: Cambridge University Press.
21. Buis, A.W.P., B. Condon, D. Brennan, B. McHugh, and D. Hadley, *Magnetic resonance imaging technology in transtibial socket research: A pilot study*. Journal of Rehabilitation Research and Development, 2006. 43(7): p. 883.
22. Torres-Moreno, R., D. Jones, S.E. Solomonidis, and H. Mackie, *Magnetic resonance imaging of residual soft tissues for computer-aided technology applications in prosthetics - A case study*. Journal of Prosthetics and Orthotics, 1999. 11(1): p. 6-11.
23. He, P., K. Xue, and P. Murka, *3-D imaging of residual limbs using ultrasound*. Development, 1997. 34(3): p. 269-278.
24. Douglas, T., S. Solomonidis, W. Sandham, and W. Spence, *Ultrasound imaging in lower limb prosthetics*. Neural Systems and Rehabilitation Engineering, IEEE Transactions on, 2002. 10(1): p. 11-21.
25. He, P., K. Xue, Q. Chen, P. Murka, and S. Schall, *A PC-based ultrasonic data acquisition system for computer-aided prosthetic socket design*. Rehabilitation Engineering, IEEE Transactions on, 1996. 4(2): p. 114-119.
26. He, P., K. Xue, Y. Fan, and Y. Wang, *Test of a vertical scan mode in 3-D imaging of residual limbs using ultrasound*. Development, 1999. 36(2).
27. Xue, K., P. He, and Y. Wang. *A motion compensated ultrasound spatial compounding algorithm*. 1997: IEEE.
28. Sansoni, G., M. Trebeschi, and F. Docchio, *State-of-The-Art and Applications of 3D Imaging Sensors in Industry, Cultural Heritage, Medicine, and Criminal Investigation*. Sensors, 2009. 9(1): p. 568-601.
29. AutoSculpt. *Infinity CAD Systems*. Accessed June 2013; Available from: <http://www.infinitycadsystems.com>.
30. R4D-CADCAM. *Rodin4D*. Accessed June 2013; Available from: <http://www.rodin4d.com>.
31. BioShape. *BioSculptor*. Accessed June 2013; Available from: <http://biosculptor.com>.
32. Rogers, B., G.W. Bosker, R.H. Crawford, M.C. Faustini, R.R. Neptune, G. Walden, and A.J. Gitter, *Advanced trans-tibial socket fabrication using selective laser sintering*. Prosthetics and Orthotics International, 2007. 31(1): p. 88-100.

33. OrtenShape. *Orten*. Accessed April 2013; Available from: <http://www.orten.fr/>.
34. Prothesis-Stem. *Proolutions GmbH*. Accessed June 2013; Available from: <http://www.proolutions.net/en>.
35. CANFIT. *Vorum Research Corporation*. Accessed June 2013; Available from: <http://www.vorum.com>.
36. OMEGA. *The Ohio Willow Wood Company*. Accessed July 2013; Available from: <http://www.willowwoodco.com/>.
37. Lin, C.C., C.H. Chang, C.L. Wu, K.C. Chung, and I.C. Liao, *Effects of liner stiffness for trans-tibial prosthesis: a finite element contact model*. *Medical Engineering & Physics*, 2004. 26(1): p. 1-9.
38. Zhang, M., A.F.T. Mak, and V.C. Roberts, *Finite element modelling of a residual lower-limb in a prosthetic socket: a survey of the development in the first decade*. *Medical Engineering & Physics*, 1998. 20(5): p. 360-373.
39. Sewell, P., S. Noroozi, J. Vinney, and S. Andrews, *Developments in the trans-tibial prosthetic socket fitting process: a review of past and present research*. *Prosthetics and Orthotics International*, 2000. 24(2): p. 97-107.
40. Mak, A.F.T., M. Zhang, and D.A. Boone, *State-of-the-art research in lower-limb prosthetic biomechanics-socket interface: A review*. *Journal of Rehabilitation Research and Development*, 2001. 38(2): p. 161-173.
41. Baars, E.C.T. and J.H.B. Geertzen, *Literature review of the possible advantages of silicon liner socket use in trans-tibial prostheses*. *Prosthetics and Orthotics International*, 2005. 29(1): p. 27-37.
42. Amali, R., S. Noroozi, J. Vinney, P. Sewell, and S. Andrews, *Predicting interfacial loads between the prosthetic socket and the residual limb for below-knee amputees - A case study*. *Strain*, 2006. 42(1): p. 3-10.
43. Amali, R., S. Noroozi, J. Vinney, P. Sewell, and S. Andrews, *An artificial intelligence approach for measurement and monitoring of pressure at the residual limb/socket interface - a clinical study*. *Insight*, 2008. 50(7): p. 374-383.
44. Amali, R., S. Noroozi, J. Vinney, P. Sewell, and S. Andrews, *A novel approach for assessing interfacial pressure between the prosthetic socket and the residual limb for below knee amputees using artificial neural networks*. *INNS-IEE International Joint Congress Neural Networks*, 2001: p. 2689-2693.
45. Sewell, P., S. Noroozi, J. Vinney, R. Amali, and S. Andrews, *Improvements in the accuracy of an Inverse Problem Engine's output for the prediction of below-knee prosthetic socket interfacial loads*. *Engineering Applications of Artificial Intelligence*, 2010. 23(6): p. 1000-1011.
46. Frillici F.S., R.P., Rizzi C., Rotini F., *The role of simulation tools to innovate the prosthesis socket design process*. *Cardiff University*, 2008: p. 214-219.
47. Faustini, M.C., R.R. Neptune, and R.H. Crawford, *The quasi-static response of compliant prosthetic sockets for transtibial amputees using finite element methods*. *Medical Engineering & Physics*, 2006. 28(2): p. 114-121.
48. Goh, J.C.H., R.S. Lee, S.L. Toh, and C.K. Ooi, *Development of an integrated CAD-FEA process for below-knee prosthetic sockets*. *Clinical Biomechanics*, 2005. 20(6): p. 623-629.
49. SilverThorn, M.B., J.W. Steege, and D.S. Childress, *A review of prosthetic interface stress investigations*. *Journal of Rehabilitation Research and Development*, 1996. 33(3): p. 253-266.

50. Zachariah, S.G. and J.E. Sanders, *Interface mechanics in lower-limb external prosthetics: a review of finite element models*. IEEE Trans Rehabil Eng, 1996. 4(4): p. 288-302.
51. Tonuk, E. and M.B. Silver-Thorn, *Nonlinear elastic material property estimation of lower extremity residual limb tissues*. Ieee Transactions on Neural Systems and Rehabilitation Engineering, 2003. 11(1): p. 43-53.
52. Tonuk, E. and M.B. Silver-Thorn, *Nonlinear viscoelastic material property estimation of lower extremity residual limb tissues*. Journal of Biomechanical Engineering-Transactions of the Asme, 2004. 126(2): p. 289-300.
53. Jia, X.H., M. Zhang, and W.C.C. Lee, *Load transfer mechanics between trans-tibial prosthetic socket and residual limb - dynamic effects*. Journal of Biomechanics, 2004. 37(9): p. 1371-1377.
54. Lee, W.C.C., M. Zhang, X.H. Jia, and J.T.M. Cheung, *Finite element modeling of the contact interface between trans-tibial residual limb and prosthetic socket*. Medical Engineering & Physics, 2004. 26(8): p. 655-662.
55. Colombo, G., S. Filippi, C. Rizzi, and F. Rotini, *A new design paradigm for the development of custom-fit soft sockets for lower limb prostheses*. Computers in Industry, 2010. 61(6): p. 513-523.
56. Cugini, U., M. Bertetti, D. Bonacini, G. Colombo, C. Corradini, and G. Magrassi, *Innovative implementation in socket design: digital models to customize the product*. Proceedings of ArtAbilitation, 2006: p. 54-61.
57. Zhang, M., Y.P. Zheng, and A.F.T. Mak, *Estimating the effective Young's modulus of soft tissues from indentation tests - nonlinear finite element analysis of effects of friction and large deformation*. Medical Engineering & Physics, 1997. 19(6): p. 512-517.
58. Kistenberg R., K.S., Mate B., Brown E., Tawfik S., Terk. M., *Utilization of magnetic resonance imaging, segmentation and finite element analysis (FEA)*. Leipzig - 13th ISPO World Congress, 2010: p. 3469-644.
59. Lacroix, D. and J. Ramírez Patiño, *Finite Element Analysis of Donning Procedure of a Prosthetic Transfemoral Socket*. Annals of Biomedical Engineering, 2011. 39(12): p. 2972-2983.
60. Portnoy, S., I. Siev-Ner, N. Shabshin, A. Kristal, Z. Yizhar, and A. Gefen, *Patient-specific analyses of deep tissue loads post transtibial amputation in residual limbs of multiple prosthetic users*. Journal of Biomechanics, 2009. 42(16): p. 2686-2693.
61. Portnoy, S., Z. Yizhar, N. Shabshin, Y. Itzchak, A. Kristal, Y. Dotan-Marom, I. Siev-Ner, and A. Gefen, *Internal mechanical conditions in the soft tissues of a residual limb of a trans-tibial amputee*. Journal of Biomechanics, 2008. 41(9): p. 1897-1909.
62. Portnoy, S. and A. Gefen, *Patient-Specific Modeling of Subjects with a Lower Limb Amputation*, in *Patient-Specific Modeling in Tomorrow's Medicine*. 2012, Springer. p. 441-459.
63. Ramírez, J.F. and J.A. Vélez, *Incidence of the boundary condition between bone and soft tissue in a finite element model of a transfemoral amputee*. Prosthetics and Orthotics International, 2012. 36(4): p. 405-414.
64. Wu, C.L., C.H. Chang, A.T. Hsu, C.C. Lin, S.I. Chen, and G.L. Chang, *A proposal for the pre-evaluation protocol of below-knee socket design - Integration pain tolerance with finite element analysis*. Journal of the Chinese Institute of Engineers, 2003. 26(6): p. 853-860.

65. Zhang, M. and C. Roberts, *Comparison of computational analysis with clinical measurement of stresses on below-knee residual limb in a prosthetic socket*. Medical Engineering & Physics, 2000. 22(9): p. 607-612.
66. Colombo, G., G. Facoetti, R. Morotti, and C. Rizzi, *Physically based modelling and simulation to innovate socket design*. Computer-Aided Design and Applications, 2011. 8(4): p. 617-631.
67. Kistenberg R., K.S., Mate B., Brown E., Tawfik S., Terk. M., *Lower limb prosthetics I: Constructing an anatomically-correct structural model of the residual limb*. Leipzig - 13th ISPO World Congress, 2010: p. 3469-644.
68. Kistenberg R., K.S., Mate B., Brown E., Tawfik S., Terk. M., *Lower limb prosthetics II: Analysis and design considerations of a prosthetic socket*. Leipzig - 13th ISPO World Congress, 2010: p. 3590-670.
69. Lee, W.C.C. and M. Zhang, *Using computational simulation to aid in the prediction of socket fit: A preliminary study*. Medical Engineering & Physics, 2007. 29(8): p. 923-929.
70. Portnoy, S., I. Siev-Ner, Z. Yizhar, A. Kristal, N. Shabshin, and A. Gefen, *Surgical and Morphological Factors that Affect Internal Mechanical Loads in Soft Tissues of the Transtibial Residuum*. Annals of Biomedical Engineering, 2009. 37(12): p. 2583-2605.
71. SilverThorn, M.B. and D.S. Childress, *Parametric analysis using the finite element method to investigate prosthetic interface stresses for persons with trans-tibial amputation*. Journal of Rehabilitation Research and Development, 1996. 33(3): p. 227-238.
72. SilverThorn, M.B. and D.S. Childress, *Generic, geometric finite element analysis of the transtibial residual limb and prosthetic socket*. Journal of Rehabilitation Research and Development, 1997. 34(2): p. 171-186.
73. Sanders, J.E. and C.H. Daly, *Normal and shear stresses on a residual limb in a prosthetic socket during ambulation - comparison of finite-element results with experimental measurements*. Journal of Rehabilitation Research and Development, 1993. 30(2): p. 191-204.
74. Zachariah, S.G. and J.E. Sanders, *Finite element estimates of interface stress in the trans-tibial prosthesis using gap elements are different from those using automated contact*. Journal of Biomechanics, 2000. 33(7): p. 895-899.
75. Zachariah, S.G. and J.E. Sanders, *Standing interface stresses as a predictor of walking interface stresses in the trans-tibial prosthesis*. Prosthetics and Orthotics International, 2001. 25(1): p. 34-40.
76. Zhang, M., M. Lord, A.R. Turnersmith, and V.C. Roberts, *Development of a nonlinear finite-element modeling of the below-knee prosthetic socket interface*. Medical Engineering & Physics, 1995. 17(8): p. 559-566.
77. Zhang, M., A.R. TurnerSmith, V.C. Roberts, and A. Tanner, *Frictional action at lower limb prosthetic socket interface*. Medical Engineering & Physics, 1996. 18(3): p. 207-214.
78. Ramos, A. and J.A. Simoes, *Tetrahedral versus hexahedral finite elements in numerical modelling of the proximal femur*. Medical Engineering & Physics, 2006. 28(9): p. 916-924.
79. Lee, V.S.P., S.E. Solomonidis, and W.D. Spence, *Residuum-socket interface pressure as an aid to socket design in prostheses for trans-femoral amputees - A preliminary*

- study*. Proceedings of the Institution of Mechanical Engineers Part H-Journal of Engineering in Medicine, 1997. 211(2): p. 167-180.
80. Silver-Thorn, M.B., *Investigation of lower-limb tissue perfusion during loading*. Journal of Rehabilitation Research and Development, 2002. 39(5): p. 597-608.
 81. Choi, A.P.C. and Y.P. Zheng, *Estimation of Young's modulus and Poisson's ratio of soft tissue from indentation using two different-sized indentors: finite element analysis of the finite deformation effect*. Medical & Biological Engineering & Computing, 2005. 43(2): p. 258-264.
 82. Lu, M.H. and Y.P. Zheng, *Indentation test of soft tissues with curved substrates: A finite element study*. Medical & Biological Engineering & Computing, 2004. 42(4): p. 535-540.
 83. Delalleau, A., G. Josse, J.M. Lagarde, H. Zahouani, and J.M. Bergheau, *Characterization of the mechanical properties of skin by inverse analysis combined with the indentation test*. Journal of Biomechanics, 2006. 39(9): p. 1603-1610.
 84. Avril, S., L. Bouten, L. Dubuis, S. Drapier, and J.F. Pouget, *Mixed Experimental and Numerical Approach for Characterizing the Biomechanical Response of the Human Leg Under Elastic Compression*. Journal of Biomechanical Engineering-Transactions of the Asme, 2010. 132(3): p. 8.
 85. Hendriks, F., D. Brokken, J. Van Eemeren, C. Oomens, F. Baaijens, and J. Horsten, *A numerical-experimental method to characterize the non-linear mechanical behaviour of human skin*. Skin Research and Technology, 2003. 9(3): p. 274-283.
 86. Zienkiewicz, O.C. and R.L. Taylor, *The Finite Element Method: Solid Mechanics*. Vol. 2. 2000: Butterworth-heinemann.
 87. Hinton, E., *Introduction to Nonlinear Finite Element Analysis*. 1992: NAFEMS.
 88. Zhang, M. and A.F.T. Mak, *In vivo friction properties of human skin*. Prosthetics and Orthotics International, 1999. 23(2): p. 135-141.
 89. Zhang, M., A.R. Turner-Smith, A. Tanner, and V.C. Roberts, *Clinical investigation of the pressure and shear stress on the trans-tibial residuum with a prosthesis*. Medical Engineering & Physics, 1998. 20(3): p. 188-198.
 90. Seelen, H.A.M., S. Anemaat, H.M.H. Janssen, and J.H.M. Deckers, *Effects of prosthesis alignment on pressure distribution at the residuum/socket interface in transtibial amputees during unsupported stance and gait*. Clinical Rehabilitation, 2003. 17(7): p. 787-796.
 91. <http://www.cooperinstruments.com/en/load-force-sensors/item/38-elf-4200-flexiforce-paper-thin-sensor.html>. Accessed September 2013.
 92. <http://www.pressuremapping.com/index.cfm?pageID=13§ion=10>. Accessed September 2013.
 93. <http://www.tekscan.com/prosthetic-in-socket-pressure-distribution>. Accessed September 2013.
 94. <http://novel.de/novelcontent/medical/prosthesis-hardware>. Accessed September 2013.
 95. Abu Osman, N.A., W.D. Spence, S.E. Solomonidis, J.P. Paul, and A.M. Weir, *Transducers for the determination of the pressure and shear stress distribution at the residuum-socket interface of trans-tibial amputees*. Proceedings of the Institution of Mechanical Engineers Part B-Journal of Engineering Manufacture, 2010. 224(B8): p. 1239-1250.
 96. Ali, S., N.A. Abu Osman, A. Eshraghi, H. Gholizadeh, N.A.b. Abd razak, and W.A.B.B. Wan Abas, *Interface pressure in transtibial socket during ascent and*

- descent on stairs and its effect on patient satisfaction.* Clinical Biomechanics, 2013. 28(9–10): p. 994-999.
97. Convery, P. and A.W.P. Buis, *Conventional patellar-tendon-bearing (PTB) socket/residuum interface dynamic pressure distributions recorded during the prosthetic stance phase of gait of a trans-tibial amputee.* Prosthetics and Orthotics International, 1998. 22(3): p. 193-198.
 98. Convery, P. and A.W.P. Buis, *Socket/residuum interface dynamic pressure distributions recorded during the prosthetic stance phase of gait of a trans-tibial amputee wearing a hydrocast socket.* Prosthetics and Orthotics International, 1999. 23(2): p. 107-112.
 99. Dumbleton, T., A.W.P. Buis, A. McFadyen, B.F. McHugh, G. McKay, K.D. Murray, and S. Sexton, *Dynamic interface pressure distributions of two transtibial prosthetic socket concepts.* Journal of Rehabilitation Research and Development, 2009. 46(3): p. 405-415.
 100. Dou, P., X.H. Jia, S.F. Suo, R.C. Wang, and M. Zhang, *Pressure distribution at the residuum/socket interface in transtibial amputees during walking on stairs, slope and non-flat road.* Clinical Biomechanics, 2006. 21(10): p. 1067-1073.
 101. Goh, J.C.H., P.V.S. Lee, and S.Y. Chong, *Comparative study between patellar-tendon-bearing and pressure cast prosthetic sockets.* Journal of Rehabilitation Research and Development, 2004. 41(3B): p. 491-501.
 102. Goh, J.C.H., P.V.S. Lee, and S.Y. Chong, *Static and dynamic pressure profiles of a patellar-tendon-bearing (PTB) socket.* Proceedings of the Institution of Mechanical Engineers Part H-Journal of Engineering in Medicine, 2003. 217(H2): p. 121-126.
 103. Krouskop, T., A. Muilenberg, D. Dougherty, and D. Winningham, *Computer-aided design of a prosthetic socket for an above-knee amputee.* J Rehabil Res Dev, 1987. 24(2): p. 31-8.
 104. Polliack, A., R. Sieh, D. Craig, S. Landsberger, D. McNeil, and E. Ayyappa, *Scientific validation of two commercial pressure sensor systems for prosthetic socket fit.* Prosthetics and Orthotics International, 2000. 24(1): p. 63-73.
 105. Rogers, B., G. Bosker, M. Faustini, G. Walden, R.R. Neptune, and R. Crawford, *Case report: Variably compliant transtibial prosthetic socket fabricated using solid freeform fabrication.* Journal of Prosthetics and Orthotics, 2008. 20(1): p. 1-7.
 106. Sanders, J., S. Zachariah, A. Jacobsen, and J. Ferguson, *Changes in interface pressures and shear stresses over time on trans-tibial amputee subjects ambulating with prosthetic limbs: comparison of diurnal and six-month differences.* Journal of Biomechanics, 2005. 38(8): p. 1566-1573.
 107. Sengeh, D.M. and H. Herr, *A Variable-Impedance Prosthetic Socket for a Transtibial Amputee Designed from Magnetic Resonance Imaging Data.* JPO: Journal of Prosthetics and Orthotics, 2013. 25(3): p. 129-137.
 108. Lee, W.C., M. Zhang, and A.F. Mak, *Regional differences in pain threshold and tolerance of the transtibial residual limb: Including the effects of age and interface material.* Archives of Physical Medicine and Rehabilitation, 2005. 86(4): p. 641-649.
 109. Commean, P.K., K.E. Smith, and M.W. Vannier, *Lower extremity residual limb slippage within the prosthesis.* Archives of Physical Medicine and Rehabilitation, 1997. 78(5): p. 476-485.
 110. Papaioannou, G., C. Mitrogiannis, G. Nianios, and G. Fiedler, *Assessment of amputee socket-residuum-residual bone kinematics during strenuous activities using Dynamic*

- Roentgen Stereogrammetric Analysis*. Journal of Biomechanics, 2010. 43(5): p. 871-878.
111. Rehabilitation Engineering Division and K.s.C.f.t.A.o.R. Equipment, *Pain-free artificial lower limb patient interfaces*, in *Evidence Review*. 2007, December 2007: London. p. 1-30.
 112. Nolte, L., M.L. Haynes, and J.M. Colvin. *Comparison of direct manufacturing technologies for the application of prosthetic sockets*. in *ORTHOPAEDIE + REHA-TECHNIK*. 2012. Leipzig - Germany
 113. Dhondt, G., *CalculiX CrunchiX USER'S MANUAL Version 2.5*. 2012.
 114. Hong, J.H., *Effect of hip moment on socket interface pressure during stance phase gait of transfemoral amputee*. Gait & Posture, 2006. 24(2): p. S259-S261.
 115. Pallas-Areny, R., J.G. Webster, and R. Areny, *Sensors and signal conditioning*. 2001: Wiley New York.
 116. Ristic, L., *Sensor technology and devices*. Measurement Science and Technology, 2000. 11(12): p. 1829.
 117. Baxter, L.K., *Capacitive sensors*. Ann Arbor, 2000. 1001: p. 48109.
 118. Yeung, L., A.K. Leung, M. Zhang, and W.C. Lee, *Effects of long-distance walking on socket-limb interface pressure, tactile sensitivity and subjective perceptions of trans-tibial amputees*. Disability and Rehabilitation, 2013. 35(11): p. 888-893.
 119. Trebbin, H., *Effects of high demand activity on gait and socket pressure in trans-tibial amputees*, in *Faculty of Engineering*. 2009, University of Strathclyde.
 120. Eshraghi, A., N.A. Abu Osman, H. Gholizadeh, S. Ali, S.K. Sævarsson, and W.A.B. Wan Abas, *An experimental study of the interface pressure profile during level walking of a new suspension system for lower limb amputees*. Clinical Biomechanics, 2012.
 121. Tekscan, *F-Scan ® User Manual*. 2012.
 122. Infinity_O&P. Accessed January 2014; Available from: <http://infinityop.com/>.
 123. Lake, C. and T.J. Supan, *The Incidence of Dermatological Problems in the Silicone Suspension Sleeve User*. Journal of Prosthetics and Orthotics, 1997. 9(3): p. 97-106.

Appendices

A

Prosthesis components

In recent years, present prostheses are an assembly of different standard components that satisfy the amputees' requirements, allowing them to accomplish different activities, from the simpler to the more complex. Taking into account the statistical data about amputations previously cited, the number of persons subject to amputations are tens of thousands every year and that means millions of persons around the world. So, since production and manufacture of prosthesis devices has assumed an industrial dimension, the concept of modularity has become established. The entire prosthesis device, excluding the socket, has been divided in small components, according to the specific function, each capable of interfacing with the other thanks to standardized connections. Standardization allows to a drastic reduction of costs thanks to a series production, simplify the assembled and disassembled of the devices, speed the set-up procedures, and allow repeatable and consistent alignment conditions of the components.

Prosthetic elements are mainly classified according to some patient's characteristics (weight, height, activity level) and the degree of mobility permitted by the component. The choice of the right component is done consulting a catalogue, selecting the specific part according to the needs and the use of the amputee, and paying attention to their compatibility.

The modular lower limb prosthesis, both transtibial and transfemoral, are principally assembled by: socket, liner, knee (only for transfemoral amputees), pylon, foot, adapters, and cosmetic part. These elements will be described in this paragraph, which also will give a brief overview on prosthetic socket types. Figure A.1 portrays an overview of common components and related variants used for modular transfemoral prosthesis.

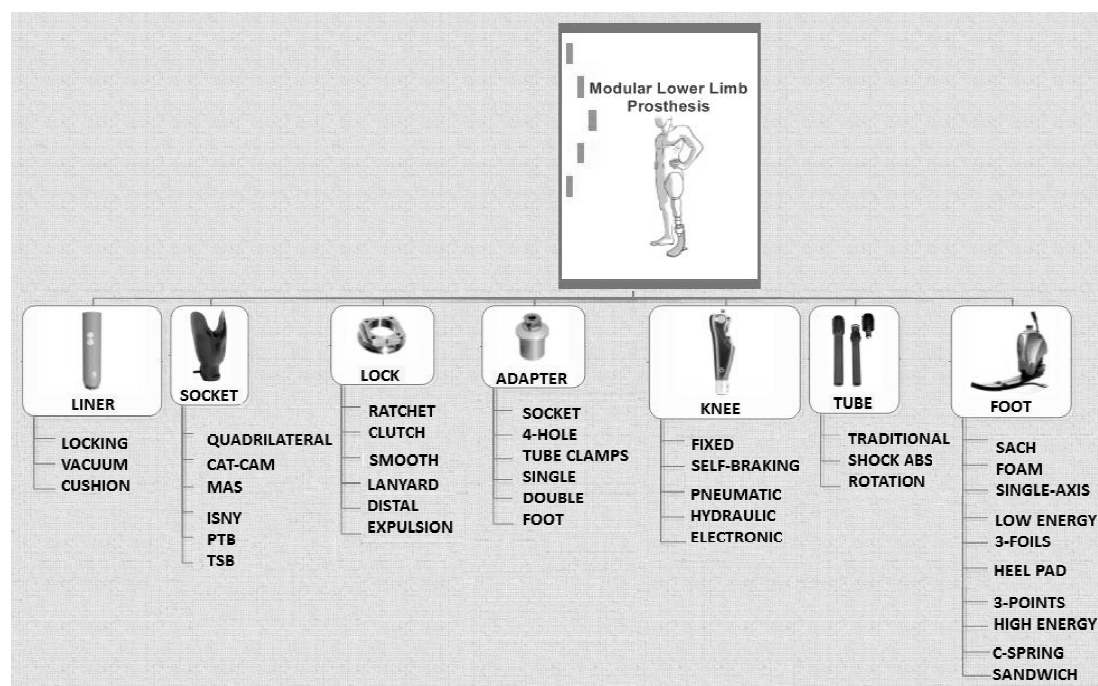


Figure A.1 - Mind map of modular lower limb prosthesis components [3].

A1. Socket

The socket is the interface between the residuum and the mechanical part of the prosthesis. It requires a high level of customization to satisfy functional and comfort requirements, so it is totally custom-fit on the patient's anatomy. It wears on the residual limb and it supports the amputee during the walking. The socket is made in wood, synthetic resin or carbon fibre, and that influences the degree of mobility associated with the prosthesis. Weight and pathologies of the patient are the most important parameters that influence the choice of the socket typology. In the following, the most diffused typologies of socket shapes are listed.

There are primarily two types of socket used for transfemoral amputees, the quadrilateral and the ischial-containment socket (in Figure A.2).

Quadrilateral socket is named for the socket shape and is borne with rigid walls, each of which has a specific function. The medial wall has to contain its respective tissues and provide counterpressure to the lateral wall. The latter should support adequately the femur in the Midstance to prevent a Trendelenburg's sign during the swing of the healthy leg. The anterior wall avoids forward movement of the residuum; while, the anterior wall offers a weight-bearing surface for the ischial prominence and the gluteus muscles. Quadrilateral sockets show some limits such as loss of adductor strength, complaint over ischial prominence, and higher pressure values due to smaller contact areas that reduce the ability to distribute pressure and forces.

Ischial containment socket solves quadrilateral limits. It allows obtaining a more uniform pressure distribution over the entire residual limb surface, including the ischium and enveloping the trochanter and all muscles. It is proposed to amputees with scars, angiopathies or bypass; excellent results are achieved for short and not very tonic residual limbs, but also with sportive people. MAS socket (Marlo Anatomical Socket) can be considered an evolution of ischial containment one, offering more mobility and a better containing ischium. It is particularly adapted for active amputees with very tonic residual limbs.

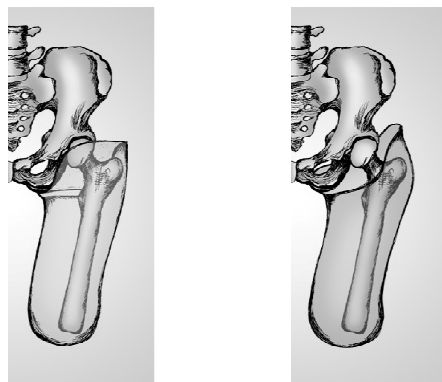


Figure A.2 - Examples of transfemoral prosthesis socket: quadrilateral (left) and ischial-containment (right) [122]

Patellar Tendon Bearing (PTB) and Total Surface Bearing (TSB) are the most diffused sockets for transtibial amputation (see Figure A.3).

The most commonly used for TT amputation the end of the '90s was the PTB socket. It uses total contact to avoid pockets and edema and it presents two different regions, the bearing and the relief area. Areas of bearing include weight tolerant parts which have a good blood supply to dissipate pressure; while the relief areas present bony prominence, poor blood supply, or near important nerves. This socket is not appropriate for sensitive skin. Other typologies of PTB socket can be identified: Supracondylar Suprapatellar Suspension (SCSP) and Supracondylar Suspension (SC) socket. The first one envelops all the patella region with higher medial, lateral and frontal walls, giving better stability but becoming more bulky; it good for patients with very short residuum, but slim. The SC socket looks like SCSP but it leaves visible the front area of patella, allowing good knee flexion.

In contrast to PTB socket, TSB socket shows a more equally pressures distribution over the transtibial residuum surface; furthermore, the use of liner assists the in distributing these pressure. This socket seems to be the best choice for below knee amputees.

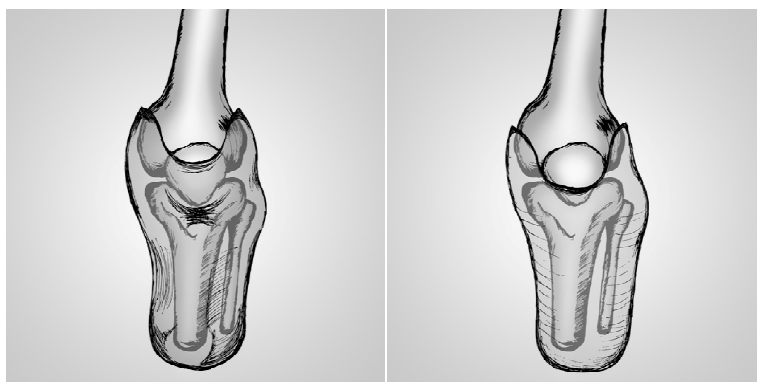


Figure A.3 - Examples of Patellar Tendon Bearing (PTB) and Total Surface Bearing (TSB) [122].

A transversal case is the flexible or ISNY (Iceland-Swedish-New York) socket because its functioning concept is applicable both for transtibial and transfemoral socket. As shown in Figure A.4, this kind of socket presents an external rigid or semi-rigid structure that sustains an internal flexible thermoplastic part. The external structure is in correspondence of bearing areas; while the flexible element permits to keep the complete prosthesis control during walking. The mix of these two parts allows reducing the internal temperature, increasing the comfort, and reducing the weight.

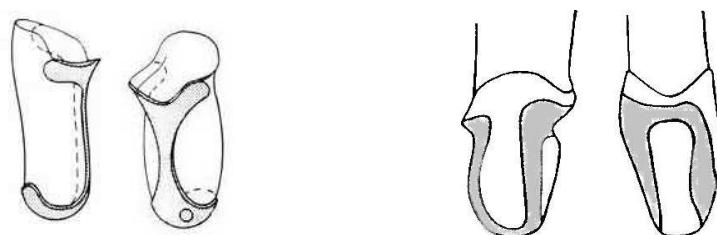


Figure A.4 - Examples of transfemoral flexible sockets (left) and transtibial flexible sockets (right).

Ischial containment socket for transfemoral amputation and TSB socket for transtibial amputation seem to be the best choice, as also confirmed at the last International Society for Prosthetics and Orthotics World Congress [56]. Nevertheless, all socket typologies are still used by amputees because the great psychological difficulties and mental inertial of their habits.

A2. Liner

The liner is a sock, usually made of different qualities of silicone, that is fit on the residuum and creates a soft gap between the skin and inner socket wall. It allows supporting in a better way the residuum, avoiding excessive forces on the residual limb, reducing shear stress, minimizing the pistoning phenomenon. Thus, it provides greater comfort to transtibial and transfemoral amputees. These benefits are analysed in Lin et al. study [37], where the liner key role in the redistribution of stresses and interface pressures comes to light. It emerged how a less rigid liner increases the slippage distance between the residuum and socket, but without ensuring a reduction of peak stress. This rather complicated behaviour is due to the combined effects of non-uniform socket shape and of different sliding distances, caused by the different stiffness of the liner.

The socket liner is not a device adopted in a systematic manner in lower limb amputees because it presents some disadvantages. It can cause a heat build-up or dermatological problems due to the directly interaction with the biological [123]. These diseases are influenced by aging, activity level and use patterns. Also Baars and Geertzen [41] objectively documented advantages of silicone liners, such as better residuum suspension, along with possible negative effects, such as excessive perspiration and itching.

Liner is commercialized in different standard sizes and thickness (usually from 3 to 9 mm), but it can be customized through a thermoformed process according to the residuum morphology or easily shortened according to patient's needs. The shape is slightly tapered and closed at the end; the outer surface may be smooth or ribbed and some complex models have particular inserts that improve damping and grip. The choice of using the liner is done according to the residuum characteristics (type, dimensions, amputation stability, tonicity, shape, and skin conditions) and the patient life style. The liner is fixed to the socket by a lock device or vacuum valve. Figure A.5 shows some examples of the last generation of liners.



Figure A.5 - Different typologies of liners by Össur.

A3. Knee

The prosthetic knee is a modular component used only for transfemoral (or above knee) amputees. It replace the function of human knee and can be classified according to its centre of rotation (monocentric or polycentric, also shown in Figure A.6), or on the basis of working principles (fixed, self-braking or friction, pneumatic, hydraulic or electronic).

In contrast to monocentric knee, the polycentric one has the centre of rotation that moves into the space in relation to the flexion angle and to the disposition of the articulation axes. It executes simultaneously the movement of rotation and translation, avoiding the foot dragging on the floor and giving a more natural movement.

Fixed knee doesn't flex during walking and it can be unlocked only to sit down. Self-braking knee allows knee movement during the gait thanks to a friction system that prevents flexion under load. Pneumatic and hydraulic knees offer high stability in static position and a more physiological way of walking. They differ mainly for the operation principle: in the first case is the air that moves from one to another chamber, in the other one is a liquid. Finally, electronic knee is totally controlled by microchips with hydraulic functioning and its behaviour depends on patient walking. It offers the best knee performance but it is expensive, has high maintenance costs and high weight.



Figure A.6 - Examples of monocentric and polycentric knee.

A4. Foot

The foot is the most important component because it conditions the way in which the prosthetic device interfaces with the ground. It has to sustain the amputee and reproduce the behaviour of a healthy foot every step of the walking, providing a shock absorption in the foot rear and an elastic reaction in the forefoot. The appropriate foot selection (see different examples in Figure A.7) is strictly related to the patient characteristics, the allowed degrees of mobility, and the knee choice in transfemoral amputees.

Foot parameters, such as supported load, weight, flexibility, and mobility, depend on the geometry and the materials that are made of (wood, rubber, foams, or composite materials). In particular, the carbon fiber has permitted to improve the functionalities and properties of the prosthetic feet. The latter are light, easy adaptable to irregular floors; and, they can store and release energy during walking, reducing the load to the contra-lateral limb. Feet can be characterized as static, dynamic, or electronic, according to the principles of operation. The main difference between static and dynamic is that the latter stores and releases energy during walking; while in electronic foot all ankle movement are controlled by a microchip.



Figure A.7 - Examples of prosthetic feet by Otto Bock: carbon foot, adjust foot, dynamic foot and SACH.

A5. Other components

Pylon

The pylon is a tube that connects the socket with the prosthetic foot, providing the same function of the tibia in a healthy subject. Generally are made of aluminium, steel, or titanium. The diameter is standard and chosen according to weight and activity level of the patient; and the length depends on the residuum length. Some pylons have a rotation adapter or shock-absorbing system.

Adapters

With the term of adapters it means all the different part that allows coupling all the different components of a modular prosthesis each others. This parts permit to easily and quickly connect the different components in a standard mode and allow to perform the alignments set-up in a much more simple and accurate way.

Adapters are made of aluminium or stainless steel when the patient weight is less than 100kg, otherwise titanium or carbon fiber. In agreement with use, they can be mainly classified as (see different examples in Figure A.8):

- *Socket adapter*, it connects the socket to the pylon in TT amputees or the knee in TF amputees;
- *Pylon clamps*, it links up the tube with the knee, or the foot or the socket;
- *Double adapter*, it substitutes the pylon when the distance between TT socket and foot is too small;
- *Foot adapter*, it connects the foot with the tube clamps or double adapters.



Figure A.8 - Examples of adapters: socket adapter, pylon clamps, double adapter, foot adapter.

Cosmetics

Cosmetics components are non-structural devices and the materials used are usually polymeric materials or elastomers. Their contribution is solely aesthetic, they try to reproduce the visual appearance of a healthy limb, and they can be used over the previously cited components.

B

Workstation technical specification

Hardware and operating system of the workstation influence significantly the simulation times, because they determine the computing performance, but few authors reported the hardware used to run simulations. These technical specifications are summarized in Table B.1. Analysing the literature, it seems that supercomputers have been replaced by PC/workstation thank to the increase of hardware performance and, for the future, parallel computing architecture will be widely diffused.

Table B.1 - Workstation technical specifications.

Researcher	Year	CPU	RAM	OS	Runtime
Zhang et al. [76]	1994	CONVEX 63840 supercomputer			
Goh et al. [48]	2004	Pentium-IV@ 3.2 GHz	2 GB		~5min
Portnoy et al. [61]	2008	Pentium-class workstation; Designated graphic processor board	1 BG		~12h
Lacorix et al. [59]	2011	Quad Core i7-880@3.06 GHz	16 GB	Windows7 Pro 64-bit	6÷8 h
Morotti	2013	Intel Xeon W3505@2.53 GHz	12 GB DDR3 @ 1333Mh	Windows7 Ultimate 64-bit	<4h